Fakultät für Medizin

Klinik für Hals- Nasen- Ohrenheilkunde des Klinikums Rechts der Isar

der

Technischen Universität München

„Inter-individual differences in human adipose derived stem cells with regards to adipogenic potential and endothelial progenitor cell differentiation potential in in-vitro experiments“

Jascha Frederik Che ELL

Vollständiger Abdruck der von der Fakultät für Medizin der Technischen Universität München zur Erlangung des akademischen Grades eines Doktors der Medizin (Dr. med.) genehmigten Dissertation.

Vorsitzender: Prof. Dr. Ernst J. Rummeny

Prüfende der Dissertation:

1. Priv.-Doz. Dr. Thomas Stark

2. Prof. Dr. Florian Bassermann

Die Dissertation wurde am 08.02.2019 bei der Technischen Universität München eingereicht und durch die Fakultät für Medizin am 06.11.2019 angenommen.

Meinen Eltern gewidmet.

Zusammenfassung:

Seit längerer Zeit besteht Einigkeit darüber, dass weißes Fettgewebe im Menschen mehr darstellt als ein Organ zur Speicherung überschüssiger Energie in Zeiten kalorischen Überangebotes. Seit mehr als 20 Jahren ist die endokrine Funktion des Fettgewebes bekannt, womit das Fettgewebe nach Volumen das größte Organ des Menschen darstellt. Weiterhin ist bekannt, dass chronische Erkrankungen, wie zum Beispiel Typ 2 Diabetes Mellitus mit Veränderungen des Fettgewebes vergesellschaftet sind. Diese Veränderungen sind von einer chronischen Entzündungsreaktion gekennzeichnet, welche in Konsequenz zu einer Infiltration mit Makrophagen führt. Längerfristig führt dieser Prozess zu einem fibrotischen Umbau des Fettgewebes, welcher hypoxische Bedingungen innerhalb des Fettgewebes zur Folge hat und somit die Aufrechterhaltung der Entzündungsreaktion weiterhin unterstützt. Auch sind diese chronisch entzündlichen Veränderungen mit Insulinresistenz des Fettgewebes vergesellschaftet. Wie die meisten anderen Gewebe ist auch das Fettgewebe einem ständigen Erneuerungsprozess unterworfen, in welchem Adipocyte Stem Cells (ASC) die Ausgangszellen für neue Adipozyten darstellen. Diese Zellen befinden sich perivaskulär im Fettgewebe und sind morphologisch kaum von Fibrozyten zu unterscheiden, lassen sich immunhistochemisch jedoch identifizieren.

Aufgrund seiner leichten und komplikationsarmen Entnahme, sowie der Abwesenheit von Fremdkörper- oder Abstoßungsreaktionen nach Replantation würde Fettgewebe theoretisch ein ideales Füllmaterial für die Wiederherstellung von Weichgewebsdefekten oder auch zur Behandlung von Stimmlippenatrophien nach Recurrensparesen ein ideales Füllmaterial darstellen, jedoch zeigen sich unvorhersehbare Resorptionsraten, die häufige Nachbehandlungen notwendig machen. Dies ist häufig weder vom Patienten toleriert noch praktisch durchführbar.

Ziel dieser Dissertation soll es sein, Hinweise auf Veränderungen auf Ebene dieser Vorläuferzellen zu finden, welche sich in unterschiedlicher Regenerationsfähigkeit des Fettgewebes manifestieren könnten und damit dazu beizutragen besser zu verstehen wieso Resorptionsraten nach autologer Fettgewebstransplantation so großen Schwankungen unterworfen sind. Dazu wurden Adipocyte Stem Cells aus Liposuktionsproben isoliert, diese nach einem standardisierten Protokoll aufgereinigt und bei Erreichen einer kritischen Dichte zur adipogenen Differenzierung angeregt. Die Zugehörigkeit der isolierten Zellen zu der Gruppe der ASC wurde mittels FACS (Fluorescence Activated Cell Sorting) bestätigt. Während der Differenzierungsphase wurden in regelmäßigen Intervallen mittels ELISA der Adiponectinspiegel im Nährmedium gemessen und nach Abschluss der Differenzierungsphase histologische Färbungen durchgeführt. Auch wurden in einem Co-Kultur Experiment mit Hilfe des kommerziell verfügbaren V2a-Assays das Potenzial der so isolierten Zellen, endotheliale Vorläuferzellen zur Differenzierung anzuregen, überprüft. Da die Expansion beziehungsweise die Aufrechterhaltung eines physiologischen Fettgewebes zu einem großen Teil von der Vaskularisation

desselben abhängt, standen hier ebenfalls mögliche Unterschiede zwischen den Proben im Fokus der Untersuchung.

Im Ergebnis konnte mittels FACS Untersuchungen gezeigt werden, dass sich in den im Rahmen von Liposuktionen isolierten Gewebeproben zuverlässig Adipocyte Stem Cells isolieren lassen. Auch ließen sich die große Mehrheit der so isolierten Proben adipogen differenzieren, wobei signifikante Unterschiede in der Wachstumsgeschwindigkeit bis zur Einleitung der Differenzierung bei Konfluenz beobachtet wurden. Histologisch wurden Unterschiede deutlich, die sich sowohl in Größe und Form der Adipozyten als auch in Anzahl und Größe beobachtbarer Vakuolen. Weiter untermauert wurden diese Ergebnisse auch durch Untersuchungen des Anstiegs des Adiponectinspiegels während der Differenzierung, der zwar generell nachgewiesen werden konnte jedoch weder im Bezug zum Zeitpunkt des Anstiegs noch zum erreichten Endwert homogen erfolgte. Schließlich zeigte das das Cokultur Experiment nach immunhistochemischer Färbung statistisch signifikante Unterschiede sowohl in der von endothelial differenzierten Zellen eingenommenen Fläche als auch im morphologischen Aspekt der Kultur.

In Zusammenschau der Ergebnisse konnte die initiale Hypothese, ASC seien bezüglich ihrer Differenzierbarkeit und ihres proangiogenetischen Potentials nicht generell vergleichbar, untermauert werden. Hier findet sich an Anschlusspunkt für weitere Forschung um das Potential von Fettgewebe als autologem Augmentationsmaterial für Gewebsdefekte oder Atrophien besser nutzen zu können.

Abstract

The fact the adipose tissue in humans is more than an organ for saving excess energy in times of excess energy uptake has been established for a considerable time. The endocrine function of adipose tissue has been known for more than 20 years making adipose tissue the largest endocrine organ in humans by volume. Furthermore, is has been shown that chronic diseases like type 2 diabetes are associated with adipose tissue changes. Chronic inflammation leading to macrophage infiltration has been found to be a hallmark of these changes. In the long term, adipose tissue is remodeled into a fibrotic state, causing adipose tissue hypoxia, which in turn further maintains inflammation. These chronic inflammatory changes are also associated with adipose tissue insulin resistance.

Like most other tissue types, adipose tissue is subject to a constant cell turnover with Adipocyte Stem Cells (ASC) representing the progenitors for new adipocytes. These cells are located perivascular in adipose tissue, can hardly be differentiated from fibrocytes morphologically but are identifiable through immunostaining.

Being easily obtainable and without risk of foreign-body- or rejection-reactions after replantation, adipose tissue would, theoretically, be an ideal filler for the reconstruction of soft tissue defects or for treatment of vocal cord atrophies following recurrens-nerve lesions. However, unpredictable resorption rates of transplanted adipose tissue necessitate frequent revision-treatments, which are often neither tolerated by patients nor practically performable.

This dissertation is aimed at finding clues for changes at the progenitor cell level, which could manifest in varying regenerative abilities of adipose tissue and thus at contributing to a better understanding of the reasons for the observed variation of resorption rates following autologous adipose tissue transplantation. To this end, Adipocyte Stem Cells were isolated from liposuction samples, purified according to a standardized protocol, and upon them reaching a critical confluence level adipogenic differentiation was induced. The isolated cells` affiliation to ASC lineage was confirmed through fluorescence activated cell sorting (FACS). During differentiation, adiponectin levels in the differentiation medium were measured regularly and after conclusion of differentiation histologic examination were conducted. Also, using the commercially available V2s-assay, the isolated cells` ability to induce differentiation in endothelial progenitor cells was examined. Since expansion respectively physiological turnover of physiological adipose tissue depends to a large extend on its vasculature, this experiment was again aimed at uncovering any possible differences between samples.

As a result, FACS demonstrated that Adipocyte Stem Cells can be reliably isolated from tissue samples obtained from liposuctions. Also, adipogenic differentiation was successful in a vast majority of the

samples with significant differences in growth speed as measured in time to 70% confluence and induction of differentiation being recorded. Histologically, differences regarding adipocyte size and shape as well as numbers and size of observable vacuoles were observed. The results were further supported by examinations of adiponectin levels during differentiation. Generally, an increase in adiponectin was observed but neither the time of first increase of adiponectin nor the reached maximum levels were homogenous. Finally, the co-culture experiment exhibited significant differences both in terms of the area occupied by endothelially differentiated cells and the morphological aspect of the co-culture.

Conclusively, the initial hypothesis of ASC not being generally comparable regarding differentiability and pro-angiogenic potential could be supported. Future research could further investigate these phenomena to eventually make use of adipose tissue`s potential as autologous filling material for tissue defects or atrophies.

Table of Contents

Inter-individual differences in human adipose derived stem cells with regards to adipogenic potential and endothelial progenitor cell differentiation potential in in-vitro experiments I

Abstract: IV

Table of Contents 1

Abbreviations 3

1. Introduction 6

1.1. White Adipose Tissue 6

1.1.1. White Adipose Tissue and the Adipocyte 6

1.1.2. Adipose Tissue Pathology 18

1.2. Adipocyte Derived Stem Cells 21

1.3. Experiment Aim 24

1.4. Experiment Design 26

2. Materials and Methods 28

2.1. Patient Demographic 28

2.2. Obtainment, Isolation and Culture of Adipocyte Derived Stem Cells 29

2.2.1. Liposuction and Immediate Processing 29

2.2.2. Tissue Digestion, Adipose Derived Stem Cell isolation and Initial Cultivation (P_0) 30

2.2.3. Quantification of Cell Yield 30

2.2.4. Cryopreservation of ASC 31

2.2.5. Thawing and Seeding of Cryopreserved ASC 32

2.3. Primary Cell Culture (P_1) 32

2.3.1. Cell Seeding 32

2.3.2. Induction and Differentiation Process 33

2.3.3. Characterisation of Adipose Derived Progenitor Cells / Flow Cytometry 34

2.4. Microscopic Analysis of P_1 Cultivated Adipocytes 35

2.4.1. Oil-Red Staining 35

2.4.2. Qualitative Examination 36

2.5. Biochemical Analyses 36

2.5.1. Adiponectin-ELISA 36

2.5.2. VEGF-ELISA 37

2.6. Adipocyte Derived Stem Cell – Endothelial Progenitor Cell Co-culture (V2A) assay 39

2.6.1. Hypothesis 39

2.6.2. Experimental Setup 39

2.6.3. Execution of the co-culture experiment 40

2.6.4. Anti-CD31 immunostaining 41
2.6.5. Evaluation 42
3. Results 43
3.1. Time to confluence in P_0 43
3.2. Time to confluence in P_1 44
3.3. Biochemical differences 45
3.3.1. Adiponectin levels in culture 45
3.3.2. VEGF levels in endothelial progenitor cell – ASC co-culture 48
3.3.3. Proof of Multipotency - Adipogenic, Osteogenic and Chondrogenic differentiation 50
3.4. Flow cytometric (FACS) Analysis of ASC 52
3.4.1. Cell Yield 52
3.4.2. Surface Marker Patterns on Analysed Cells 52
3.5. Histological Findings 54
3.5.1. Qualitative Morphological Variances in Oil-red-stained Cultures 54
3.5.2. Variances in Anti-CD31 Immunostained Adipocyte Derived Stem Cell – Endothelial Progenitor Cell Co-cultures 62
4. Discussion 67
4.1. Conclusion of Findings 67
4.2. Limitations 68
4.3. Interpretation and Outlook 69
5. Appendix 75
5.1. References 75

Abbreviations

ADIPOR– Adiponectin receptor

AMPK – Adenosine monophosphate kinase A

AP – Alkaline phosphatase

ASC – Adipocyte derived stem cell(s)

ATGL – Adipocyte specific triacylglycerol lipase

BMI – Body mass index

BMP – Bone morphogenetic protein

BRCA – Breast cancer early onset

BSA – Bovine serum albumin

CAMP – Cyclic adenosine monophosphate

CD – Cluster of differentiation

CREB – CAMP-responsive element binding protein

CRP – C-reactive protein

CRTC – CAMP-responsive transcriptional co-activator

CTSS – Cystin protease cathepsin S

DMEM – Dulbecco's Minimum Essential Medium

EC – Endothelial cell(s)

ECGM – Endothelial cell growth medium

ECM – Extracellular matrix

ELISA – Enzyme-linked immunosorbent assay

FACS – Fluorescence-activated cell sorting

FAT – Fatty acid translocase

FCS – Foetal calve serum

FGF – Fibroblast growth factor

GFP – Green fluorescent protein

GLUT – Glucose transporter

GTP – Guanosine triphosphate

HEPES – 4-(2-hydroxyethyl)-1-piperazineethanesulfonic acid

HIF-1α – Hypoxia inducible factor 1α

HRP – Horseradish peroxidase

HSC – Haematopoietic stem cell(s)

HSL – Hormone sensitive lipase

IFN – Interferon

IL – Interleukin

IRS1 – Insulin receptor substrate 1

LCN2 – Lipocalin 2

LEPR – Leptin receptor

LOX – Lysyl oxidase

LPL – Lipoprotein lipase

MEM – Eagle's minimum essential medium

MGL – Monoglycerol lipase

MMP – Matrix metalloprotease

MSC – Mesenchymal stem cell(s)

NFκB - Nuclear factor kappa B

NO – Nitrogen monoxide

NPY – Neuropeptide Y

PBS – Phosphate buffered saline

PDGF(R) – Platelet derived growth factor (receptor)

Pdx1 – Pancreatic and duodenal homeobox

PI3K – Phosphatidylinositide 3-kinase

PKA – Protein kinase A

PKC – Protein kinase C

PPAR – Peroxisome proliferator-activated receptor

ROS – Reactive oxygen species

Smad – Combination of names of the *sma* (*Caenorhabditis elegans*) and *mad* proteins (*Drosophila*)

SVF – Stromal vascular fraction

TACE – TNF-α transforming factor

TAG – Triacylglyceride

TGF-β – Transforming growth factor beta

TMB – Tetramethylbenzidine

TNF-α – Tumour necrosis factor alpha

VEGF – Vascular endothelial growth factor

VWF – Von-Willebrand Factor

WAT – White adipose tissue

1. Introduction

1.1. White Adipose Tissue

1.1.1. White Adipose Tissue and the Adipocyte

White adipose tissue (WAT), commonly referred to as “fat tissue” or simply “fat”, has for some time been known to play a more complex physiological role than that of a mere organ of long-term energy storage. Adipose tissue forms a considerable but variable percentage of the mass of a human being. Increases and decreases in total body fat levels are dependent on the difference between total energy uptake and total energy consumption. Fat distribution patterns depend on a multitude of hormonal and genetic factors, which, in turn, depend on factors such as gender, age and nutritional habits. Some of these aspects will be explained in more detail in the following section.

Adipose tissue is abundantly present in all but severely underweight individuals. Whereas no significant differences in body fat percentages are present in groups of similar body mass indexes (BMI) across ethnicities, women generally exhibit a higher percentage of body fat than men and older individuals a higher percentage than younger individuals of the same sex [1]. Unsurprisingly, body fat percentages also correlate positively with BMI. In one study, physiological body fat percentages for adults with a BMI between 18.5 and 25 have been calculated to range between 21% and 36% for women and 8% to 25% for men across all age groups, with fat percentage rates above 36% and 25% for women and men, respectively, being indicators of obesity [1]. Another study has found physiological body fat percentage to range in similar magnitudes - between 9-18% for men and 14-28% for women [2]. Although virtually no upper limit exists for the body fat percentage in morbidly obese subjects, a body fat percentage of 2.5% has been described as the lower limit of fat mass in healthy adult men [3]. Existing in most body regions in the form of subcutaneous fat pads and in addition to its obvious function as a storage for energy, fat serves as mechanical protection for regions of the body prone to mechanical stress (e.g. the gluteal region or the soles of the feet), provides structural support, for example, in the perirenal fat capsule and shapes and defines our physical appearance as exemplified by subcutaneous facial fat. Nevertheless, visceral adipose tissue (which is predominantly found in the omentum majus and minus and has been suggested to be divided into even further sub-classifications [4]) has been found to be significantly different from subcutaneous adipose tissue with regard to its plasticity, resilience to metabolic stress (i.e. the effects of hypernutrition) and the impact of metabolic dysregulation as seen in obesity (see also 1.1.2.). The

differences are so significant that the notion of all WAT being equivalent should be abandoned and replaced with a more differentiated understanding of the different physiology of adipose tissue in the two main niches, namely subcutaneous and visceral. This is underlined by the findings that, despite subcutaneous and visceral adipose tissues being histologically identical and descendants of the same pool of progenitor cells, specific adipocytes retain a "memory" of their origin and maintain insulin sensitivity and glucose uptake when autologously transferred between the two depots [4,5]. These effects are stable and can be attributed to the different gene expression pattern expressed by adipocyte progenitor cells. Notably and in line with the higher differential potential, the expression of PPARμ, a cornerstone of adipocyte growth and differentiation, is upregulated in subcutaneous adipose tissue. In the study conducted by Tchkonia et al., 503 gene products in total were found to exhibit different expression levels in subcutaneous versus visceral adipose progenitor cells [6]. The underlying causality for the observed differences has not yet been identified. Moreover, subcutaneous adipose tissue exhibits a higher regenerative potential, as measured in proliferation and adipogenesis rates [7,5].

Independently of location, adipose tissue is composed of the eponymous adipocytes, which are comparatively large (50-150 μm) cells and, in physiological WAT, mostly univacuolar. At the cellular level, a lipid droplet fills most of the volume of the cell; the organelles and cell nucleus can usually be found peripherally. As large quantities of lipoproteins and other lipid double-layer subunits have to be produced continuously, the Golgi apparatus is also generally clearly distinguishable electro-microscopically in adipocytes [8]. Other cells found in WAT include cells of the immune system, such as macrophages, T lymphocytes, dendritic cells and others (see also 1.1.2.), fibrocytes, fibroblasts, and progenitor cells of stromal cells and adipocytes (adipocyte stem cells, ASC). As adipose tissue is excellently perfused, with every adipocyte being in direct contact with at least one capillary, vascular endothelial cells and smooth muscle cells are also found in WAT samples [9–11]. In line with the dense vasculature, adipose tissue physiologically receives 3-7% of total cardiac output (and up to 30% in cases of extreme obesity) [12]. In the context of adipose tissue research, the *stromal vascular fraction* (SVF) is the term for all contents of adipose tissue other than the adipocytes (therefore, including cells and extracellular matrix (ECM)). This name is derived from the centrifugation properties of the latter, with the adipocytes being located in a pellet at the bottom of centrifugation tubes, and the remaining cells, membranes and debris remaining in the supernatant, thus separating this cell pool from adipocytes. Dysregulation of this diverse environment plays an important role in various pathologies that affect WAT, such as metabolic syndrome and type 2 diabetes (see 1.1.2.)

The ECM of WAT is also crucial for its physiological function [13]. Analogous to other tissues, it is predominantly composed of proteoglycans and fibril-forming proteins, with the ECM of adipose tissue

exhibiting some characteristic features. Collagen type II is almost absent in human adipose tissue [14]. Collagen IV, fibronectin, laminin and the heparin sulphate proteoglycan perlecan (itself consisting of 10-15 heparan sulphate chains) can be found surrounding adipocytes [15]. The basal laminas of both adipocytes and endothelial cells are mostly composed of collagen IV and the other mentioned proteins, proteoglycans, and glycoproteins, which serve primarily as anchors to other ECM constituents and act as providers of structural support. As cells expanding in size (in hypertrophic states) or in number (in hyperplastic states), they need an non-rigid and adaptive environment, and hence, the degradation of collagen IV and collagen V and their remodelling is crucial during WAT expansion [16,17]. The same principle applies to fibronectin, a glycoprotein found throughout the body and also in WAT. Spiegelmann and Ginty reported as early as 1983 that a fibronectin-rich environment can impair the adipogenic differentiation of mouse 3T3 preadipocytes in an in-vitro setting [18]. Once fibronectin degradation was established as being essential for the adipogenic differentiation of ASC, cystin protease cathepsin S (CTSS) was identified as being secreted by differentiating adipocytes and able to degrade fibronectin [19]. By creating space for adipocyte expansion and by participating in the activation of growth factors, such as transforming growth factor β (TGF-β), zinc dependent matrix metalloproteases (MMP), a subgroup of the proteoglycan family, play another important role in these aforementioned processes. MMP 2 (also known as “Gelatinase A”) is secreted by adipocytes and its activity has been shown to be crucial to de novo adipogenesis in the recent gene knockout experiment of Bauters et al. [20]. MMP 9 (also known as “Gelatinase B”) is also secreted by adipocytes [21]. Whereas both Gelatinases are able to catalyse the activation of extracellular but are compounded and inactivated TGF-β by catalysing its break-up from binding proteins such as latent TGF-β binding protein (LTBP) and latency associated peptide (LAP), a knockout of MMP 9 does not impair in vitro adipogenesis [22,23]. Notwithstanding this finding, MMP 9 is elevated during WAT remodelling and in inflamed adipose tissue and is the target of the adipokine lipocalin-2 (LCN2), suggesting an as yet unknown physiological role [24,21]. TGFβ plays a twofold role in adipogenesis with observations of both the stimulation of adipogenesis during early adipogenesis and the inhibition of adipogenesis in vitro. Additionally, TGFβ levels are elevated in obese individuals. The most characteristic collagen type in WAT is collagen VI, which is closely connected to various metabolic and neoplastic diseases (see 1.1.2.). Collagen VI is a heterotrimeric protein consisting of three subunits ColVIα1, ColVIα2 and ColVIα3, and binds, among other proteins, Col IV. Collagen VI, in turn, has been attributed a role in anchoring a adipocyte basement membrane to the ECM and in providing structural support for the comparatively large lipid laden adipocytes [25,26]. See Figure 1 for an overview.

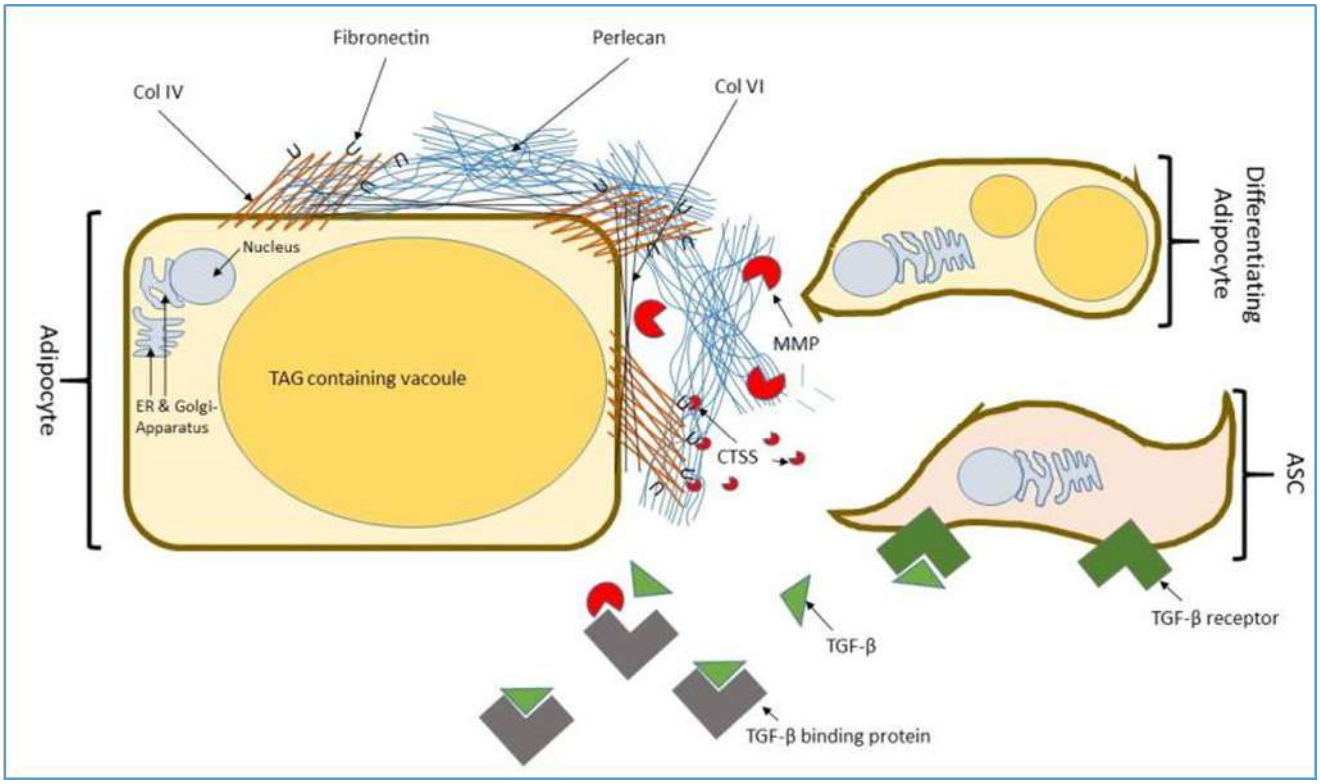

Figure 1: Overview of important components of the ECM and its degradation during WAT expansion. Collagen IV (brown) and VI (black) anchor other ECM proteins / proteoglycans / glycoproteins (here exemplified by Perlecan (blue)) to cells via fibronectin (black Us). In order to expand, the ECM must be degraded, a process catalysed by proteases such as Matrix-metalloproteases (MMP) and cystin protease cathepsin S (CTSS), which are secreted by adipocytes. Additionally, TGF-β (green triangles) is released from protein binding (grey dented cubes) and is transduced into its activated form by MMP interaction allowing it to exert its pro-adipogenic properties.

Attribution of adipocytes to one particular cell lineage has long been difficult, because of the unclear lineage attribution of the adipocyte progenitor cell. Nevertheless, evidence increasingly suggests that ASC are of mesodermal origin and descendants from mesenchymal stem cell (MSC) [27]. MSC were first found to reside in the same biological niche as the ASC, whereas in-vitro adipogenesis could also be achieved in cultures of MSC that where not initially perivascular [28,29]. Tomiyama et al. were able to show the expression of green-fluorescent protein (GFP) in adipose tissue following GFP+ bone-marrow derived MSC transplantation in a mouse experiment, further supporting the thesis of MSC being the progenitor of ASC [30]. Matches in the CD expression patterns of HSC, MSC, fibroblasts and various adipocyte progenitor cell types have been described [31]. Rodeheffer et al. eventually demonstrated that a Lin-, CD29+, CD34+, Sca-1+, CD24+ subpopulation, amounting to 0.08% of the total SVF cells, acted as specific adipocyte progenitors in vivo; they were characterised as being able to form fat pad in vivo without preconditioning or seeding onto artificial scaffolds [32]. Adipocyte progenitor cells have multilineage differentiation capabilities, at least in vitro, and have also been found to be involved in the angiogenesis in WAT in times of WAT expansion, remodelling and maintenance in vivo (also see 1.2.) [33].

Mature adipocytes are post-mitotic and in order to store excess energy, WAT reacts to positive available energy balances primarily through boosting the cell hypertrophy of adipocytes, as the hyperplastic potential of WAT in response to excess energy appears to be age-dependant, with its hyperplastic potential decreasing with increasing age [34–36]. Under physiological conditions, a constant turnover of aging adipocytes has been reported in humans with adipocyte life expectancy being about 8 years [35,37]. The maintenance of physiological size has been shown to be crucial for adipocyte physiology; the underlying reasons for these findings, however, are not fully understood [38–40]. Notwithstanding, a limited amount of hyperplasia has been shown to be evoked by the continued overfeeding of adult rats [41]. As, even in this engineered case adipocyte hypertrophy predates hyperplasia, we can assume that adipocyte hyperplasia does not contribute significantly to WAT expansion during physiological fluctuations of WAT mass but that it may play a role in WAT growth during extreme obesity. Although many questions about the underlying causes for the priority of hyperplasia remain, an experiment by Naaz et al. underscored the importance of maintained adipocyte numbers for a healthy metabolic profile. His team was able to be show, in a mouse experiment, that the knock-out of cell cycle inhibitors p21 or p27 caused a shift back to disproportionate adipocyte hyperplasia under a high fat diet; this was, however, accompanied by decreased insulin sensitivity. A double knock-out of p21 and p27 aggravated the effects observed in the single knock-out model and worsened the insulin resistance to the point of glucose intolerance [37]. A relatively recent experiment comparing the adipocyte turnover rates of visceral and subcutaneous adipocytes in an obese setting confirmed the findings, highlighting a decrease in the number of adipocyte precursors attributable to a so far unexplained exhaustion of this cell pool that predates the hypertrophy of mature adipocytes [40]. Thus, hypernutritive states cannot be considered as physiological promotors of WAT hyperplasia in adult individuals. Moreover, whereas in vitro, p21 knockout ASC exhibited spontaneous adipogenesis, this was accompanied by significant apoptosis in adipocytes that had differentiated from these cells, indicating that the environment of adipose tissue in adults is not intrinsically supportive of adipocyte hyperplasia once its development has come to an end [42].

The regulation of adipogenic differentiation is still shrouded in considerable mystery, in particular with little knowledge being available about the physiological coordination of the process during childhood. However, insulin signalling is likely to be crucial for the creation of physiological adipose tissue pre- and postnatally. Epidemiological studies have found that children born with intra-uterine growth restriction are at an increased risk of developing obesity and obesity-related diseases later in life [43]. Based on the observation of inheritable factors increasing the risk of the development of type II diabetes, whose hallmark is insulin resistance of adipocytes, insulin signalling has been investigated during intra-uterine development. Even short disruptions of insulin signalling through insulin receptor

substrate 1 (IRS-1) were observed to give rise to a pronounced metabolically dysregulated obese phenotype [44]. When intra-uterine growth restriction was simulated in an animal experiment setting, key elements of insulin signalling were detected as being post-translationally modified resulting in them having lower active levels. The proteins affected were not the insulin receptor itself but IRS-1 and the catalytic subunit of phosphatidylinositide 3-kinase (PI3K), named p100β; increased adipocyte size and lower total adipocyte numbers resulted, together with a poorer metabolic profile (as measured by insulin, leptin, triacylglcerides and cholesterol levels) than that in a control group. Interestingly, these variances remained stable, even when the animals were allowed to recover from their low birth weight immediately after birth, suggesting that epigenetic changes had taken place [45]. Mechanically, the link between adipocytes and the surrounding ECM (which, for example, is established by ColVI) also plays a role in the adipogenic differentiation of adipocyte precursors: Rigid ECM, which are rich in Col I, have detrimental effects on the adipogenicity of MSC [46,47]. Moreover, MSC under pulling forces show WNT pathway activation whose “canonical” activation involving the frizzled and low-density lipoprotein-related 5 and 6 (LRP5 and LRP6) protein signalling is known to inhibit adipogenesis [48]. A recent review by Hauner et al. further highlights the futility of “easy” solutions to the problem of determining the “right” number of adipocytes. This review notes that specific diets rich in polyunsaturated fatty acids and administered during early childhood with the aim of reducing the risk of the development of obesity did not deliver conclusive results, despite evidence that essential polyunsaturated acids (specifically those with a double bond at the third carbon atom of the chain, i.e. the so-called ω-3 fatty acids) might decrease the hyperplastic potential of growing adipose tissue [49].

Insulin is the key anabolic hormone; it stimulates adipocyte hyperplasia during foetal development and early childhood [45,50,51]. Not only has insulin resistance in adult individuals been shown to be associated with adipocyte hypertrophy, but also adipocyte hypertrophy has been demonstrated to be present in non-obese individuals with impaired insulin sensitivity [40,52]. Following empirical findings on the beneficial effect of insulin on ASC differentiation, it is also contained in most differentiation media for the adipogenic differentiation of ASC in vitro. Many pathways inhibit or stimulate the insulin sensitivity of mature adipocytes. Among the stimulating agents are fibroblast growth factor 21 (FGF21), adiponectin and the drug class of glitazones, which act as PPARγ agonists and are used as potent antidiabetics [53–55]. Incidentally, the glitazone class of antidiabetic drugs have been suggested to exert their antidiabetic effects through the promotion of adipocyte hyperplasia in obese type II diabetic patients [42]. However, as PPARγ is found in many tissues, the unselective stimulation by glitazones use brought with it numerous serious side effects, including a significant increase in the risk of cardiovascular events and bladder cancer, causing a withdrawal rosiglitazone and pioglitazone from European markets. Corticosteroids, hypoxia and agents associated with inflammation (e.g. free fatty

acids and TNF-α), on the other hand, have detrimental effects on insulin sensitivity [56–60]. Decreased insulin sensitivity is a symptom of adipose tissue pathologies (see section 1.1.2. for further information).

The pathways governing the effects of insulin on adipocytes beyond the activation of the ubiquitous insulin receptor signalling are less clear. Insulin increases the amount of energy stored in adipocytes through an increase in the translocation of lipoprotein lipase (LPL) to the cell membranes, increasing the availability of fatty acids, which are then, actively and passively, incorporated into adipocytes. The knowledge that available energy (especially in the form of fatty acids) has a stimulating effect on adipocyte hyperplasia and growth completes the link between insulin and WAT expansion [42].

Nevertheless, the downstream regulation of adipocyte differentiation requires the peroxisome proliferator-activated receptor γ (PPARγ), which has been identified as a key factor for adipogenesis. Whereas PPARγ has two activating domains, one ligand-independent and one ligand-dependent, and existing data shows that activation via the ligand-independent domain suffices to maintain adipogenesis and that ligand-dependent activation appears to be necessary for the initialisation of adipogenesis. Numerous substances of various types (including prostaglandins, polyunsaturated fatty acids, xanthine oxidoreductase, cytoplasmic phospholipase A_2, and others) have been identified as stimulating PPARγ activity through the ligand-dependent binding site. The step in the activation pathway(s) that the aforementioned agents represent remains unclear. A relatively recent paper by Hallenborg et al. [42] proposes the provision of derivates of polyunsaturated fatty acids, especially linoleic and arachidonic acid, as being the driver of PPARγ activation. Hallenborg et al. suggest that the key to PPARγ ligand-dependent domain activation is the release of arachidonic and linoleic acid from lipid membranes. This might be accomplished by cytoplasmic phospholipase A_2 (cPLA2), which has been shown to be upregulated in proliferating cells. In order to be activated, cPLA2 needs to be phosphorylated by p22 and p44 map kinases. These kinases are activated by elevated CAMP levels. The transformation of free arachidonic and linoleic acids into hepoxilin analogues capable of stimulation the ligand-dependent domain of PPARγ might include CCAAT / enhancer binding protein (C/EBP) transcription factor signalling, which has been shown to induce xanthine oxidoreductase (XOR). With XOR increasing the availability of reactive oxygen species, this could lead to the auto-oxidation of polyunsaturated fatty acids, which, in turn, are substrates for epidermal type 3 lipooxygenase (eLOX3). According to Hallenborg et al., eLOX3 would then convert the oxidised lipids into hepoxilin analogons, which are ligands of the ligand-dependent domain of PPARγ [42]. This suggests that, physiologically, WAT reacts to excess energy similar to the way in which myocytes react to physical training, with relatively low numbers of adipocytes being capable of maintaining energy homeostasis. As the number of adipocytes is set during childhood, insulin resistance and its

consequences would arise when the lipid storage system is stretched beyond its physiological limits, which are determined by the hypertrophic capability of the adipocytes. The pathway explained in this

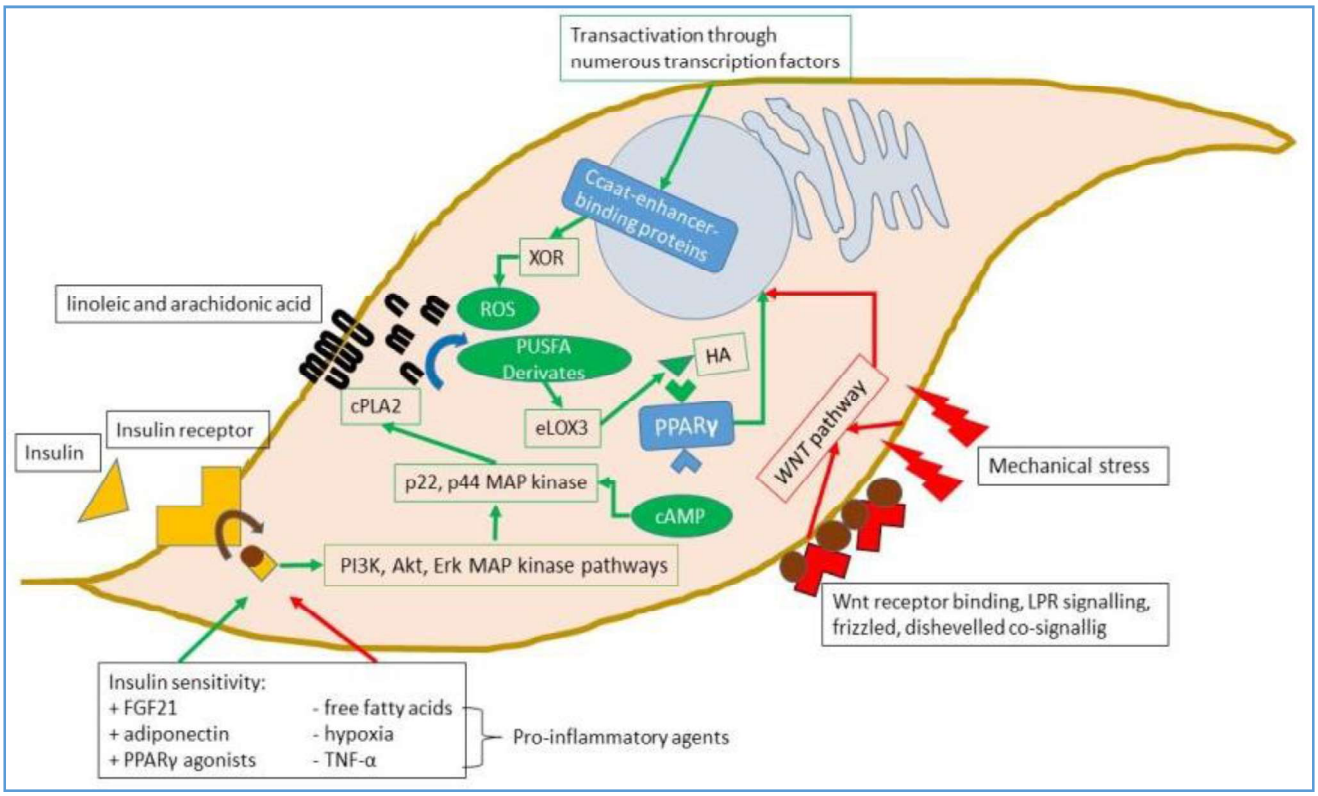

Figure 2: The pathway involved in adipogenesis (according to the sources mentioned in the above paragraph): Phosphorylation of insulin receptor substrate 1 (IRS1, small yellow cube, phosphate brown circle) is the intracellular starting point following the binding of insulin at the insulin receptor. Insulin sensitivity can be influenced positively (green arrow) and negatively (red arrow) by the factors mentioned and by others. Insulin signaling stimulates the PI3K, Akt, Erk and MAP kinase pathways, which eventually cause in increase in p22 and p44 MAP kinase, which is activated in the presence of cAMP, a signal of energy saturation. p22 and p44 activate cytoplasmic phospholipase A2 (cPLA2), which releases linoleic and arachidonic acid from double-layer lipid membranes. Ccaat-enhancer binding protein is a transactivated transcriptional factor that increases xanthine oxidoreductase (XOR), which leads to an increase in reactive oxygen species (ROS) allowing for an autooxidation of the fatty acids released by cPLA2. The resulting poly-unsaturated fatty acids (PUFA) derivates are a substrate of epidermal type 3 lipooxygenase, which converts them into hepoxilin analogons (HA). HA are potent activators of the ligand-dependent binding site of PPARγ. Binding of this site is an important promotor of adipogenesis. Also included in this representation is the downregulation of adipogenesis through WNT pathway signalling, which can be activated through "canonical" binding of the low-density lipoprotein receptor with WNT, frizzled and dishevelled proteins acting as co-factors or through mechanical stress on the ASC.

paragraph is summarised in figure 2.

In 1950, the first genetic mutation causing type II diabetes and a morbidly obese phenotype in house mice was described by Ingalls et al. and named the *obese (ob)* mutation [61]. However, it was not until 1994 that Zhang et al. could demonstrate that the transcriptional product of the *ob* gene is a secreted protein that is not only found in rodents, but also in a similar form in humans [62]. This secreted protein would later be named *leptin*. These findings immediately made WAT the largest endocrine organ by volume, with the regulation of energy homeostasis (i.e. controlling hunger) being heavily reliant on hormones secreted by WAT. Apart from the aforementioned leptin, adiponectin also plays a crucial

role in energy homeostasis. These hormones have, since their discovery, been coined “adipokines”, a term that is used to describe hormonally active substances secreted by adipose tissue. Adiponectin and leptin are the best studied adipokines and are secreted by adipocytes dependent on the body’s energy balance, with pathologies of fat tissue being related to a multitude of endocrine disorders (see 1.1.2.) [63–65]. They can be thought of as partial antagonists, both with regard to their function regulating energy homeostasis and to their blood plasma levels at times of fasting and food intake. Adiponectin promotes intracellular lipid oxidation, increases adipocyte insulin sensitivity and acts as a promotor of hunger in the arcuate hypothalamus. Its plasma levels are the highest physiologically in times of fasting, being elevated as a sign of the underlying pathology in cachectic and anorexic patients, and lowest in obese patients [66,55]. Accordingly, adiponectin levels have been shown to be inversely correlated not only to body-mass index (BMI), but also to insulin-resistance / type 2 diabetes, CRP and TNF-α, all well-studied indicators of the inflammatory response [67,57,68,69]. However, adiponectin must not be underestimated as a mere surrogate marker of a dysregulated metabolic state, as numerous intrinsic anti-inflammatory properties of adiponectin have been demonstrated. Hypoadiponectinaemia has been recognised as an independent risk factor for the development of hypertensive disease [70]. Furthermore, adiponectin is considered as a protective factor against atherosclerosis and associated conditions. It inhibits the release of reactive oxygen species (ROS), which are hallmarks of an inflamed environment such as that in atherosclerosis, and in the vascular endothelium irrespective of ROS - triggers such as oxidised low-density lipoprotein [71]. Moreover, adiponectin directly increases the release of nitrogen monoxide (NO) in endothelial cells and inhibits the proliferation of smooth muscle cells (through oligomerisation and the inactivation of smooth muscle cell growth factors with adiponectin molecules), thus improving blood circulation and preventing blood vessel stenosis [72,73]. With regards to adipose tissue pathology (see also 1.1.2.) the direct interactions of adiponectin with macrophages deserve special attention. First, pro-inflammatory proteins such as TNF-α or interleukin 6 (IL-6) form complexes with adiponectin, thus decreasing their availability for leucocyte activation [74]. Second, macrophages express adiponectin receptors 1 and 2 (ADIPOR 1 and ADIPOR 2), whereby two purportedly contradictory effects of adiponectin exposure have been demonstrated. Adiponectin increases the secretion of IL-6 and TNF-α by macrophages through the activation of the nuclear factor kappa B (NFκB) and ERK1/2 (extracellular regulated kinase 1/2) pathways following ADIPOR signalling. However, this is only true for short-term administration (approximately 30 minutes) of adiponectin [75]. Prolonged exposure, on the other hand, causes a desensitisation of macrophages towards pro inflammatory stimuli and even stimulates the expression of anti-inflammatory IL-10 and tissue inhibitor of matrix metalloproteases (TIMP) in macrophages [75–77]. The molecular basis for this observation is not fully understood, although the anti-atherosclerotic effects of adiponectin are obvious. With regards to energy homeostasis, adiponectin promotes fatty

acid oxidation in peripheral tissues through the ADIPOR 1 mediated activation of AMPK (adenosine monophosphate kinase) and through an increase in PPARα (peroxisome proliferator-activated receptor) ligand availability in myocytes [68]. AMPK is considered to be a key peptide of energy homeostasis, curbing energy storage by gluconeogenesis, lipogenesis and lipolysis in adipocytes while facilitating energy expenditure and a build-up of energy reserves in striated myocytes [78]. In adipocytes, the AMPK-mediated inhibition of lipolysis is achieved by the phosphorylation of the protein perilipin, reducing access of the lipid-droplet-stored TAG by lipases (see also below) [79]. Adiponectin additionally promotes hepatic ketogenesis through adiponectin receptor 2 (ADIPOR 2) binding predominantly expressed in the liver and also resulting in AMPK and PPARα activation [69]. All of the above findings lead to the conclusion that adiponectin is an adipokine whose physiological role appears to prime the body for physical exercise. These effects are mainly achieved by boosting the provision of energy to the musculature while curbing long-term energy storage.

Leptin, on the other hand, is widely regarded as a hormone of energy saturation. In the central nervous system (CNS), it decreases appetite and, indirectly, sympathetic tone through leptin receptor (LEPR) signalling predominantly in the arcuate nucleus and to a lesser extent in the ventromedial, dorsomedial and other nuclei of the hypothalamus [80,81]. For a long time, leptin was thought of as an antagonist to adiponectin and was suggested to have a pro-inflammatory nature, specifically through its ability to increase oxidative stress through an increase in ROS and a secretion of pro-inflammatory cytokines [82–84]. At transcriptional levels, activated protein kinase C (PKC) is the mediator for the leptin-induced upregulation of TNF-α and ROS via the MAP pathway [85]. Only recently has evidence of the anti-inflammatory properties of leptin emerged, whereby leptin has been shown to contributes to a sympathetic upregulation of cyclic adenosine monophosphate (CAMP) in WAT resident macrophages. Elevated CAMP levels in macrophages leads to an activation of histone deacetylase HDAC4 through dephosphorisation attributable to the inhibition of the phosphorylation of salt-dependent kinase activity, which, in turn downregulates, the pro-inflammatory NFκB pathway. Additionally, elevated macrophage CAMP levels act as a stimulus on the camp-responsive transcriptional co-activator (CRTC) family and the camp-responsive element binding protein (CREB), which, among a multitude of other functions, increases the secretion of the anti-inflammatory IL-10 in macrophages [86,87]. Like its counterpart adiponectin, leptin is expressed and secreted by adipocytes but, unlike its antagonist, its plasma levels positively correlate with BMI, adipocyte size and adipocyte number. A gender difference also exists, with women having higher leptin levels then men (normalised to body fat mass) [88]. Elevated leptin levels lead to increased glucose uptake in the musculature, decreased insulin sensitivity in WAT and decreased pancreatic insulin production [89,90]. Simultaneously, elevated leptin levels trigger a vagal-nerve-mediated decrease in hepatic gluconeogenesis [90]. Transgenic leptin-deficient mice exhibit early-onset extreme obesity, as a decisive negative feedback mechanism for hunger and

appetite control is disabled [91]. At least one documented case has been reported of a young human patient with functionally inactive leptin, presenting with symptoms similar to those observed in animal models [92]. Additionally, leptin appears to have a centrally inhibitory effect on pancreatic insulin secretion.

Lipocalin 2 (LCN2), also known as neutrophil gelatinase associated lipocalin, is another relatively recently discovered adipokine, being only first described in 2007 by Yan et al. [93]. The limited existing data about LCN2 effects is incomplete and suggests both pro- and anti-inflammatory effects. TNF-α and dexamethasone were the first agents shown to stimulate LNC2 transcription, indicating LCN2 release under inflamed conditions. Apart from its secretion in inflamed environments, LCN2 decreases insulin sensitivity in WAT and is associated with elevated MMP 9 activity (because of a supposed protective effect of LCN2) facilitating macrophage migration into WAT. However, it also affects macrophages, stimulating an anti-inflammatory response [94,93].

Neuropeptide Y (NPY) is not an adipokine *sensu stricto* as, apart from adipocytes, is also identically produced by the arcuate and paraventricular nuclei of the hypothalamus. Centrally produced NPY is released under (physical and psychological) stress conditions in conjunction with norepinephrine from sympathetic nerve endings, which also permeate WAT. NPY exhibits complex central effects, such as regulating appetite, but low NPY levels have also been associated with anxiety and post-traumatic stress disorder. However, NPY has also been shown to be expressed by adipocytes in times of proliferation and excess energy availability / hypernutrition, making it an adipokine. It has been shown to promote the differentiation of ASC into adipocytes and the expansion of stored fat mass in visceral WAT. Out of the five known and identified NPY receptors, four different NPY receptors have been identified in humans; as yet, not all have had their specific functions identified. The receptors found in humans act as g-protein coupled receptors and are named Y_1, Y_2, Y_4 and Y_5, with Y_1 and Y_2 being mentioned in the literature in conjunction with adipocyte differentiation and reactions to stimuli. The Y_1 receptor has been identified as the driving force behind adipogenic ASC differentiation [95]. In contrast, adipocyte response to stress and sympathetic stimuli is mediated by a corticosteroid-triggered upregulation of the Y_2 receptor [96].

The energy homeostasis of adipocytes is tightly regulated. As in all cell-types, glucose is the main source of energy for adipocytes in which two types of glucose transporters are found. Mature adipocytes (and striated myocytes) react to stimuli indicative of a positive energy balance by translocating (and increasing the rate of synthesis of) glucose transporter GLUT 4 receptors to their cell membrane, thereby allowing rapid passive glucose uptake into the adipocyte. Insulin is the main stimulus for this process. After binding the insulin receptor, insulin receptor substrate is recruited and binds the insulin receptor. This activates a cascade of kinases (phosphatidylinositol-3 kinase and

protein kinase B) eventually leading to an inhibition of TBC1D4 (TBC1 domain family member 4) mediated guanosine triphosphate (GTP) hydrolysis [97]. Elevated GTP levels then prevent the inhibition of Rab proteins and monomeric G proteins, which are necessary for the integration of GLUT 4 into the cell membrane [98]. In contrast, baseline energy expenditure is covered by constitutively expressed glucose transporter GLUT 1 mediated glucose influx, GLUT 1 being a transmembrane protein allowing for the facilitated diffusion of glucose. With insulin being the prime anabolic hormone, insulin signalling also activates de-novo lipogenesis by the enzyme fatty acid synthase, which allows surplus intracellular glucose in the form of acetyl-CoA to be used to synthesise fatty acids. Nevertheless, only 2-4% of glucose uptake is utilised by adipocytes; the hepatic and adipocytic de-novo synthesis of fatty acids amounts to only 1-2 g / day, whereas 60-80 g / day of triacylglycerides (TAG) are adsorbed daily through the intestines and, following a hepatic first pass, are distributed in the form of VLDL (very low density lipoproteins) or as albumin-bound non-esterised fatty acids (NEFA) [79]. The extracellular lipase lipoprotein lipase (LPL) is synthesised by adipocytes (and by striated myocytes) and hydrolyses TAG into two fatty acids and monoaclyglyceride; hepatically synthesised apoprotein C-II found on chylomicrons and VLDL is an essential co-factor for this reaction. Thus, VLDL and chylomicrons are the primary means of transport of fatty acids for the use and / or storage in peripheral tissues such as WAT. Of note, as the point of action of LPL is the endothelial epithelium where it is anchored to endothelial cell membranes, a transfer from synthesising adipocytes (and myocytes) is necessitated [99]. A glycosylphosphatidylinositol anchored glycoprotein of lymphocyte antigen 6 family, GPIHBP1, synthesised by endothelial cells, has been shown to be responsible for the transcytosis of LPL through endothelial cells and for anchoring LPL in the luminal cell membranes of these cells [100]. In this context, the ECM again plays an important role. This was revealed by Bishop et al. who were able to show that collagen XVIII (Col XVIII) is necessary for the proper translocation of LPL to endothelial cells and who speculated that the thickness of the endothelial cell basal lamina, which is influenced by Col XVIII, played a role in LPL migration [101]. Several isoforms of this protein exist, with adipose tissue LPL activation being insulin-dependent [102]. Moreover, prolonged hypernutrition increases the availability of LPL in the capillaries of adipose tissue [103]. In addition to passive diffusion, a specialised transport protein, fatty acid translocase (FAT, also known as CD36), which is a class B scavenger protein, mediates the uptake of fatty acids into adipocytes [104]. Again, insulin acts as a stimulus for FAT; conversely, pro-inflammatory cytokines such as TNF-α effectively inhibit adipocytic FAT-mediated fatty acid uptake [105]. Once fatty acids have been incorporated into adipocytes, they are re-esterised into TAG and stored in the lipid droplet. De-novo lipogenesis is achieved by promoting the dephosphorylation, and thereby the activation, of the pacemaker enzyme of lipogenesis, namely acetyl-CoA-carboxylase. Newly produced fatty acids are also stored as TAG in the lipid droplet of adipocytes, which have been shown to regulate triacylglyceride storage primarily by means of

expanding or decreasing the volume of their respective lipid droplet. In times of excess energy / triacylglyceride availability, the volume of stored lipid can quadruple compared with normal levels.

Fasting, hypoglycaemia and exercise resulting in elevated levels of glucagon, together with elevated adrenalin levels, promote lipolysis. Apart from circulating hormones that mediate the release of energy from adipocytic storage, WAT is influenced by the sympathetic nervous system. The main hormones mediating catabolic effects are glucagon and catecholamines. Sympathetic signalling inhibits the hyperplasia of and facilitates the provision of energy from adipocytes through increased lipolysis [106]. Glucagon acts through its namesake glucagon receptor, with insulin acting via the β2-adrenoreceptor. Both are g-protein coupled receptors that activate the enzyme adenylate cyclase, resulting in elevated intracellular levels of CAMP. During lipolysis, TAG undergo three enzymatic reactions resulting in three fatty acids and one glycerol molecule. However, under non-catabolic conditions, the surface of the lipid droplet is covered in perilipin, protecting it from spontaneous hydrolysis by ubiquitous intracellular lipases and hydrolases. Only when phosphorylated by activated PKA, can perilipin disassociate from the lipid droplet and allow the mobilisation of fat reserves. This phosphorylation is the actual mechanism by which β-adrenergic stimulation enhances lipolysis. The aforementioned PKA is activated by elevated CAMP levels, which at catabolic states, are the result of the β-adrenergic activation of adenylate cyclase [79]. Hydrolysis of the fatty acids is catalysed by adipocyte specific triacylglycerol lipase (ATGL), hormone-sensitive lipase (HSL) and, finally, monoglycerol lipase (MGL). ATGL and HSL are capable of hydrolysing the first fatty acid from a TAG, namely the reaction-speed-determining step of enzymatic lipolysis following perilipin dissociation from the lipid droplet. The second fatty acid is hydrolysed by HSL and the third by MGL. As implied by its name, HSL is under the hormonal control of insulin and catecholamines, with insulin inhibiting and catecholamines promoting lipolysis. Neuropeptide Y (NPY), a peptide released by the paraventricular and arcuate hypothalamus under stress conditions, also inhibits lipolysis. Apart from fatty acids, glycerol is an end product of lipolysis; it is a metabolite that cannot be utilised by adipocytes becaause of their lack of glycerol kinase. Via a signalling cascade involving the activation of protein kinase A (PKA), intracellular Ca^{2+} increases as membrane calcium channels are activated by phosphorylation.

1.1.2. Adipose Tissue Pathology

WAT is more than just an organ of energy storage. Metabolic disorders such as type 2 diabetes or obesity are correlated with a low-grade chronic inflammatory process that occurs within WAT and that cause an increase in ECM proteins, leucocyte migration and insulin resistance. Adipocyte hypertrophy appears to be more detrimental to the physiological state of WAT than does hyperplasia (although the actual amount of adipose tissue hyperplasia in adult humans is likely to be minimal [35]), with the underlying principles of this observation not yet being understood (compare 1.1.1.). In an experiment

conducted on obese women, Hoffstedt et al. were able to show that visceral fat cell size is positively correlated with plasma levels of cholesterol, low-density lipoprotein, triacylglycerides and apolipoprotein B, which are all indicators of metabolic syndrome [107,108], but is uncorrelated with BMI or fat distribution [7]. In addition, subcutaneous adipocyte size was found to be correlated with insulin resistance to a higher degree than visceral adipocyte size [7]. The altered adipose tissue microenvironment may predate the onset of metabolic diseases as a comparative study has found that hallmarks of WAT inflammation (TNF-α secretion and fibrosis) and adipocyte hypertrophy are present even in otherwise healthy first-degree relatives of patients with type II diabetes [38]. In the same group of individuals, gene assays of adipocytes have furthermore revealed decreased levels of messenger RNA (mRNA) of GLUT4 and adiponectin [52]. The aforementioned inflammation is maintained by constant hypoxia, which cannot be compensated for by adequate neovasculogenesis [109]. The size of adipocytes, which can grow up to 200 µm in diameter under hypertrophic conditions, has been suggested to be sufficient to cause an intracellular hypoxic state, this possibly being a starting point for the vicious circle of inflammation and aggravating hypoxia [60]. The finding of increased post-prandial blood flow in the adipose tissue of obese individuals hints at an insufficient counter regulatory measure aimed at alleviating the hypoxic state [110]. As early as 1993, Hotamisligil et al. could show that TNF-α levels are increased in animal models of obesity and diabetes, and that TNF-α is secreted by adipose tissue resulting in insulin resistance [57]. In 2003, Hotamisligil went as far as suggesting that actual inflammation (as opposed to a dysregulated inflammatory response) of adipose tissue is a hallmark of metabolic diseases [111]. In 2009, Khan et al. coined the term "adipose tissue fibrosis" when they first demonstrated "*general upregulation of several extracellular matrix components in adipose tissue in the diabetic state, therefore implicating "adipose tissue fibrosis" as a hallmark of metabolically challenged adipocytes*" [25]. Elevated levels of collagen VI, a collagen subtype characteristic of adipose tissue [112], are found in patients suffering from insulin resistance and obesity [34]; moreover, an increase in ECM might be responsible for the hypoxic conditions that maintain a state of chronic adipose tissue inflammation by increasing the distance between capillaries and adipocytes [109]. Elevated levels of collagen V and less functional elastin further add to hypoxia by acting as a barrier to sufficient capillary vasculogenesis [17]. As hypoxic ASC have been shown to secrete proangiogenic HIF-1α and VEGF [113,114], the presence of dysfunctional ECM proteins may also contribute to explaining the failure of proangiogenic factors secreted by hypoxic ASC to promote adequate vasculogenesis in obese/insulin-resistant subjects as opposed to their success in doing so in healthy subjects and in experiments involving the 3T3-L1 cell-line [109,17]. The idea of a dysregulation of the response to hypoxia being fundamental to WAT inflammation is further supported by the finding that the overexpression of HIF-1α triggers adipose tissue fibrosis in vitro [60]. This hypoxia and the dysregulation of ECM protein synthesis are accompanied by a similarly dysregulated response of

cytokines and inflammatory cell activation and migration. Inflammatory cytokines (especially TNF-α) are released in inflamed WAT and contribute, by adding to the decrease of partial O_2 pressure (this being a hallmark of inflammation), to hypoxic stress, thus posing an additional cause of insulin resistance under these conditions [115]. However, these cytokines are not secreted by ASC or mature adipocytes. Instead, immune cells such as macrophages, dendritic cells and T-lymphocytes maintain WAT inflammation and can be found in increased numbers in inflamed WAT compared with healthy WAT [116,117,34,118]. In contrast, the aforementioned NPY, is expressed (as quantified by elevated mRNA levels) by adipocytes in response to co-stimulation with corticosteroids. This NPY, which is identical to the centrally expressed NPY, acts in an autocrine and paracrine manner in WAT, stimulating adipocytes through the Y_2 g-protein coupled receptor. Stimulation of the Y_2 receptor growth and pathological hyperplasia in adipocytes lead to an obese phenotype in animal models and humans. Furthermore, macrophage invasion is stimulated, as is WAT angiogenesis [96]. These findings lead to the proposal of a link between the psyche and stress-triggered metabolic disorders established by centrally and peripherally produced NPY, as its appetite-enhancing effects aggravate the oxidative stress already present in metabolically challenged WAT. Macrophages are the key player in WAT inflammation. Not only are WAT resident macrophages activated by hypoxia and cell-cell interactions in inflamed tissues, but also circulating macrophages home into inflamed WAT. Both M1 and M2 macrophages are present in inflamed WAT. In obese subjects, the percentage of M2 macrophages is elevated [117,34]. These findings are interesting, as M1 macrophages are considered to be "pro-inflammatory" and release TNF-α and IL-6, whereas M2 "anti-inflammatory" macrophages are thought to be associated with tissue remodelling and wound healing. Thus, a dysbalance of the two macrophage subtypes is probably to blame for the maintenance of inflammation. The number of dendritic cells is also elevated in inflamed adipose tissue [119,116]. Of note, as opposed to adipose tissue resident macrophages (CD11b+, F4/40+), macrophages freshly recruited to inflamed adipose tissue macrophages express the traditional dendritic cell marker CD11c (in addition to the classic macrophage markers CD11b and F4/80) [120]. Circulating CD11c+ macrophages have been shown to be recruited by CD8+ cytotoxic T-cells, which also increase in frequency in inflamed adipose tissue [118]. Notwithstanding this observation, the number of CD103+ dendritic cells, which are known to promote the differentiation of anti-inflammatory regulator T cells, is decreased in inflamed WAT, whereas the dendritic cells isolated from inflamed WAT have been shown to promote the differentiation of pro-inflammatory IL-17-expressing T-cells in vitro [116]. This is important as CD4+ Foxp3+ regulatory T-cells (Tregs), which are physiologically found in higher numbers in healthy WAT than in any other tissue, appear to be pivotal in preventing an uncontrolled immune reaction in WAT [121]. Lymphocytes also play a role in WAT inflammation. The number of IFN-μ-expressing CD4+ Th1-cells is elevated in obese subjects, whereas Th2-cells, which promote a shift from M1 to M2

macrophage polarisation appear with decreased frequency [122,123]. Available studies remain inconsistent concerning the principles underlying the adaptive response of the immune system to WAT inflammation but agree that (1) T-cell functioning is shifted towards an escalating immune reaction and (2) T-cell receptor patterns in WAT show distinct differences from those observed in other tissues [122,123]. The aforementioned CD8+ cytotoxic T-cells also appear with increased frequency in inflamed WAT and the rise in CD8+ T-cell numbers predates the rise in macrophage numbers. CD8+ T-cells are outstanding in that their proliferation can be triggered by co-culture with adipocytes under oxidative stress, thereby offering another possible entry to the circle of inflammation, hypoxia and fibrosis of WAT [118]. Activated natural killer cells (NK cells) are present in inflamed WAT and, whereas their role attributable to the ability of their T-cell receptors to recognise and bind lipid antigens is interesting, results on their effects on inflamed WAT are inconsistent [124]. Consistent with the association of granulocytes with bacterial infections, they have not been found to play an important role in the maintenance of chronic WAT inflammation. Likewise, mast cells and basophile granulocytes are found in inflamed WAT but no evidence as yet exists of an effective contribution to the chronic inflammation process [125]. The chronic inflammation of WAT can be concluded to be a hallmark and possibly the cause for a number of pathological conditions. The starting points of this circle of hypoxia, dysregulated ECM proliferation and inflammatory response remain unclear. However, an epigenetic "first hit" caused by prolonged overfeeding might increase a susceptibility to later adipose tissue fibrosis [126]. Strong evidence has been presented that epigenetic changes (especially those bringing with them an evolutionary advantage in times of famine) are inheritable and pose a risk for the development of diabetes and / or metabolic syndrome in later generations not suffering from food shortages [127–130]. Jufvas et al. have demonstrated that such phenotypic changes are likely to stem from alterations in histone methylation. This knowledge necessitates that genetic predisposition should be added to the list of possible causes of WAT inflammation [131]. Furthermore, prolonged high-fat diets have been shown to increase TNF-α levels and subsequently to cause adipose tissue fibrosis by means of elevated expression of TACE (TNF-α converting enzyme), suggesting a negative effect of overnutrition per se [132]. Moreover, adipocyte necrosis rates increase during WAT expansion, possibly causing an influx of macrophages that might stimulate a pathological immune response [133]. In conclusion, Evidence exists for the assumption that adipose tissue inflammation can be evoked by a number of factors, both inheritable and acquired. The common result, however, is adipose tissue fibrosis, which greatly impairs WAT functioning.

1.2. Adipocyte Derived Stem Cells

The adipocyte derived stem cell (ASC) is the progenitor cell of the adipocyte. Morphologically, it is indistinguishable from fibrocytes, with whom it shares the similarity of being found perivascularly in

the SVF of WAT. With WAT having a turnover rate of 10 % of adipocytes, even under non-expanding conditions (i.e. in adults as mentioned in 1.1.1.), and with adipocytes not being mitotically active, the task of rejuvenation falls to a pool of progenitor cells. Whether these preadipocytes are committed ASC or an entity of their own remains unclear; nonetheless, research has been able to characterise ASC and to demonstrate signalling pathways involved in adipogenic differentiation and the regulation of WAT turnover. Being derived from the mesenchymal lineage, ASCs are characterised as being plastic-adherent, morphologically fibrocyte-like and multipotent, as they have the capacity to differentiate into adipocytes, oesteoblasts and chondrocytes in vitro. Furthermore, the differentiation capacity of those cells can be extended over all three germ layers depending on the specific differentiation media [134]. Phenotypically, among others, MSC show the surface expression of CD73, CD90 and CD29, while being negative for CD34, CD14, CD31 and HLL-DR [135]. Knowledge about ASC is expanding rapidly. However, the term "ASC" is used inconsistently in the literature. Unsorted SVF cells have been named ASC, just like distinct SVF subpopulations characterised through surface marker / cluster of differentiation (CD) analysis. Furthermore, a differentiation between adipocyte progenitor cells and committed preadipocytes can be made. In this definition, adipocyte progenitor cells are bound for adipogenic differentiation but will not differentiate without other stimuli, whereas preadipocytes are committed cells about to undergo adipogenic differentiation. *Sensu stricto* ASC are a subgroup of the SVF, distinguished by being CD166+, CD31-, CD45- and von-Willebrand-factor (vWF) negative. This selector removes endothelial cells (CD31-, vWF+) and cells descendent from the haematopoietic stem cells (CD45+) from the pool of SVF cells, while including, in the broadest sense, other cells descending from MSC (CD166+) [136]. Whereas ASC isolated from lipoaspirate samples or otherwise are pluripotent SVF cells, those committed to the adipocyte lineage, i.e. true adipocyte progenitor cells, appear to be CD31-, CD105-, CD140a+ and CD140b+. A surface antigen configuration that remains preserved even in mature adipocytes is CD31- and CD105-. Interestingly, ASC not committed to adipocyte differentiation are CD105+, creating the notion of CD31-, CD105+, CD140a+ cells being actual pluripotent ASC, and CD31-, CD105-, CD140a- cells belonging to the distinct entity of adipocyte progenitor cells. However, with conflicting findings about the expression of these surface antigens at various levels of differentiation, an assumption of a continuity in adipogenic differentiation from uncommitted CD105+ ASC to committed CD105- ASC might be fairer, since the absence of CD105 and CD140a expression is the only hallmark of the "preadipocyte" cell type. A Lin-, CD29+, Sca-1+, CD24+ subpopulation, amounting to 0.08% of SVF cells, has subsequently been shown to act as the last cell pool at the progenitor cell level before division into the post-mitotic mature adipocyte in a self-regenerative mitosis step [32]. Being evolutionary close to the multipotent MSC, ASC (or certain subpopulations linked to the various stages of adipocyte commitment) have demonstrated impressive pluripotent differentiation abilities in vitro and, in part, in vivo. Beyond the formation of adipose tissue

in vitro and in vivo (possible without prior induction when seeded on three dimensional scaffolds or following an induction step leading to engraftment), the osteogenic differentiation has been demonstrated in the presence of exogenous or endogenous (following trauma) BMP (bone morphogenetic protein) 2 or 4 (among the main promotors of bone growth and healing). Chondrocytic differentiation has also been shown in in-vitro experiments. ASC potential for striated skeletal and cardiac myocyte differentiation must be questioned. Whereas experiments involving un-purified SVF cells have shown the incorporation of SVF cells into damaged myofibrils, these were conducted by using CD34- cells, which do not appear to have maintained their potential for adipogenic differentiation. In contrast to these findings, CD140b+ ASC can differentiate into smooth muscle cells with α-smooth muscle actin (SM22α) expression when co-cultured with endothelial cells in vitro [137]. ASC differentiation into endothelial cells has been reported in vitro and in vivo. In vitro, ASC have demonstrated their ability to form tubules, to upregulate the endothelial cell progenitor marker CD31 (PECAM 1 / Platelet endothelial cell adhesion molecule) and CD309 (VEGFR-2 / vascular endothelial growth factor receptor 2) and to secrete VEGF, when seeded in a methylcellulose scaffold [138] [139]. In vivo, ASC have been shown to enhance healing-associated angiogenesis by releasing VEGF, by differentiation into endothelial cells and by rearranging existing endothelial cells [140]. Furthermore, and of therapeutic interest, CD105- ASC exhibit the potential for differentiation into hepatocytes in vitro and in vivo. Interestingly, in vivo hepatocytic engraftment is possible without preconditioning when ASC are implanted into injured livers. However, whether the reconstitution of liver function is achieved by the proliferation of ASC-turned-hepatocytes or by the fusion of ASC with injured pre-existing hepatocytes is not fully understood. Following pre-conditioning and artificial transfection to enable them to express Pdx1 (Pancreatic and duodenal homeobox 1, a promotor of pancreas development), ASC were also able to be grafted into pancreatic tissue and to restore pancreas function in diabetic rodents. However, as the latter application required extensive pre-conditioning and genetic modifications, ASC are unlikely to be naturally able to differentiate into pancreatic tissue. Calcium-activated potassium channels also play a role in the adipogenic differentiation of ASC [141]. Two K^+ channels have been found in preadipocytes. An inhibitory (repolarising) Ca^{2+}-triggered outward K^+ current (I_{KCa}) was found in more than 90% of preadipocytes and a 4-aminopyridine-sensitive transient outward K^+ channel (I_{to}) in just more than one third of preadipocytes. Evidence of their contribution to differentiation arose from the finding that selective blockade of these channels significantly reduced adipogenic differentiation in these cells [141].

The origin of an ASC influences its adipogenicity. When the two main pools of adipose tissue and thus of ASC, namely the visceral and subcutaneous adipose tissues, were compared, a significantly higher in vitro adipogenicity was found in ASC originating from subcutaneous fat depots [5]. Throughout differentiation, the expression of genes indicating adipogenesis, such as PPARμ during early

differentiation, and fatty acid binding protein 4 (FABP4) and adiponectin as markers of late differentiation was found to be upregulated in ASC from subcutaneous biopsies when compared with those of visceral origin. Although many questions about the regulation of adipogenesis remain unsolved, adipogenic commitment has been shown to be concomitant with the downregulation of CD105 and CD140a, thereby removing inhibitors of adipogenesis. CD105, also called *endoglin*, a peptide representing a part of the TGF-β (transforming growth factor beta) receptor complex. CD140a is another name for PDGFR-α (platelet derived growth factor alpha). Both TGF-β and PDGF signalling is known to inhibit adipogenesis. TGF-β acts through the phosphorylation and activation of Smad3, which activates downstream gene transcription by signal transduction from extracellular TGF-β ligands to the cell nucleus, whereas PDGFR-α signalling downregulates PPARμ (peroxisome proliferator-activated receptor gamma / glitazone receptor), with PPAR ligands such as polyunsaturated fatty acids being known promotors of adipogenesis. Another central element of adipocyte differentiation and adipocyte metabolism is the transcriptional factor PPARγ, although its physiological ligand(s) remain(s) unknown [142]. BMP 2 and 4 promote the adipogenic differentiation of ASC. These hormones, also members of the TGF family of hormones, bind type 1a and 2 BMP receptors and activate Smad 1, 5, and 8 through phosphorylation. Phosphorylated Smads 1, 5 and 8 form active heterodimers with Smad 4, with the Smad 1/4 complex promoting the transcription of the PPARμ gene through activation of zinc finger proteins (Zfp). Moreover Smad 1/4 complexes upregulate the transcription of lysyl oxidase (LOX), an enzyme crucial for adipocyte differentiation through ECM remodelling [143]. NPY has also been shown to stimulate adipogenic differentiation in vivo. Y_1 receptor signalling induces the differentiation of ASC, whereas NPY exhibits a six-fold increase in messenger RNA concentration during the adipogenic differentiation of ASC. Not only does this underline the endocrine properties of adipose tissue, but it also suggests an auto- and paracrine aspect of ASC-secreted NPY under physiological conditions [95].

1.3. Experiment Aim

In theory, adipose tissue would make an excellent filling material for soft tissue defects. In most patients, it is abundantly available, easily obtained through minimally invasive techniques, can be handled without specialised surgical equipment and does not provoke rejection because of it proposedly being an autologous transplant. Moreover, subcutaneous adipose tissue exhibits excellent regenerative potential. However, the still unpredictable resorption rates of the transplanted fat remain a major factor of uncertainty linked to this method. For the practicing physician, lack of knowledge of the definite volume of the augmented tissue often restricts the use of grafted adipose tissue, especially in delicate operation areas, such as vocal fold augmentation following recurrens nerve paresis or when repeated correctional operations are undesirable or unfeasible. The individual resorption of

transplanted adipose tissue is apparently triggered and regulated by a multitude of factors. These include some that can by influenced by the surgeon. However, these techniques have the highest impact when larger volumes of adipose tissue are to be transplanted (mostly in plastic and aesthetic surgery). Among the most important physician-dependent factors for graft survival rate, which can also be easily assessed, evaluated and addressed, is the fan-shaped grafting technique when higher graft volumes are required, the injection of the lipograft while pulling back the cannula and the use of suitable (blunt-tipped) cannulas. Moreover, centrifugation of the aspirated fat prior to reinjection in order to separate it from the possibly cytotoxic tumescence solution is speculated to result in a higher "concentrated" lipograft and is a semi-experimental approach that may contribute to improved results [144]. Nevertheless, as a significantly varying resorption rate between patients has been observed by skilled surgeons conducting operations involving adipose tissue transplantation routinely, the existence of factors influencing a patient's individual resorption rate independently of the surgeon's skill and technique must be assumed [145,146]. Unfortunately, these factors are neither readily assessed, nor analysed and are the least predictable.

In the experiments reported here, an assessment of possible inter-individual differences between human-patient-obtained subcutaneous ASC as contained within their surrounding SVF has been attempted with regard to parameters that might reflect the viability and ability of the cells for engraftment. An in-vitro approach was chosen in order to be able to focus on ASC behaviour in an environment free of stressors (hypoxic, inflammatory, nutritive or situative as in animal experiments) and as standardised as possible, with the goal of only highlighting possible intrinsic inter-individual ASC differences. Whereas many experiments investigating the role of ASC in soft tissue transplant engraftment and healing processes have been conducted in animal studies, these in vivo studies, while giving much insight into engraftment and wound healing, were undertaken in an inflamed and / or hypoxic environment. This appears as a shortcoming, as, invariably, (1) confounding factors would be present that could not be monitored or accounted for and (2) the conditions expected to be encountered in autologously augmented tissue would probably be characterised by a lower degree of inflammation and hypoxia. Contrasting the setting chosen here, animal studies involving larger sample sizes were almost exclusively conducted on the well-established 3T3-L1 cell line. Despite being easier to handle, as human biological material triggers rejection in all but athymic animals, and despite the results from these experiments being readily comparable, possible inter-individual differences in patient-obtained ASC fail to be highlighted in such a setting. However, as detailed above, the possibility of inherited or acquired epigenetic changes in subcutaneous ASC manifesting themselves as variable adipogenic potential must be assumed. These differences may take the form of inherited risk factors for metabolic dysregulation (in first-degree relatives of type II diabetes patients) or may have been acquired during the life of the donor patient. The experiments presented here were designed to

feature a comparatively large number of human samples for streamlined analysis allowing conclusions to be made pertaining to key determinants of ASC viability and adipogenicity.

1.4. Experiment Design

A two-fold strategy was pursued in order to investigate the aforementioned possible inter-individual differences. In total, 52 ASC samples were initially isolated from lipoaspirates obtained from 41 female patients undergoing aesthetic or reconstructive procedures involving liposuction. Following an immediate digesting step, ASC were cultured in ECGM medium ("Endothelial cell growth medium" purchased from Promocell, Heidelberg, DE), which was previously shown not to interfere with ASC differentiation potential [147].

In an effort to attempt an approach that would be practical when hypothetically employed in a clinical setting, no extensive sorting of the obtained cells was conducted. Instead, as SVF cells (including ASC) adhere to plastic surfaces in vitro and can only be disrupted by enzymatic means, several washing steps were employed to remove debris and non-adherent cells from cultures in order to obtain a purified SVF culture. On the assumption that ASC are the only cell type exhibiting significant proliferation, ASC should make up the vast majority of cultured cells. Although this approach makes it impossible to rule out the presence of non-adipogenic progenitor cells in culture, this method is easy to perform and could also be used in a clinical setting. Moreover, flow cytometry and randomly selected samples were used to demonstrate that cells isolated and cultured by this method exhibited the expected stem cell markers and that the viability of the cells was not significantly impaired by the handling process and to rule out contamination with other proliferating cell types, in agreement with results previously published by Bunnell et al. [148]. Adherence to plastic surfaces itself also constitutes an essential property postulated as one of the "*Minimal criteria for defining multipotent mesenchymal stromal cells*" by the International Society for Cellular Treatment [135].

After 24 hours, debris and non-adherent cells were removed from the flasks in a first medium change before the P_0 culture was again incubated in ECGM to a 75% cell confluence. When this confluence level was achieved, the ASC / preadipocytes were harvested by using trypsin to detach the adherent ASC. The cell yields were then registered, and the cells were seeded in 6-well plates for further differentiation. In order to be able to attain the two-fold experimental approach, the remaining cells were frozen in liquid nitrogen for later use in the ASC-endothelial progenitor cell co-culture experiment. For the differentiation part, 50000 ASC now in P_1 were seeded into each well of 3.5 cm diameter (equalling a well surface area of 9.62 cm^2) resulting in an initial cell density of ~ 5000 cells / cm^2. When the P_1 cells had again reached 75 % confluence, the induction and differentiation protocol

was initiated. Induction medium replaced the ECGM and the cultures were incubated for 48 hours under induction conditions. The cell cultures began the 11-day differentiation course in differentiation medium on day two of the experiment. Medium supernatants were retrieved on day 0 (i.e. before differentiation from 48-h-old induction medium) and on the second, fourth, eighth, and eleventh day after the initiation of differentiation. These supernatants were immediately frozen at -20°C for later adiponectin enzyme-linked immunosorbent assay (ELISA). After completion of the differentiation process, cultures were oil-red stained and analysed for morphological differences. Similar to the setup of the first part of the experiment, the ASC / preadipocytes - endothelial progenitor cell co-culture experiment used P_1 cells, although, in this case, cryopreserved P_0 cells were thawed and used instead of "fresh" cells as this experiment took place after the differentiation experiment had been concluded. The P_1 cells used in this second experiment originated from the pool of those cells cryopreserved directly after being isolated. Five hundred ASC were added to endothelial progenitor cells that had been pre-cultured in 24-well plates for one day. The co-culture experiment had a 14-day runtime; again supernatants were repeatedly stored for later adiponectin and VEGF ELISA and cultures were immunostained to visualise endothelial cell differentiation. In parallel, P_1 ASC cultures were seeded into 24-well plates at a density of 100000 per well and grown until confluency. From those undifferentiated ASC cultures, supernatants were collected and frozen for later use in VEGF ELISA.

The first part of the experiment allowed a comparative analysis of growth times, gave insights into adiponectin levels during differentiation into mature adipocytes and permitted a qualitative histological analysis of cultivated adipocytes. Adiponectin levels are an established indicator of successful adipocyte proliferation, whereas cell growth rate as reflected by the time taken to reach confluence after initial seeding in P_1 further provides another easily comparable indicator of ASC viability.

The co-culture component of the experiment spotlighted the endocrine / paracrine properties of ASC as promotors of endothelial cell differentiation, whereas vasculogenesis served to demonstrate possible inter-individual differences not characterised by variances in adiponectin secretion or morphological changes. This experimental part was performed by seeding defined numbers of ASC / preadipocytes with pre-cultured endothelial progenitor cells and subsequently by observing the development of mature (i.e. CD 31+) endothelial cells and the tubular networks formed by them. Observations were undertaken by means of immunostaining for both qualitative and quantitative analysis by VEGF ELISA and image analysis software. For this part of the experiment, another random sample of cells from the pool was used in an attempt to prove the hypothesis.

2. Materials and Methods

All laboratory work involving the handling of cell cultures and all preparatory steps pertaining to the experiments with living cell cultures outlined in the following chapter were performed in a biological safety cabinet (Herasafe KS, Thermo Fisher Scientific, Waltham, MA, USA), which was disinfected with 70% denatured ethyl alcohol (prepared by the in-house pharmacy) before and after work. At the end of every working day, it was further disinfected by 1 hour of UV radiation exposure. Gloves were always worn when cells or biological materials were handled or experiments conducted. Contaminated materials were disposed of in compliance with the established biohazard disposal protocol of the Institute. Additionally, non-sterile work areas were also always wiped with 70% denatured ethyl alcohol before and after experiments. All statistical analysis was performed using IBM® SPSS® Statistics Version 23 for Microsoft Windows.

2.1. Patient Demographic

All research was approved by the authors' ethic committee of the Technical University of Munich, and all clinical investigations were conducted according to the principles expressed in the Declaration of Helsinki. All patients gave their written consent, which was approved by the ethic committee of the Technical University of Munich (Permit Number: 5623/12). In total, 52 samples of lipoaspirate were obtained from 41 female patients undergoing liposuction for aesthetic or reconstructive purposes. Three patients were operated upon three times and four patients twice because of initially unsatisfactory aesthetic results. All patients who underwent reconstructive breast augmentation involving autologous adipose tissue grafting had undergone mastectomy and some had also had adjuvant radio- or chemotherapy because of breast cancer before this operation but had been staged preoperatively and were declared cancer-free. Patients were aged from 21 years to 67 years with a median age of 50 years. A reliable medical history could only be obtained from 27 of the 41 patients (65.9 %): 19 of the 41 patients (46.3 %) had a confirmed history of breast cancer with one of the patients in this group being BRCA 1+2 positive; 8 of the patients (19.5 %) suffered from benign conditions, such as fibrocystic breast disease or breast abscesses, or had selected to undergo purely aesthetic mamma augmentation through autologous fat transplantation. Two patients (4.8 %) underwent breast reconstruction following pre-emptive mastectomy because of their positive BRCA1 status but with no tumour being detected in the pathological analysis in these two cases. All 6 patients (14.6 %) who had a history of nicotine abuse received reconstructive breast augmentation following mastectomy because of breast cancer. All patients had voluntarily consented to surplus biological material being used for scientific purposes prior to their operation. Out of this pool, 28 samples were positively selected for inclusion into a standardised differentiation scheme aimed at unveiling possible

inter-individual differences in ASC behaviour under controlled conditions. Medical histories could be obtained for 14 of these samples. Of note, one patient was operated upon three times resulting in 3 of the 28 samples being from this patient.

2.2. Obtainment, Isolation and Culture of Adipocyte Derived Stem Cells

2.2.1. Liposuction and Immediate Processing

Fifty-two individual ASC samples were isolated from lipoaspirates of 41 female patients who underwent mamma reconstruction or augmentation procedures or aesthetic liposuctions at the Clinic for Plastic and Reconstructive Surgery at the Klinikum Rechts der Isar der TU München, Munich, Germany. The operation was performed under sterile conditions and general anaesthesia. In order to reduce bleeding and to facilitate the removal of adipose tissue, a 1:1000 adrenaline – sodium chloride tumescence solution was injected subcutaneously in the areas from which fat was to be removed prior to the actual liposuction. The infiltration with tumescence solution is the hallmark of the “wet” technique that was pioneered in the 1980s by Y.G. Illouz and is the method of choice for liposuction today [145,149]. Following the infiltration with tumescence solution, a blunt-tipped liposuction cannula with an opening near the tip of the cannula was inserted subcutaneously below the fascia superficialis through small incisions of less than 1 cm. Adipose tissue was removed through fan-shaped movements of this cannula, which was attached, under a negative pressure of approximately 0.8 bar controllable by the surgeon, to a sterile collection system. During liposuction, emphasis was placed on (1) the level of movement of the cannula at the appropriate skin level (below the fascia superficialis) and (2) the application of the vacuum only during the withdrawal of the cannula tip with the opening facing towards the patient (downward). The diameter of the cannula used was determined by the body region in which the liposuction took place. As the larger volumes of adipose tissue required for breast reconstruction were almost exclusively obtained from the abdominal and femoral region, the cannulas used usually had a diameter of 2.5 – 3.5 mm. The lipoaspirate was collected in a sterile container, transferred into 20 ml tubes and centrifuged at 2000 rpm for 3 minutes (Hettich EBA 20, Hettich Lab Technologies, Tuttlingen, DE) to separate the adipose tissue from the tumescence solution. Tumescence solution was discarded after centrifugation and the majority of adipose tissue was used for breast augmentation and / or reconstruction purposes. Surplus centrifuged tissue was saved to be studied in experiments outlined on the following pages. These adipose tissue samples were transported into the laboratory immediately for further processing and cultivation.

2.2.2. Tissue Digestion, Adipose Derived Stem Cell isolation and Initial Cultivation (P_0)

Of the centrifuged lipoaspirate from step 2.2.1., 10 ml aliquots were subsequently digested in 50 ml tubes (Cellstar®, Greiner Bio-One, Kremsmünster, AT) by using Collagenase solution at a concentration of 0.2 U / ml Collagenase NB4 (Serva, Heidelberg, DE) in collagenase buffer supplied by the hospital's in-house pharmacy (23.8g/l Hepes; 4-(2-hydroxyethyl)-1-piperazineethanesulfonic acid, Merck, Darmstadt, DE), 7g / l NaCl , 3.6 g KCL / l, 0.15 g / l $CaCl_2$, 1 g / l D-Glucose to 1 litre distilled water), supplemented with 1.5% BSA (Sigma Aldrich, St. Louis, MI, USA). Lipoaspirate and Collagenase were mixed at a 1:1 ratio. Samples were then incubated in a 37°C water bath with gentle agitation for 1 hour. Digestion was stopped by adding 2 volumes (i.e. 20 ml) of DMEM (Dulbecco's Minimum Essential Medium, Invitrogen, Carlsbad, CA, USA) supplemented with 10% FCS (Invitrogen, Carlsbad, CA, USA). After fractionation of the mixture by sedimentation centrifugation (Hettich Rotina 380 R, Hettich, Tuttlingen, DE) at 2000 rpm for 10 min at 20°C, the upper fluid layer was removed. The pellet of cells at the bottom of the tube was resuspended, washed up, aspirated with PBS (Invitrogen, Carlsbad, CA, USA) and filtered through a 70-µm-mesh cell strainer (BD Bioscience, Bedford, MA, USA) to remove debris. This cleaning step was performed twice. Following the second washing step, PBS was removed, the pellet was re-suspended with 25 ml ECGM (Endothelial Cell Growth Medium (Promocell, Heidelberg, DE) supplemented with Endothelial Cell Growth Medium – Supplement mix (Promocell, Heidelberg, DE) and 1% Antibiotic-Antimycotic (Invitrogen, Carlsbad, CA, USA), all pre-warmed to 37°C and directly transferred into 75 cm^2 cell culture flasks (Sigma-Aldrich, St. Louis, MI, USA). Culturing took place in an incubator with a humidified atmosphere at 37°C and 5% CO_2 (Heracell 150i; Thermo Fisher Scientific, Waltham, MA, USA). Attempts at cell counting at this step were waived after it became clear that excessive debris prevented any evaluable results. After 24 hours, medium was removed and the flask was carefully washed with PBS pre-warmed to 37°C in order to remove interfering erythrocytes, cell debris and non-adherent cells. Subsequently, 20 ml fresh pre-warmed ECGM, prepared as described above, was added and renewed every 3-4 days, if necessary. Cells were initially cultured until a confluence level of 75% was reached. Confluence levels were monitored by means of a Leica DM IL inverted contrasting microscope (Leica, Wetzlar, DE).

2.2.3. Quantification of Cell Yield

After showing a confluence of >75%, cells were harvested. In a first step, ECGM was removed and the culture was washed twice by using PBS (Invitrogen, Carlsbad, CA, USA) to remove non-adherent cells and cell debris. Detachment of the adherent ASC was achieved by using a trypsin solution (Trypsin 0, 05% in EDTA, Invitrogen, Carlsbad, CA, USA); 3 ml of this solution was added to the cells after the PBS used for washing had been removed. Under occasional gentle agitation, cell detachment was achieved

after 5 minutes of trypsin presence. Once adequate detachment had been microscopically confirmed, the action of the trypsin was neutralised by using 7 ml FCS supplemented DMEM (same as used in step 2.2.2.). The cell solution was then transferred into 50 ml tubes (Cellstar® tubes, Greiner Bio-One, Kremsmünster, AT). To determine the number of ASC per ml of cell solution, a disposable haemocytometer (C-Chip disposable haemocytometer, Biochrom, Berlin, DE) was employed together with trypan blue (trypan blue 0.4% in 0, 81% sodium chloride and 0.06 % potassium phosphate, Sigma-Aldrich, St. Louis, MI, USA) exclusion staining to allow distinction between viable cells and those with damaged cell membrane, which took on a blue shade. The term "exclusion staining" was derived from the finding that trypan blue is unable to permeate intact cell membranes. For cell counting, 10 µl ASC suspension was pipetted into a well of a 96-well plate for mixing, following which, 10 µl of 0.4 % trypan blue solution was added and thoroughly mixed by repeated re-pipetting. After the cell suspension and trypan blue were mixed completely, all 20 µl fluid were taken up with a pipette and transferred into the counting chamber of the disposable haemocytometer. Cell numbers were recorded in all four large quadrants independently and the mean number of cells per large quadrant was determined. The dilution factor of 2 was factored in, as was the factor 10000 to convert cells / µl into cells / ml. The following is the complete formula used to determine the total cell count per millilitre.

$$\bar{n}_{cells\ per\ large\ square} \times 2\ (dilution\ factor) \times 10000\ (conversion\ cells \div \mu l \rightarrow\ cells \div ml) = n_{cells} \div ml$$

2.2.4. Cryopreservation of ASC

At this point, cells not used in the experiment were cryopreserved by using DMSO-free (dimethylsulphoxide-free) Biofreeze solution (Biochrom, Berlin, DE) and prepared for long-term storage in liquid nitrogen. In preparation for cryoconservation, 1 ml Biofreeze solution at room temperature was filled into 1.5 ml cryotubes (1.5 ml mikrotubes, Sarstedt, Nümbrecht, DE). Aliquots of 1.5 ml cell suspension were transferred from the 50 ml Falcon tubes used for cell quantification (see 2.2.3.) into 1. 5 ml Eppendorf tubes (Eppendorf, Hamburg, DE), which were then centrifuged at 2000 rpm for 5 minutes (Hettich Rotina 380 R, Hettich, Tuttlingen, DE). Next, all fluids were removed before the cell pellet was broken up by gentle vortexing (Vortex Genie 2, Scientific Industries, NY, USA). By means of a disposable transfer pipette, the 1 ml biofreeze solution was mixed with the broken up cell pellet in the respective Eppendorf tube while avoiding excessive foam formation. Once the cells and biofreeze had been thoroughly mixed, the suspension was transferred into the cryotube and immediately placed in a cooling container (Mr. Frosty™, Thermo Fisher Scientific, Waltham, MA, USA) that had been pre-cooled to 6° C. The cooling container, which was able to provide a constant rate close to -1°C per minute (well suited for cell freezing), was then placed in a -80°C freezer for at least

90 hours. The samples, which were at -80°C by this time, were then transferred into a -196°C liquid nitrogen tank for long-time storage.

2.2.5. Thawing and Seeding of Cryopreserved ASC

In order to thaw and re-cultivate ASC that had been cryopreserved as described in 2.2.4., an appropriate volume of 20 % FCS in MEM "thawing medium" (for example, 10 ml FCS + 40 ml MEM) was prepared in a 50 ml tube (Cellstar®, Greiner Bio-One, Kremsmünster, AT) and pre-warmed to 37°C in a water bath (TW8, Julabo, Seelbach, DE). The cryotube(s) were then removed from the liquid nitrogen tank and placed in the 37°C water bath under constant monitoring until only minimal ice crystals remained. At this point, the vials were quickly wiped with 70% denaturised ethyl ethanol for disinfection and 1 ml thawing medium was added to the cryotube by using a transfer pipette. By means of the same transfer pipette, the contents of the cryotube were thoroughly mixed and eventually transferred into a 25 cm^2 cell culture flask (Cellstar®, Greiner Bio-One, Kremsmünster, AT), 5 ml thawing medium was added and the flask was incubated at 37°C under a humidified 5% CO_2 atmosphere (Heracell 150i incubator) overnight to allow for cell adherence to the plastic surface of the flasks. On the next day, the thawing medium was removed and replaced with 5 ml ECGM. Cells were then incubated until 75% confluence was reached, as confirmed microscopically (by using a Leica DM IL inverted contrasting microscope; Leica, Wetzlar, DE), at which point cells were trypsinised and counted (see 2.2.3.).

2.3. Primary Cell Culture (P_1)

2.3.1. Cell Seeding

Following the determination of the cell count (see 2.2.3.), cells were seeded into 6-well plates (Cellstar® Cell Culture Multiwell Plate, Greiner Bio-One, Kremsmünster, AT). After the necessary volume had been calculated, 50000 cells were seeded into each respective well. For a well surface area of approximately 10 cm^2, this equalled a cell density of 5000 cells / cm^2. A volume of 3 ml ECGM was then added to each well and the cells were incubated at 37°C under a humidified 5% CO_2 atmosphere in an incubator (Heracell 150i, Thermo Fisher Scientific, Waltham, MA, USA). Growth was monitored by daily microscopic checks (Leica DM IL inverted contrasting microscope, Leica, Wetzlar, DE) and a medium change of 3ml fresh ECGM was carried out on the third day if 75-80% confluence had not been achieved by that time. Once cell confluence levels had reached 75-80%, the induction and differentiation process was initiated.

2.3.2. Induction and Differentiation Process

Microscopically confirmed 75-80% cell confluence was selected as the starting point for the induction of adipogenic differentiation. The induction and differentiation sequence consisted of 2 days of induction and 12 days of differentiation. Induction medium was based on supplemented Eagle's minimum essential medium (MEM, Life technologies, Carlsbad, CA, USA). To prepare the induction medium, 25 ml FCS (Life technologies, Carlsbad, CA, USA), 5 ml Antibiotic-Antimycotic (Life technologies, Carlsbad, CA, USA), 500 µl Insulin (10 mg /ml Sigma-Aldrich, St. Louis, MI, USA) giving a final concentration of 1 µg / ml, 5 µM Hydrocortisone (Sigma-Aldrich, St. Louis, MI, USA), 50 µg 3-Isobutyl-1-methylxanthine (IBMX, Sigma-Aldrich, St. Louis, MI, USA), 10 µg indomethacine (Sigma-Aldrich, St. Louis, MI, USA), and 5 ml glutamine (equivalent to 200 mM glutamine; GlutaMAX 100x, Life technologies, Carlsbad, CA, USA) were added to a 500 ml bottle of MEM. The composition of the induction medium was based on the results published by Bunnel, Zuk and many others and experience at this laboratory [148,33,150]. Differentiation medium was also based on MEM but was solely supplemented with 25 ml FCS (Life technologies, Carlsbad, CA, USA), 5 ml Antibiotic-Antimycotic (Life technologies, Carlsbad, CA, USA), 500 µl Insulin (10 mg / ml; Sigma-Aldrich, St. Louis, MI, USA) to give a final concentration of 1 µg / ml and 25 ml (equivalent to 200 mM) glutamine (GlutaMAX 100x, Life technologies, St. Louis, MI, USA). Similar to the induction medium, its composition was based on published studies and laboratory experience [33,150,148,148,148]. Once a cell confluence of 75-80% had been reached, ECGM was exchanged for induction medium and cells were incubated at 37°C under a humidified 5% CO_2 atmosphere (Heracell 150i, Thermo Fisher Scientific, Waltham, MA, USA) for 48 hours. Subsequently, 1 ml induction medium was removed from each well, transferred into a 1.5 ml Eppendorf tube (Eppendorf, Hamburg, DE) and frozen at -20°C for later adiponectin ELISA. The remaining induction medium was then discarded and replaced by 3 ml differentiation medium per well. The cell culture plates were again placed in the incubator and 1 ml aliquots of medium supernatants were taken on days two, five, eight, and eleven after incubation. These aliquots were also immediately frozen at -20°C; they were never drawn from the same well twice but always from the 3 ml differentiation medium. For osteogenic induction, ASCs were plated at a concentration of $1x10^5$ cells into 24 well plates in duplicates and cultured in ECGM. After reaching confluency, the medium was replaced by MSC Osteogenic Differentiation Media (Promocell). Cells were incubated for 21 to 28 days and changes of media were performed every third day. After this time period, cells were submitted to a standard Alizarin red staining protocol.

During the induction and differentiation process, cells were occasionally monitored microscopically for viability and adipogenesis. However, the necessary sterility of the cultures did not allow routine photographic documentation as samples would have had to be transported to another room.

2.3.3. Characterisation of Adipose Derived Progenitor Cells / Flow Cytometry

The differentiation capacity of adipose derived progenitor cells was evaluated. In order to fulfil the minimal criteria outlined by Dominici and Zuk for the definition of the adipogenic progenitor cells as adipose derived stem cells (ASCs), cells were induced in parallel by means of an adipogenic and an osteogenic differentiation regime. To further support these criteria, undifferentiated cells were analysed by standard flow cytometry procedure (FACS) in a BD FACS-Accuri (Becton Dickinson Biosciences, Heidelberg, Germany) cell analyser and Accuri software

For the characterisation of ASC, the following monoclonal antibodies (mAB), conjugated with either fluorescein isothiocyanate (FITC), phycoerythrin (PE) or allophycocyanin (APC) and directed against membrane-associated proteins corresponding to the mesenchymal lineage were used:

- CD90-FITC (mouse anti human, clone 5E10, IgG1, cat.nr. A15761, Life technologies GmbH Darmstadt, Germany)
- CD44-FITC (mouse anti human, clone MEM85 (IgG2a) cat.nr. MHCD4401), Life technologies GmbH Darmstadt, Germany),
- CD29-PE (mouse anti human, clone MEM-101A (IgG1) cat.nr. CD 2901, Life technologies GmbH Darmstadt, Germany),
- CD73-APC (mouse anti human, clone AD2 (IgG1) cat.nr. A16356, Life technologies GmbH Darmstadt, Germany)

To reinforce a certain lineage specificity, cells were also stained with mAbs directed against proteins of the endothelium (CD31), the haemopoietic lineage (CD34) or immune cells such as antigen presenting cells (HLA-DR and CD 14).

- CD31-APC (mouse anti human, clone WM59 (IgG1) cat.nr. A16224, Life technologies GmbH Darmstadt, Germany)
- CD34-PE (mouse anti human, clone 4H11 (IgG1) cat.nr. A16203, Life technologies GmbH Darmstadt, Germany
- HLA-DR-PE (mouse anti human, clone L243 (IgG2a) cat.nr. sc18875, Santa Cruz-Biotechnology, Inc. Heidelberg, Germany

- CD14-FITC (mouse anti human, clone Tük4 (IgG2a) cat.nr. MHCD1401, Life technologies GmbH Darmstadt, Germany

ASCs cultured at P1 or P2 were grown to confluence and subsequently harvested and brought into suspension. Cells were washed once with PBS. After centrifugation and removal of the PBS, the cell pellet was aspirated in 2 ml FACS-buffer (PBS supplemented with 2% FCS). Cells were counted and, for each staining, adjusted to an amount of 100000 cells in a volume of 100µl in 1.5 ml Eppendorf tubes. Then, 5 µl of the above enumerated specific antibodies was added to each sample. The tubes were gently vortexed and incubated for 30 minutes at room temperature in the dark. After the incubation period, 1 ml FACS-buffer was added to the samples and centrifuged for 5 minutes at 300g. The supernatant was removed and the washing step repeated.

After the final washing step, the cells were aspirated in 500 µl of FACS buffer and subsequently analysed with a BD ACCURI cell analyser.

2.4. Microscopic Analysis of P_1 Cultivated Adipocytes

2.4.1. Oil-Red Staining

Red O staining is an assay performed to stain fat droplets in tissue samples. It is therefore a useful tool for qualitative histological evaluation of adipose tissue (both cultured and ex vivo).

After completion of the 14-day cultivation curse outlined in 2.3.2., the medium was completely removed from the aforementioned 6-well cell culture plates and the wells were then rinsed three times with PBS (Invitrogen, Carlsbad, CA, USA). With the washing step complete, PBS was removed, and 10 ml buffered 10% formalin solution in PBS (Sigma-Aldrich, St. Louis, MI, USA) was added. The plates were then incubated for 30 minutes at room temperature, the formalin was removed from the wells and the plate was gently rinsed with 5 ml purified water. Subsequently, 5 ml 60% isopropanol (Sigma-Aldrich, St. Louis, MI, USA) was carefully pipetted into the plate. These steps had to be performed with great care so as not to disturb the fragile cell layer. Isopropanol was allowed to remain in the tissue culture plates for 5 min before being discarded. Finally, 2.5 ml of Oil Red O working solution (Sigma-Aldrich, St. Louis, MI, USA) sufficient to cover the entire monolayer was added to each well. The plates were then incubated for 2 hours at 4°C in a refrigerator before the Oil Red O solution was discarded. In a last step, cultures were rinsed repeatedly in PBS solution until the rising fluid remained clear and no colour bleeding could be observed with the naked eye. Oil-red-stained cultures were examined microscopically as soon as possible as colour fading occurred within days, even under dark and cold storage conditions.

2.4.2. Qualitative Examination

The Leica microscope DMI 600B and Leica software DFC 425 C Application Suite 357 were used to examine oil-red-stained cultures. Attention was especially paid to inter-individual differences pertaining to adipocyte morphology, the number and size of lipid droplets and any possible abnormalities in adipocyte configuration. Images were taken in bright field mode at 10x and 40x magnification and saved in the TIFF format.

2.5. Biochemical Analyses

2.5.1. Adiponectin-ELISA

Medium supernatants from the differentiation experiment and the co-culture experiment (see below) were collected and immediately frozen at -20°C. Quantitative analysis of adiponectin content was performed by using an ELISA kit (R&D Systems human adiponectin ELISA development kit, R&D Systems, Minneapolis, MN, USA). The ELISA protocol is described below.

After preparation of the provided mouse monoclonal capture antibody against the Adiponectin globular domain by reconstituting it with 1 ml PBS (Invitrogen, Carlsbad, CA, USA) and creating a 10 ml working solution by diluting 28 µl of the reconstituted capture antibody with 10 ml PBS, each well of a 96-well immunograde tissue-culture plate (Greiner Bio-One, Kremsmünster, AT) was coated with 100 µl of the 1 µg/ml Adiponectin capture antibody working solution. The 96-well plate was sealed by using single use adhesive plate sealing tape (Thermo Fisher Scientific, Waltham, MA, USA) and incubated overnight at room temperature. On the second day, the capture antibody was removed and each well was washed with 400 µl wash buffer (PBS with 0.05% Tween® 20, Sigma-Aldrich, St. Louis, MI, USA) per well. This process was repeated 3 times. The plates were then blocked by adding 300 µl blocking buffer / reagent diluent (1% purified BSA in PBS, R&D Systems, Minneapolis, MN, USA) per well. After incubation for 1 hour at room temperature, the plate was washed again three times with wash buffer. Towards the end of this incubation period, frozen samples were thawed in a 37°C water bath (TW8, Julabo, Seelbach, DE) and vortexed before being diluted to the desired level with reagent diluent. Standards and samples were then added in a volume of 100 µl per well, the plate was resealed and incubated for 2 hours at room temperature. Standards were prepared by serial dilution, achieving a high-concentration standard of 4000 pg adiponectin / ml and a low-concentration standard of 62.5 pg adiponectin / ml. 500 ng concentrated lyophilised adiponectin protein standard was included in the kit and reconstituted with 0.5 ml reagent diluent. According to the analysis supplied with the kits, a mix of 28 µl of the reconstituted adiponectin standard with 972 µl reagent diluent would result in a 4000 pg / ml adiponectin concentration necessary for the high-concentration standard. Samples

obtained from 6-well plates of the ASC differentiation experiment were added at a 1:20 dilution (5 µl medium supernatant + 95 µl reagent diluent); supernatants from the V2a co-culture experiment were not diluted for this ELISA. Following incubation of the standards and samples 2 hours, the plate was washed 3 again times with wash buffer before the addition of 100 µl detection antibody working solution per well. The secondary mouse monoclonal detection antibody against the adiponectin globular domain was supplied with the kit and reconstituted with 1 ml reagent diluent prior to first use. For the assay, 10 ml of working solution was prepared by diluting 55 µl reconstituted secondary antibody in 10 ml reagent diluent. Following this step, the plates were again sealed and allowed to incubate for 2 hours at room temperature. Two hours later, the washing step was repeated, before 100 µl of the working dilution of Streptavidin conjugated to HRP (horseradish peroxidase) (1:200 dilution of the Streptavidin-HRP provided in the kit in reagent diluent as specified on the vial) was added to each well. The plate was incubated in the dark for 20 minutes at room temperature, followed by three washes in wash buffer in order to remove all non-bound Streptavidin-HRP from the wells. Subsequently, 100 µL substrate solution (1:1 mixture of stabilised hydrogen peroxide (H_2O_2) and tetramethylbenzidine / TMB) was added to each well. Plates were kept in the dark for 6-8 minutes until a blue colour developed through HRP-mediated oxidation of TMB into blue TMB diimine. Nevertheless, the colour development was unpredictable and so the development process was always monitored and stopped at an appropriate time. The reaction was stopped by pipetting 50 µl stop solution (10% H_2SO_4, Sigma-Aldrich, St. Louis, MI, USA) into each well. The optical density of each sample was immediately determined by using a microplate reader (Multiskan SC, Thermo Fisher Scientific, Waltham, MA, USA) set to a wavelength of 450 nm. Readings were taken directly at 450 nm without correction with a 570 nm blank measurement subtracted from the 450 nm readings.

2.5.2. VEGF-ELISA

Medium supernatants from the differentiation experiment and the co-culture experiment (see below) were collected and immediately frozen at -20°C. Quantitative analysis of VEGF content was performed by using an ELISA kit (R&D Systems human VEGF ELISA development kit, R&D Systems, Minneapolis, MN, USA). The protocol used to perform the ELISA is described below. It is similar to the protocol for the aforementioned adiponectin ELISA in all but the employed antibodies and their concentrations.

After preparing the provided mouse monoclonal capture antibody against VEGF by reconstituting it with 1 ml PBS (Invitrogen, Carlsbad, CA, USA) and creating a 10 ml working solution by diluting 28 µl of reconstituted capture antibody with 10 ml PBS, each well of a 96-well immunograde tissue-culture plate (Greiner Bio-One, Kremsmünster, AT) was coated with 100 µl 1 µg/ml Adiponectin capture antibody working solution. The 96-well plate was sealed by using single use adhesive plate sealing tape

(Thermo Fisher Scientific, Waltham, MA, USA) and incubated overnight at room temperature. On the second day, the capture antibody was removed and each well was washed with 400 µl wash buffer (PBS with 0.05% Tween® 20, Sigma-Aldrich, St. Louis, MI, USA) per well. This process was repeated 3 times. The plates were then blocked by the addition of 300 µl blocking buffer / reagent diluent (1% purified BSA in PBS, R&D Systems, Minneapolis, MN, USA) per well. After incubation for 1 hour at room temperature, the plate was washed again three times with wash buffer. Towards the end of this incubation period, frozen samples were thawed in a 37°C water bath (TW8, Julabo, Seelbach, DE) and vortexed before being diluted to the desired level with reagent diluent. Standards and samples were then added at a volume of 100 µl per well and the plate was sealed and incubated for 2 hours at room temperature. Standards were prepared by serial dilution, achieving a high-concentration standard of 2000 pg VEGF / ml and a low-concetration standard of 31.3 pg VEGF / ml. 500 ng of concentrated lyophilised VEGF protein standard was included in the kit and reconstituted with 0.5 ml reagent diluent. According to the analysis supplied with the kits, a mix of 28 µl of the reconstituted VEGF standard with 972 µl reagent diluent would result in a 2000 pg / ml VEGF concentration necessary for the high-concentration standard. Supernatants from the V2a co-culture experiment were not diluted for this ELISA. The plate with the added standards and samples was incubated for 2 hours and then washed 3 times with wash buffer before the addition of 100 µl detection antibody working solution per well. The secondary goat monoclonal detection antibody against VEGF was supplied with the kit and reconstituted with 1 ml reagent diluent prior to first use. For the assay, 10 ml of working solution was prepared by diluting 55 µl reconstituted secondary antibody in 10 ml reagent diluent. Following this step, the plates were again sealed and allowed to incubate for 2 hours at room temperature. 2 hours later, the washing step was repeated, before 100 µl of the working dilution of Streptavidin-HRP (1:200 dilution of the Streptavidin conjugated to HRP provided in the kit in reagent diluent as specified on the vial) was added to each well. The plate was incubated in the dark for 20 minutes at room temperature and then washed three times with wash buffer in order to remove all non-bound Streptavidin-HRP from the wells and 100 µL substrate solution (1:1 mixture of stabilised hydrogen peroxide (H_2O_2) and tetramethylbenzidine / TMB) were added to each well. Plates were kept in the dark for 6-8 minutes until a blue colour developed through HRP-mediated oxidation of TMB into blue TMB diimine. As mentioned above this process was always monitored and stopped at an appropriate time by pipetting 50 µl stop solution (10% H_2SO_4, Sigma-Aldrich, St. Louis, MI, USA) into each well. The optical density of each sample was immediately determined by using a microplate reader (Multiskan SC, Thermo Fisher Scientific, Waltham, MA, USA) set to a wavelength of 450 nm. Reading was made directly at 450 nm without correction with a 570 nm blank measurement subtracted from the 450 nm readings.

2.6. Adipocyte Derived Stem Cell – Endothelial Progenitor Cell Co-culture (V2A) assay

2.6.1. Hypothesis

Interactions between endothelial cells (EC) and both adipocytes and ASC are crucial for the maintenance of physiological WAT. The connective tissue surrounding the vasculature, namely the stromal vascular fraction (SVF), is not only the location of adipocyte progenitor cells but its composition also greatly influences WAT functioning, especially pertaining to the complex vasculature in WAT. ASC have multilineage differentiation capabilities, at least in vitro, and have also been found to be involved in the angiogenesis in WAT during times of WAT expansion and during general WAT remodelling and maintenance. Animal experiments have indicated that certain cells within the SVF are recycled pre-existing blood EC, when creating new vasculature. Other studies have revealed that ASC are able directly to differentiate into EC in vitro and in vivo after prior cultivation. Recent research further suggests that the addition or implantation of ASC into wounds or models of ischaemia in vivo can significantly improve healing or survival of the lesion-affected tissue. These findings suggest a role for ASC in reorganising and healing processes outside of orthodox adipose tissue and in subcutaneous and other tissue. As vivo studies highlight that ASC do not simply coexist next to "their" connective tissue but that physiological functioning and tissue turnover can only happen if crosstalk takes place between endothelial cells, ASC and adipocytes and possibly other cell types.

The hypothesis is that possible inter-individual differences in ASC might be reflected in their differing ability to promote endothelial cell differentiation. The commercially available V2a Vasculogenesis to Angiogenesis Kit® (Caltag-Medsystems Ltd., Buckingham, UK) was used in a co-culture experiment to examine whether these assumed pro-angiogetic properties of ASC are exerted on EC and to determine any possible inter-individual differences of this pro-angiogetic effect. At the same time, the chosen experimental setup eliminated confounding factors that would have been impossible to control in animal studies, such as hypoxic stress and inflammation in artificially created ischaemia.

2.6.2. Experimental Setup

The V2a Vasculogenesis to Angiogenesis Kit ® (Caltag-Medsystems Ltd, Buckingham, UK) included primary EC progenitor cells, "V2a seeding medium" and "V2a growth media" (with associated supplements), mouse anti-human CD31 primary antibody, goat anti-mouse IgG AP (Alkaline phosphatase) conjugate secondary antibody, the reagents for tubule visualisation through AP detection by BCIP (5-Bromo-4-chloro-3-indolyl phosphate) and NBT (nitro blue tetrazolium), validated positive control (VEGF) medium additive and validated negative control (Suramin) medium additive. A detailed description of all working steps was provided with the kit. The assay was performed following

the manufacturer's guidelines, as explained below, with one exception: Cells were added to the growth medium on the second day instead of soluble additives or otherwise conditioned media as suggested in the protocol (the addition of cells for co-culture was not mentioned or suggested in the manufacturer's protocol). Detailed composition of the media included in the kit cannot be provided as it is proprietary information was not disclosed.

2.6.3. Execution of the co-culture experiment

On the first day, "V2a seeding medium" was prepared by thawing "seeding medium supplement" and adding it to the 25 ml V2a seeding medium provided with the kit. The seeding medium was then pre-equilibrated at 37°C in a humidified atmosphere with a CO_2 content of 5%. Endothelial progenitor cells were thawed in a 37°C water bath (TW8, Julabo, Seelbach, DE)until almost no crystals remained, the vial with the V2a cells was wiped with 70% isopropanol and its contents were added to a 20 ml Falcon tube (BD Biosciences, Bedford, MA, USA) with 12 ml seeding medium. Cells were thoroughly mixed, seeded into a 24-well plate and incubated under a humidified 5% CO_2 atmosphere for 24 hours prior to co-culture with ASC. After 24 hours (on the second day), thawed cryopreserved ASC that had been pre-cultivated by using the above-mentioned protocol (following the culture process outlined in 2.3.1.) were harvested by trypsination and counted by using trypan blue staining and a disposable haemocytometer (as explained in 2.2.3.). Samples containing 1000 cells were transferred into 2-ml Eppendorf tubes (Eppendorf, Hamburg, DE) and centrifuged for 5 minutes at 2000 rpm on a micro-centrifuge (SPROUT, Heathrow Scientific, IL, USA). During the preparation of the samples, "V2a growth medium" was prepared by thawing "growth medium supplement" and adding it to the 125 ml "V2a growth medium" supplied. It was also pre-equilibrated for 30 minutes at 37°C in a humidified 5% CO_2 atmosphere according to the manufacturer's protocol. Following centrifugation, media supernatants were carefully removed and the cell pellets were aspirated in 500 µl pre-equilibrated V2a growth medium. Endothelial progenitor cell seeding medium was discarded and replaced by 500 µl V2a growth medium with added ASC. For positive and negative controls, V2a growth medium containing VEGF and suramin at a respective volume of 11 ml was prepared and added to control wells instead of the ASC-containing V2a growth medium. The positive control consisted of V2a growth medium with a 2 ng / ml VEGF concentration; the negative control had 220 µl of 1 mM suramin solution added to V2a growth medium. On the first run, samples and controls were assayed in triplicate, whereas for the second and third runs, a decision was made to use duplicates (since the results of triplicate assays were comparable) in order to obtain a higher number of analysed samples. Plates were incubated at 37°C with 5% CO_2 in a humidified incubator (Heracell 150i; Thermo scientific, Waltham, MA, USA) for a total of 14 days including 13 days of co-cultivation. Growth and control media were exchanged and collected

every other day. At all media changes, pre-equilibrated V2a growth medium was used. The collected supernatants were immediately frozen at -20°C and used for laterELISA of VEGF and adiponectin.

2.6.4. Anti-CD31 immunostaining

After 14 days in culture, the experiment was terminated. In preparation for the immunostaining process, primary and secondary antibodies were thawed and diluted 1:400 (35 µl concentrated primary antibody + 14 ml 1 % BSA in PBS) for the primary anti-human CD31 antibody and 1:500 (28 µl concentrated secondary antibody + 14 ml 1% BSA in PBS) for the secondary anti-mouse IgG AP-conjugates antibody. V2a growth medium was removed (and immediately frozen at -20°C for later ELISA analysis) and the cell culture was rinsed very carefully with PBS pre-warmed to 37° C. The washing solution was removed and the cells were immediately covered in 0.5 ml of 70 % ethanol in distilled water (Sigma-Aldrich, St. Louis, MI, USA) cooled to below zero temperature prior to use, per cell culture well. The 24-well plate was then left for 30 minutes at room temperature. Next, the ethanol was discarded and the wells were washed three times with 1 % BSA (Sigma-Aldrich, St. Louis, MI, USA) in PBS (Invitrogen, Carlsbad, CA, USA). After the third wash, the washing solution was removed and 0.5 ml of prepared 1:400 diluted primary anti anti-human CD31 antibody was added to each well. The samples were then incubated at 37°C for 60 minutes. After this incubation step, the primary antibody solution was removed and each well was again washed with 1% BSA in PBS solution, which was left in the wells for 5 minutes at room temperature before being decanted. This rinsing was repeated two more times, with the 1% BSA in PBS solution remaining in the wells for 5 minutes each. Following the third washing/blocking step, 0.5 ml of the secondary anti-mouse IgG AP conjugate diluted 1:500) was added to each well. The incubation time for the secondary antibody was 60 minutes at 37°C. The cells were subsequently washed with distilled water three times; as for the washing steps, the distilled water was left in the wells for 5 minutes before being decanted. The wells were then allowed to dry. To visualise tubule formation, cultures were subsequently stained with BCIP/NBT substrate. To this end, two BCIP/NBT tablets (included in the kit) were dissolved in 20 ml distilled water. The solution was filtered by using a 20 ml syringe (B. Braun, Melsungen, DE) and an 0.2 µm filter (B. Braun, Melsungen, DE); 0.5 ml of this filtered substrate solution was added to each of the dry cell culture wells. The staining process took place at room temperature and the samples were continuously monitored until a satisfactory staining level was achieved, usually after approximately 6-7 minutes. To avoid overstaining, the BCIP/NBT substrate solution was removed at the onset of satisfactory staining levels and the samples were subsequently washed three times with distilled water. After the final rinsing water had been removed, the now successfully immunostained samples were left to air-dry in the dark.

2.6.5. Evaluation

Following anti-CD31 immunostaining (described in 2.6.4.), wells were photographed at 5x magnification by using the bright field grid mode of a Leica Microscope DMI 600B and Leica Software DFC 425 C Application Suite 357 (both Leica, Wetzlar, DE) in order to create a composite image of the entire well. In addition to qualitative visual analysis, the ImageJ program (open source, created by Wayne Rasband (wayne@codon.nih.gov) at the Research Services Branch, National Institute of Mental Health, Bethesda, MD, USA) with the Threshold_Colour Plugin (open source, created by Gabriel Landini (G.Landini@bham.ac.uk), University of Birmingham, Birmingham, UK, available at www.dentistry.bham.ac.uk/landinig/software/software.html) was used to quantify the percentage of darker shaded (CD31-positive) well surface area. A representative rectangular area as large as possible was selected from the native image and duplicated into a secondary image By using the Threshold Colour Plugin (brightness threshold pass filter set to 125), a black and white picture was created from the secondary image with the area to be analysed remaining white. The picture was then colour inverted and converted into 8-bit format. A threshold was applied and the percentage of image area passing that threshold was analysed and quantified by using the Analyze Particles function of ImageJ. Thus, a percentage value was calculated that represented the share of dark (i.e. CD31+ surface area) as a proportion of the total surface area.

3. Results

3.1. Time to confluence in P_0

Since the initial number of cells isolated from the lipoaspirate samples could not be determined because of the large amounts of cell debris and cells other than ASC, the confluence times obtained at this step should be interpreted reservedly, as the likeliness of initially diverging ASC numbers and variable external conditions (such as time under hypoxic stress during transportation to the laboratory) is considerable. Thus, comparisons of cell growth rates at this step suffer from immense uncertainty because of the number of unattributable confounding factors. During the study, 30 ASC samples were investigated directly after isolation (i.e. cells were cultured directly without intermediate cryopreservation). One sample did not exhibit any growth following cell isolation from lipoaspirate. Another sample became contaminated before reaching 75% confluence and had to be disgarded. Four samples exhibited growth arrest and apoptosis following initial growth during P_0. Among the remaining 25 samples, the mean time to confluence following cell isolation was 9.2 days (median 8 days), exhibiting a relatively large standard deviation of 3.7 days with a minimum of 5 days and a maximum of 20 days. Nine additional samples that had been previously cryopreserved were thawed and cultivated to 75-80% confluence. Again, an initial cell count was not performed. Time to confluence in formerly cryopreserved samples extended from a minimum of 1 day to a maximum of 5 days. All formerly cryopreserved cell samples could be successfully cultivated (figure 3).

	Growth arrest / Apoptosis during P_0	**Contamination**	**Successfully cultured to 80% confluence**
Samples isolated natively from lipoaspirates: (n=30)	4 (13.3%)	1 (3.3%)	25 (83.3%)
Samples obtained from cryopreserved cells: (n=5)	0 (0%)	0 (0%)	5 (100%)
All samples: (n=35)	***4 (11.4 %)***	**1 (2.9%)**	**30 (85.7%)**

Figure 3: Success rate of ASC cultivation in native cultivation and cultivation from formerly cryopreserved samples.

These results indicate that ASC can routinely be cultivated to 80% confluence following initial isolation from lipoaspirates or after earlier cryopreservation, albeit with the common risk of contamination inherent to all primary cell cultures from patient samples. The observed apoptosis in four primary

culture samples cannot be explained by the standardised isolation procedure. In these cases, damage to the cells sustained by prolonged transportation times to the laboratory and subsequent hypoxia, temperature differences or other factors must be considered.

3.2. Time to confluence in P_1

The majority of samples (27 out of 30 successfully isolated samples or 90%) achieved 75-80 % confluence between three and six days after being seeded in P_1 culture. All 30 samples reached the confluence level determined as the starting point for induction. The median time from seeding to induction was 6 days. Whereas 5 samples were cryopreserved prior to being induced and differentiated, 25 samples were seeded directly following their initial isolation from fresh lipoaspirates. Native samples had, on average, a growth time that was one day longer than the formerly cryopreserved samples (median time to confluence for freshly isolated samples 6.1 days versus median time to confluence for thawed samples 5.1 days). Moreover, the standard deviation among the (larger) group of native samples was almost twice that in the group of formerly cryopreserved samples (figure 4). Times to confluence in total ranged from 3 to 16 days after P_1 seeding. The longest time to confluence (16 days) was taken by a sample natively isolated from lipoaspirate, whereas a three-day period (the shortest measured) from seeding in P_1 to 75-80% confluence occurred in both natively isolated and previously cryopreserved samples. These findings suggest that, even after standardised conditions are achieved (in this case, equal cell densities after seeding), the growth rates of undifferentiated ASC are inter-individually different with larger differences occurring in freshly isolated cells. Observed differences in standard deviations and time taken to 80% confluence displayed a higher variance in freshly isolated samples than in thawed samples. This could suggest a positive selection of cells more resistant to external stress in the cryopreservation process resulting in a more homologous cell population in thawed samples.

	Mean time to 75-80% confluence	**Median time to 75-80% confluence**	**Standard deviation**
Samples obtained natively from lipoaspirates (n=25)	6.1 days	6 days	3.2 days
Samples obtained from cryopreserved cells (n=5)	5.1 days	6 days	1.9 days
All samples (n=30)	5.9 days	6 days	3.0 days

Figure 4: Mean and median time periods from seeding in P_1 to induction at 75 - 80% confluence. Also given are standard deviations for each group.

3.3. Biochemical differences

3.3.1. Adiponectin levels in culture

In general, following an initial absence of adiponectin, an increase in adiponectin concentration could be observed during the differentiation period. The vast majority of samples investigated responded to the induction and differentiation protocol with a measurable increase in adiponectin in medium supernatants. However, three samples (10.7%) did not react to differentiation in a way that would have resulted in an increase in adiponectin in medium supernatants. As figure 5 shows, only in 6 out of 28 samples (21.4%) was adiponectin detectable prior to differentiation, i.e. in the induction medium supernatant obtained on the day of differentiation. On day 2 of differentiation, adiponectin was found in 11 of the 30 samples (39.3%). 20 of 30 samples (71.4%) secreted adiponectin on day 5 of differentiation. On day 8, 22 samples (78.6%) exhibited detectable amounts of adiponectin in the medium supernatant. On the 11th day post differentiation, which was the last day on which medium supernatants were taken from all samples, 25 of 30 samples (89.3 %) secreted adiponectin (figure 5).

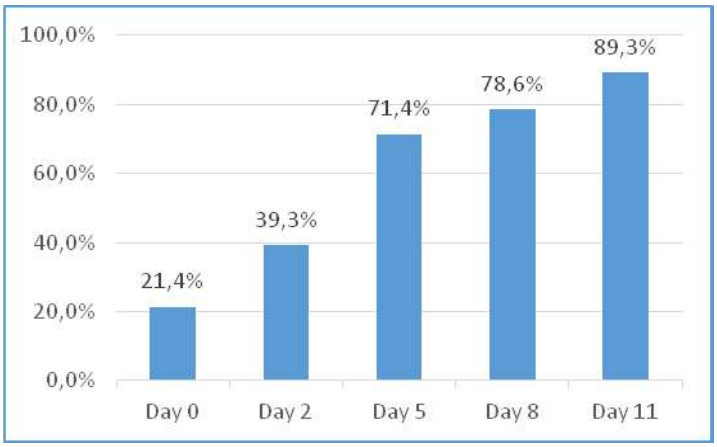

Figure 5: Percentage of adiponectin-secreting samples during differentiation.

The maximum adiponectin concentration measured in medium supernatant on day 0, prior to differentiation was 25.45 ng/ml. This increased to 30.70 ng/ml adiponectin on day 2 of differentiation and to 120.85 ng/ml adiponectin on day 5 of differentiation. On day 8, the highest measured adiponectin concentration was 120.27 ng/ml. On day 11 post differentiation, the highest absolute adiponectin level was recorded at 162.27 ng/ml. Of note, whereas the highest adiponectin levels on days 0 and 2 were obtained from different samples, the highest adiponectin levels on days 5, 8 and 11 were all measured in supernatants of the same sample. The sample in this case had been natively

isolated from lipoaspirate and had exhibited a time to confluence in P_0 of 6 days and a time of confluence in P_1 of 4 days.

In general, beginning at day 5 of differentiation, an increase in adiponectin secretion, not only as measured by the total number of adiponectin-secreting samples, but also by the rate of adiponectin secretion, was mirrored by the mean and median adiponectin secretion per sample. The mean adiponectin secretion on day 2 post differentiation was 4.88 ng/ml (or 5.52 ng/ml when non-differentiating samples were excluded) and the median adiponectin concentration was 0 ng/ml in both groups (all samples and excluding non-responders to differentiation). This had changed on day 5 post differentiation, when the mean adiponectin concentration was 33.61 ng/ml overall (37.64 ng/ml with non-responders to differentiation excluded) with the median adiponectin concentration in both groups amounting to 23.73 ng / ml. Although total adiponectin secretion continued to increase over the following days, the rate of secretion showed a continuous decrease. Mean and median adiponectin levels on day 8 of differentiation had risen to 42.00 ng/ml and 29.08 ng/ml (or 47.04 ng/ml and 34.22 ng/ml, respectively, excluding the non-differentiating samples) and to 48.72 ng/ml and 32.40 ng/ml (or 54.57 ng/ml and 39.87 ng/ml excluding non-differentiating samples) on day 11 of differentiation (figures 6, 7 and 8).

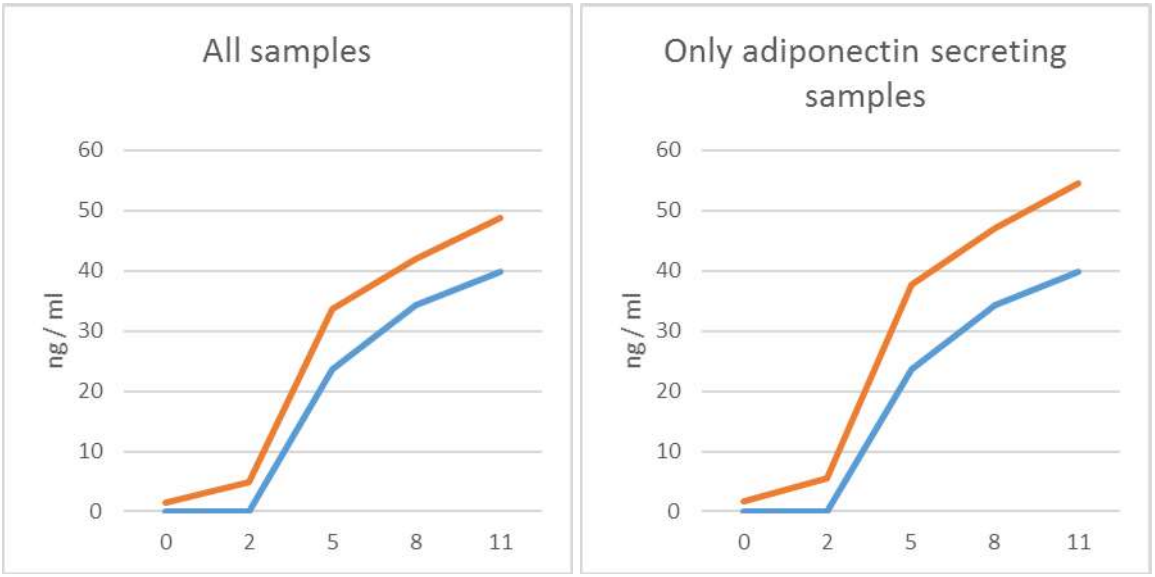

Figure 6: Mean (red) and median (blue) adiponectin level concentrations in ng / ml in medium supernatants taken on days 0, 2, 5, 8 and 11 of the differentiation process.

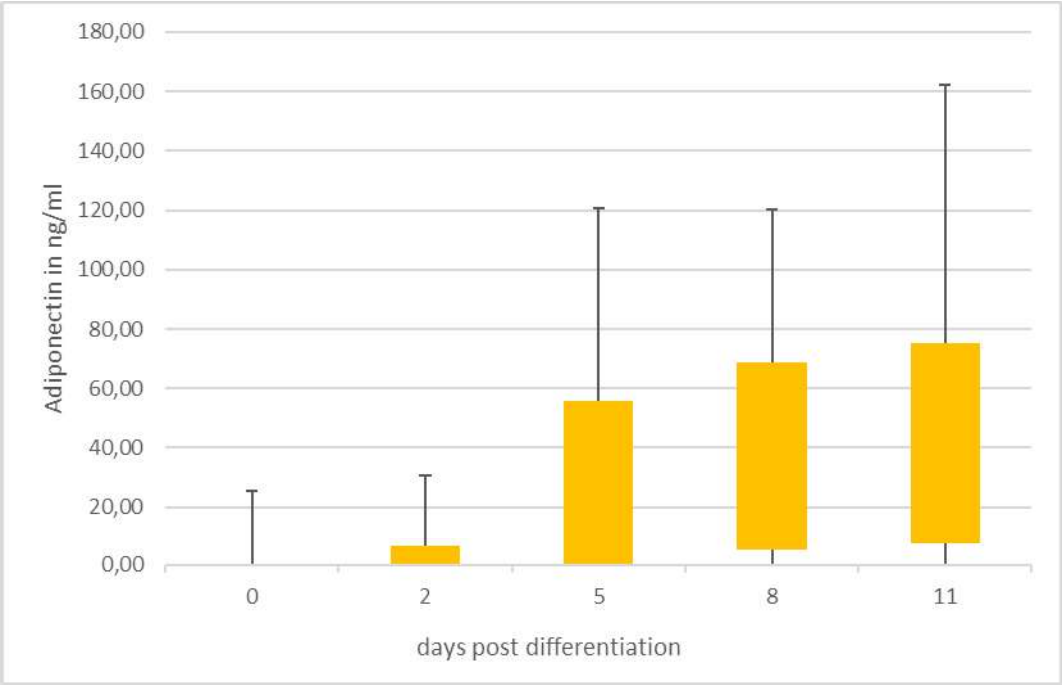

Figure 7: Boxplot of adiponectin levels in medium supernatants taken on day 0, 2, 5, 8 and 11 of differentiation. This figure includes all samples (also non-differentiating). The box indicates the p25 and p75 quartiles, whereas thin lines show minima and maxima.

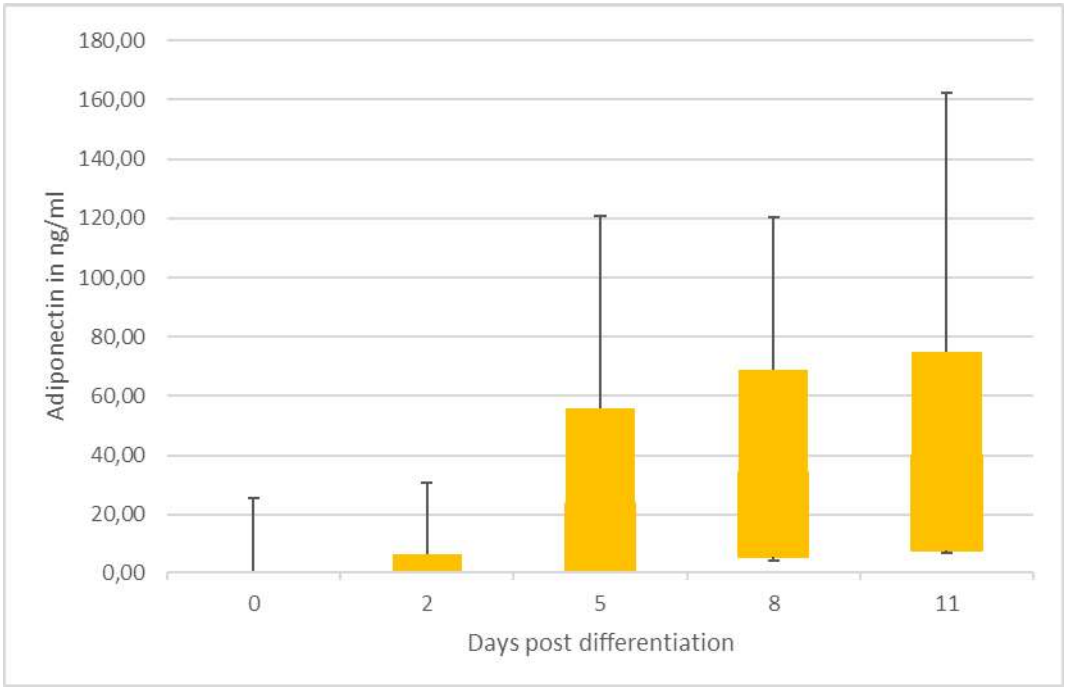

Figure 8: Boxplot of adiponectin levels in medium supernatants taken on day 0, 2, 5, 8 and 11 of differentiation. This figure excludes non-differentiating samples. The box indicates the p25 and p75 quartiles, whereas thin lines show minimums and maximums.

All 11 samples (39.3%) that were adiponectin-positive on day 2 of differentiation maintained robust adiponectin secretion throughout the differentiation process. Out of the samples that would (eventually) secrete adiponectin, only 3 samples (12%) failed to be adiponectin-positive on day 5 of differentiation. Furthermore, 2 of those 3 samples exhibited the lowest and the second lowest

adiponectin concentration on day 11 of differentiation. Interestingly, these low adiponectin secreting samples were all obtained from previously cryopreserved cells, possibly indicating cell-damage resulting in impaired differentiation potential. Of the samples, 14 exhibited their peak adiponectin level (as shown by ELISA) on the 11th day, 6 on the 8th day of differentiation and 4 on the 5th day of differentiation. Relativising these findings, the mean difference between the highest measured adiponectin level and the adiponectin level on day 11 of differentiation was only 2.2 ng/ml (standard deviation 5.1 ng/ml). The largest measured difference in between the highest and lowest adiponectin level was 25.4 ng/ml. A lower adiponectin-level steady state instead of a peak with a subsequent decrease in this protein.

The results of the analysis of adiponectin levels during the differentiating culture of ASC are twofold. First, in most cases, samples secreted adiponectin from a certain point in their differentiation process, with the adiponectin level either increasing steadily or reaching a plateau or steady secretion rate at some point of differentiation. Second, the absolute amount of adiponectin secreted varied greatly inter-individually.

3.3.2. VEGF levels in endothelial progenitor cell – ASC co-culture

To monitor the progress of V2a-cell differentiation, a VEGF ELISA was performed. Since V2a growth medium was changed every other day, the VEGF concentration measured reflects two days of VEGF secretion by the cells (unlike the adiponectin ELISA, whereby the adiponectin concentration measured reflected the total adiponectin secretion from the time of the initiation of differentiation). Overall, in co-culture wells, VEGF was present in all but 4 (3.6%) samples, at least at one measurement point. VEGF levels in the samples were generally lower (mean VEGF overall 138 ng/ml; ranging from 59 ng/ml to 200 ng/ml) than VEGF levels in the positive control (VEGF in V2a growth medium with a mean VEGF of 626 ng/ml; albeit this is composed of VEGF added to the medium and cell-secreted VEGF) and VEGF levels in the negative control (suramin in V2a growth medium with a mean VEGF of 138 ng/ml). Of note, these lower VEGF levels did not curb endothelial cell differentiation as visualised by anti-CD31 immunostaining, thus underlining the importance of intracellular interaction in this experimental setup. In some samples, endothelial differentiation was comparable with those observed in the positive control, whereas close to no tubule formation was detectable in negative controls (see also 3.4.2.). Whereas VEGF was generally lower on day 0 (i.e. before the co-culture was established by the addition of ASC) with mean VEGF amounting to 59 ng/ml and ranging from 6 ng/ml to 57 ng/ml, VEGF means lay between 92 ng/ml and 200 ng/ml. VEGF levels in individual days spanned from 0 ng/ml to 213 ng/ml on day 2 of co-culture, from 0 ng/ml to 258 ng/ml on day 4, from 36 ng/ml to 256 ng/ml on

day 6, from 42 ng/ml to 297 ng/ml on day 8, from 18 ng/ml to 183 ng/ml on day 10 and from 14 ng/ml to 439 ng/ml on the 12th and last day (figure 9).

	Minimum	Maximum	Mean	Standard deviation
Before co-culture start	6.5	86.7	58.6	29.6
Day 0 to day 2	0.0	213.3	69.4	69.7
Day 2 to day 4	0.0	257.6	139.4	75.3
Day 4 to day 6	36.6	256.3	148.0	73.0
Day 6 to day 8	41.9	297.1	151.3	73.6
Day 8 to day 10	18.1	182.8	94.0	59.3
Day 10 to day 12	14.2	439.0	200.1	131.4
Overall (all samples, day 0-12)	0.0	439.0	137.9	92.1

Figure 9: Minima, maxima, means and standard deviations of VEGF levels (in ng/ml) over various periods of time and overall. "Before co-culture start" refers to a VEGF ELISA performed on growth medium and V2a cells before addition of ASC.

VEGF concentration in the VEGF positive control ranged between 325 ng/ml and 1265 ng/ml over the 14-day period. As mentioned above, this represents the sum of the external VEGF added into the medium as a stimulus of EC differentiation and EC-secreted VEGF.

When VEGF levels dependent on time were analysed further, statistically significant different variances ($p<0.05$) were found between the VEGF levels prior to the addition of ASC and VEGF levels on the day 2 to day 4, day 4 to day 6, day 6 to day 8 and day 10 to day 12 periods. Furthermore, VEGF levels during the day 8 to day 10 period were statistically significantly ($p<0.05$) lower than those of the day 6 to day 8 and day 10 to day 12 periods (figure 10).

	d 10 – d 12	d 8 – d 10	d 6 – d 8	d 4 – d 6	d 2 – d 4	d 0 – d 2
d 0	*	n	*	*	*	n
d 0 – d 2	n	n	n	n	n	
d 2 – d 4	n	n	n	n		
d 4 – d 6	n	n	n			
d 6 – d 8	n	*				
d 8 – d 10	*					

Figure 10: Table of statistically significant differences in VEGF levels during cultivation intervals. "n" indicates no statistical significance ($p>0.05$); "" indicates statistical significance ($p<0.05$). Note that, where indicated, VEGF on d 0 (prior to addition of ASC) was significantly lower than that in the compared groups. Also, VEGF in the d 8 – d 10 interval was statistically significantly lower than the respective groups.*

Nine samples (50%) had their respectively highest VEGF secretion in the day 10 – day 12 (i.e. last) interval, four (22.2%) in the day 8 – day 10 interval, one (5.6%) at the day 6 – day 8 interval, one (5.6%) at the day 4 – day 6 interval, three (16.7%) at the day 2 – day 4 interval and none at the day 0 – day 2 interval. The samples that peaked their VEGF secretion in the day 10 – day 12 interval exhibited a mean peak VEGF concentration of 318 ng/ml, whereas those that peaked their VEGF secretion earlier had a lower mean peak VEGF concentration (day 8 – day 10: 148 ng/ml, day 6 – day 8: 194 ng/ml (only one sample), day 2 – day 4: 183 ng/ml). Connecting these findings allows two general forms of VEGF secretion to be discerned: first, a continuous increase in VEGF secretion over the cultivation time and, second, a peak in VEGF concentration before the end of the co-culture period followed by a VEGF secretion lower than the peak value. The differences in VEGF concentrations between the two groups were found to be highly ($p<0.005$) statistically significant (figure 11).

	Minimum	**Maximum**	**Mean**	**Standard deviation**
Continuous increase in VEGF secretion	238.7	439.0	318.1	64.9
Peak in VEGF secretion during co-culture period	81.4	257.6	163.2	53.3

Figure 11: Minima, maxima, means and standard deviations of peak VEGF concentrations (in ng/ml) in the two groups "continuous increase of VEGF secretion" and "peak in VEGF secretion during co-culture period". The variances are statistically highly significant ($p<0.005$).

3.3.3. Proof of Multipotency - Adipogenic, Osteogenic and Chondrogenic differentiation

During the process of adipogenic differentiation, cells undergo a phase of growth arrest that is induced by components of the induction medium. During the growth phase, immature adipocytes are morphologically similar to fibroblasts. After the induction of differentiation, the cells take on a spherical shape, accumulate lipid droplets and progressively acquire the morphological and biochemical characteristics of mature white adipocytes. Oil-Red O staining established the adipogenic potential of the ASCs by staining intracellular lipid droplets. As shown in Figure 12 a significant fraction of cells contained many intracellular lipid-filled droplets that accumulated Oil Red –O as a marker for adipogenic differentiation.

Induction of osteogenesis lead to the process of mineralisation, with induced osteoblasts producing extracellular calcium deposits in vitro. These deposits can specifically be stained with Alizarin Red S and establish successful in vitro bone formation (figure 12b).

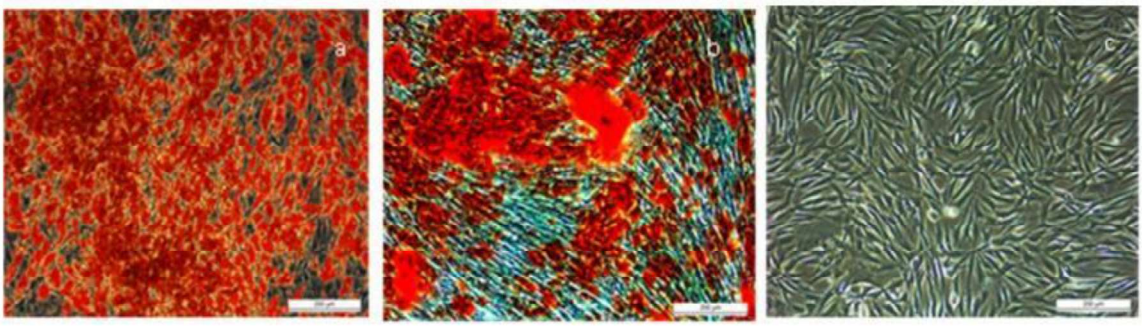

Figure 12 Representative light microscopic images of adipogenically and osteogenically differentiated ASCs (10x magnification)

a) *intracellular oil-red-stained lipid droplets at day 7 post induction and differentiation.*
b) *Extracellular calcium deposits stained with alizarin red as a marker for osteogenic differentiation on day 24 of differentiation*
c) *Undifferentiated cells*

Chondrogenic differentiation was also carried out but, because of the spheroid nature of the differentiated chondrocytes, staining with alzian blue was difficult to show by means of light microscopy.

3.4. Flow cytometric (FACS) Analysis of ASC

3.4.1. Cell Yield

Flow cytometry was used to determine the yield of five different cell samples cultivated according to the protocol.

The forward side scatter (FSC), which appears on the x-axis, is proportional to cell-surface area and size, whereas the side scatter (SSC), which can be seen on the y-axis, represents the granularity and internal complexity of the cells. A clear majority of the cells (a minimum of 75.8%) were shown to be viable. The exact values of the viable cells were: 75.8%, 77.1%, 80.3%, 84.5% and 88%. Figure 13 below shows a representative dot blot of a cell sample.

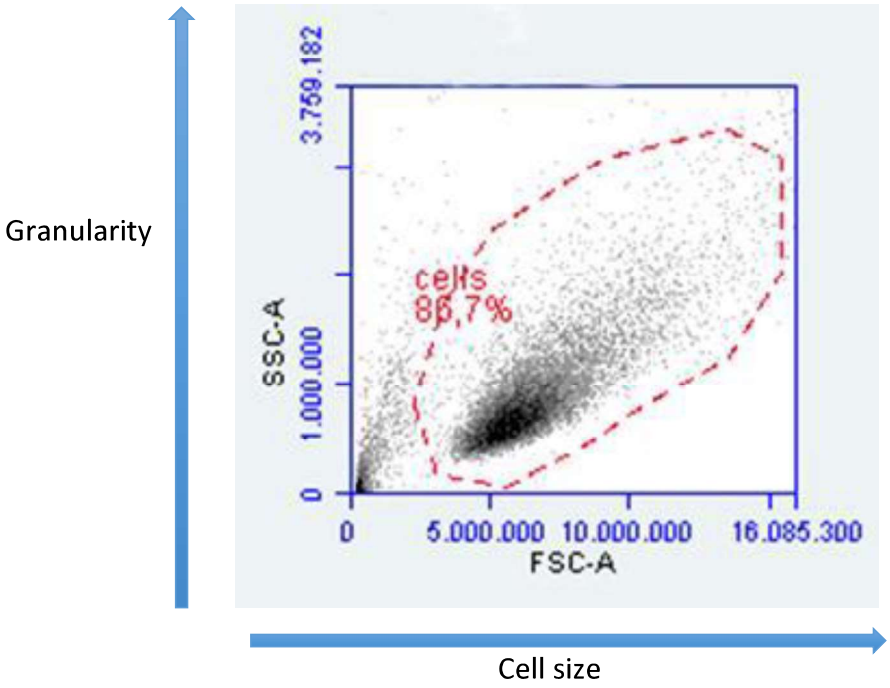

Figure 13: Scatter blot of representative cell sample.

3.4.2. Surface Marker Patterns on Analysed Cells

Once the presence of a high percentage of living cells had been confirmed in the analysed sample, a test was undertaken for antigen patterns indicating the multipotency of the cells. To rule out the presence of significant amounts of endothelial cells or non-mesenchymal stem cells (i.e. haematopoietic cells), samples were first tested for endothelial cell marker CD31 (PECAM-1) and haematopoietic stem cell marker CD34 (figure 14). In none of the five samples (0 %) could CD31 and CD34 be detected simultaneously, e.g. one sample exhibited CD31 positivity levels exceeding 1% (6%) but no CD34. The analysed cells were found to express commonly accepted cell lineage markers for

mesenchymal stem cells, namely CD29 (beta 1 integrin), CD44 (homing cell adhesion molecule, HCAM), CD73 (5' ribonucleotide phosphohydrolase) and CD90 (thymus cell antigen, Thy-1), as exemplified in figure 16. A detailed summary of the percentage of marker positive cells can be found in the following table (figure 14).

	Sample 1	Sample 2	Sample 3	Sample 4	Sample 5
CD 73	96	98.5	56	97	60
CD 90	76	96	6	6	77
CD29	97	98.3	97	95	98
CD 44	98	99.6	66	60	15
CD 14	0	0	0	0	0
CD 34	0	0	0	0	0
CD 31	1	6	1	1	1
HLA-DR	0.2	0.5	0	0	0

Figure 14: Comparison of marker expression in flow cytometric analysis of five randomly selected cell samples (percentages). Note that, in all samples, a clear majority of cells expressed stem cell markers and a significant contamination with CD31+ endothelial cells or CD34+ haematopoietic stem cells could not be detected.

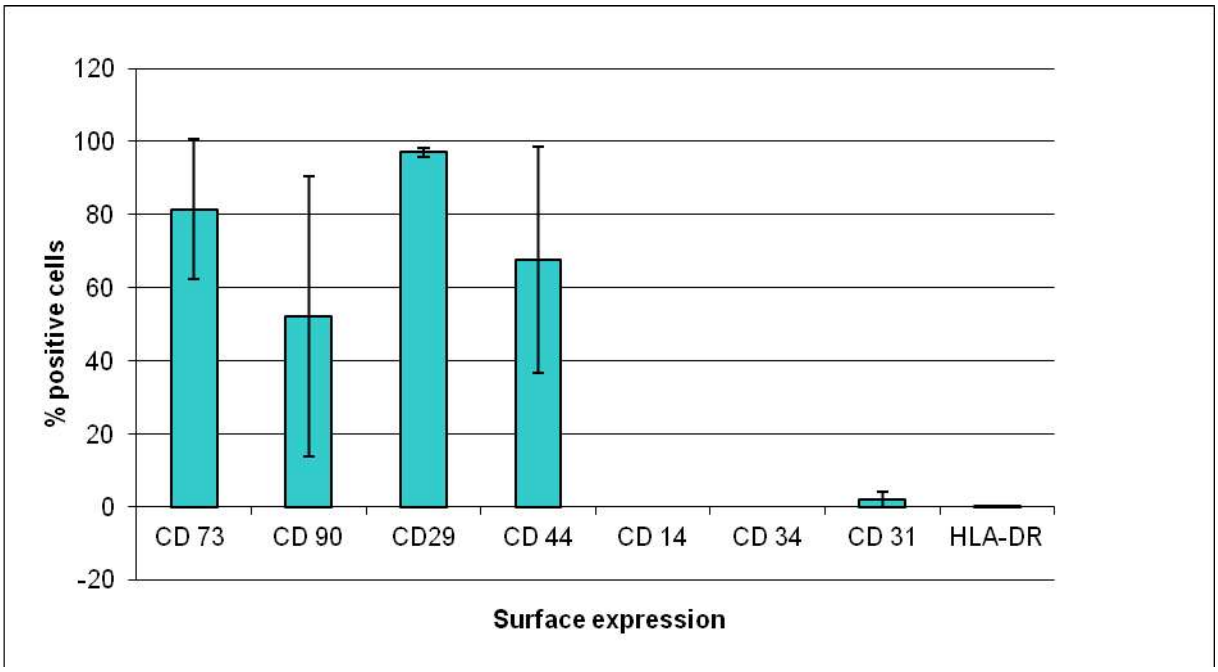

Figure 15: Comparison of marker expression in flow cytometric analysis of five randomly selected cell samples. Note that, in all samples, a vast majority of cells expressed stem cell markers and a significant contamination with CD31+ endothelial cells or CD34+ haematopoietic stem cells could not be detected.

In figure 15, the dot plot analysis of patient 2 demonstrates the positively labelled ASCs, which are also negative for CD34 and HLA-DR. These findings indicate that the native cells obtained after purification of the lipoaspirate are indeed either MSC or committed adipocyte progenitor cells at an early stage of differentiation.

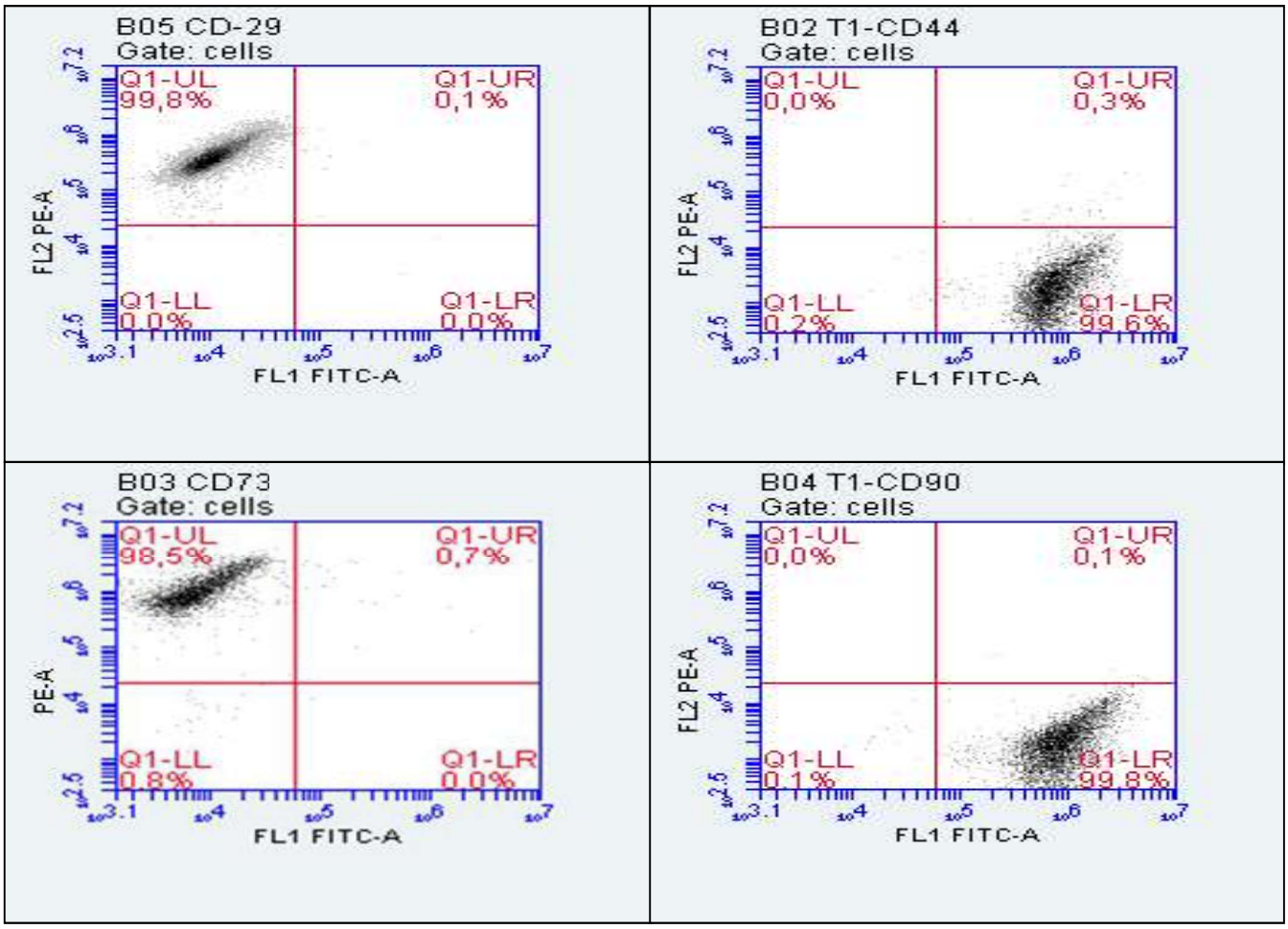

Figure 16: Flourescence activated cell sorting (FACS) used to demonstrate positivity for CD29, CD44, CD73, and CD90 of the analysed cells. Fluorescence 1 (FL1) on the x-axis represents cells positive for FITC and the Fluorescence 2 on the y-axis stands for cells positively labelled with antibodies conjugated either with PE or APC

In conclusion, the flow cytometric experiments were successful in demonstrating: (1) a high percentage of living cells in the analysed sample, (2) the absence of significant contamination of endothelial cells/fibrocytes (which would macroscopically be difficult to differentiate from adipogenic precursor cells) and (3) support for the hypothesis of the feasibility of obtaining a purified culture of cells exhibiting MSC lineage markers by using simple cultivation technique of the reported experiments. Thus, the cells investigated can be concluded to be, at least to a high percentage, mesenchymal stem cells and thus ASC.

3.5. Histological Findings

3.5.1. Qualitative Morphological Variances in Oil-red-stained Cultures

Oil-red staining proved to be a very useful method for qualitative microscopic analysis of adipocytes. Lipids (intracellular lipid droplets) appear in a bright orange-red shade after staining, whereas cell

outlines remain visible in bright field microscopy. Cell culture samples were analysed by using the aforementioned bright field microscopy following the completion of the 12-day differentiation period and most samples exhibited at least some degree of lipid droplet formation. Samples responded to the differentiation medium with variable lipid droplet formation. Cells generally adopted a fusiform shape and spread evenly across the well surface. Not all cells of a given sample formed microscopically visible lipid droplets, with lipid-droplet-forming cells congregating in thread-like or cluster formations. Moreover, samples that exhibited lower lipid droplet formation tended to be characterised by a higher prevalence of less fusiform but more spherical adipocytes. As expected, adiponectin levels seemed to correlate with lipid droplet formation. Accordingly, sample 2, which exhibited a later onset of adiponectin secretion, was found to consist of many cells that had apparently not initiated lipogenesis until late in the differentiation process or had arrested lipogenesis during differentiation. In short, whereas samples generally responded to the differentiative treatment, the overall amount of lipogenesis exhibited inter-individual differences. These differences could not be accounted for by factors investigated in the work reported this thesis. Six different representative oil-red-stained samples illustrating the aforementioned variances are presented below.

Sample 1:

ASC in this sample were freshly isolated from lipoaspirate on the same day that it was obtained from a 34-year-old healthy female patient undergoing aesthetic breast surgery. Time in P_0 until 80% confluence was 8 days (mean time 8.6 days); time in P_1 until induction at 80% confluence was 14 days (mean time 6.3 days, 14 days being the 2^{nd} longest time to confluence). Adiponectin was first detectable on day 2 of differentiation at a level of 20.3 ng/ml. This level rose to 41.9 ng/ml on day 5 of differentiation, peaked at 47. 4 ng/ml on day 8 of differentiation and fell slightly to 45.4 ng/ml on day 11 of differentiation. Bright field microscopy revealed consistent lipid droplet formation in most cells, with many of the cells having numerous lipid droplets; higher magnifications revealed that almost all cells had initiated the synthesis of lipids. Moreover, cells were of the typical fusiform shape and no signs of significant apoptosis were detectable. Figure 17 is a representative image.

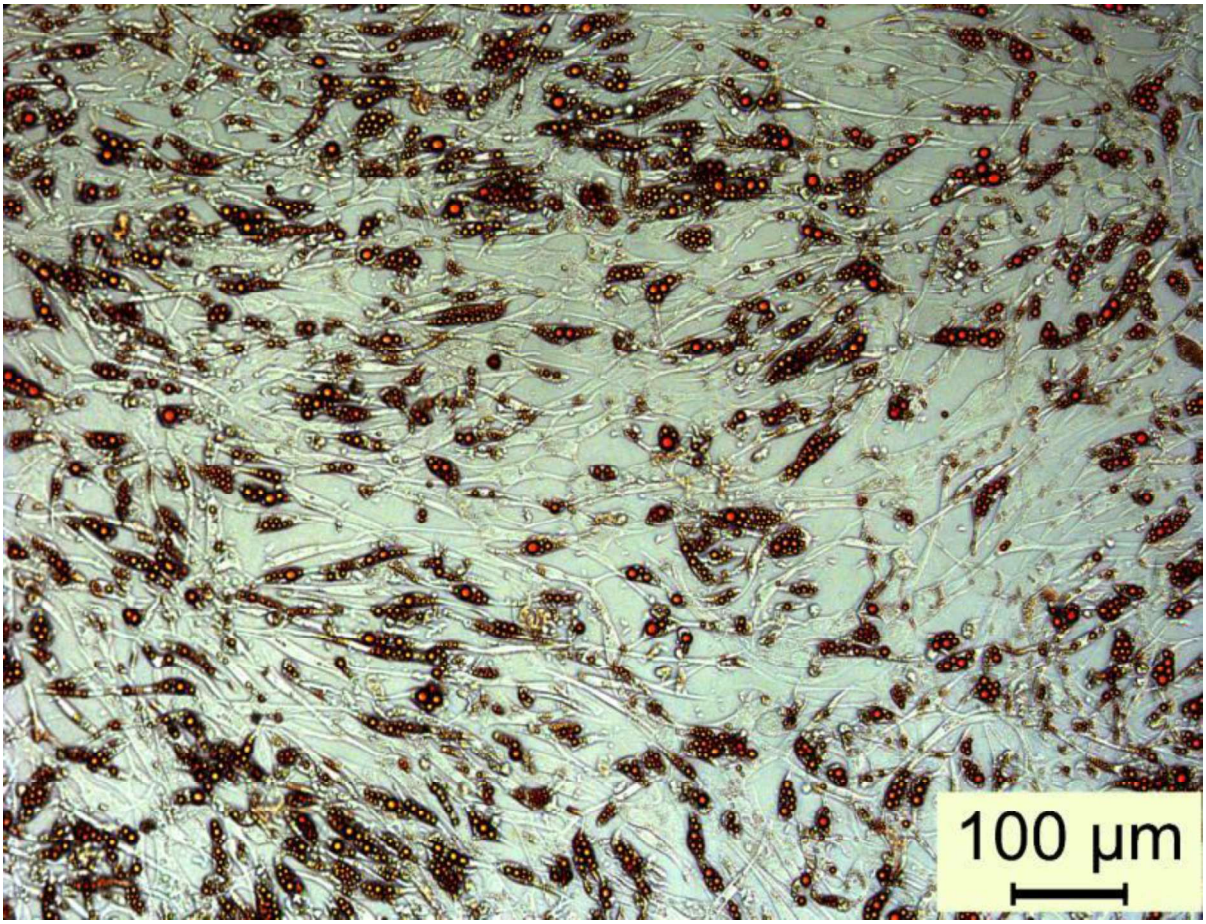

Figure 17: Sample 1, representative section, oil-red-stained.

Sample 2:

ASC in this sample were freshly isolated from lipoaspirate on the same day that it was obtained from a female patient. Time from isolation to 80% confluence was 15 days (mean time 8.6 days; 15 days being the 2nd longest time to confluence); time in P_1 to induction was 6 days (mean time 6.2 days). Adiponectin was first detectable on day 5 of differentiation at a level of 12.6 ng/ml. It rose to 36.0 ng/ml on day 8 of differentiation and peaked at 42.2 ng/ml at day 11 of differentiation. Cells in this sample were of a considerably stretched but fusiform appearance and not all cells appeared to have initiated lipogenesis. Those cells that had, however, exhibited significant lipogenesis with many medium to large-sized droplets. Upon closer inspection, minimal lipid storage could be detected in almost all cells. No significant signs of apoptosis were found. Figure 18 shows a representative view of these cells.

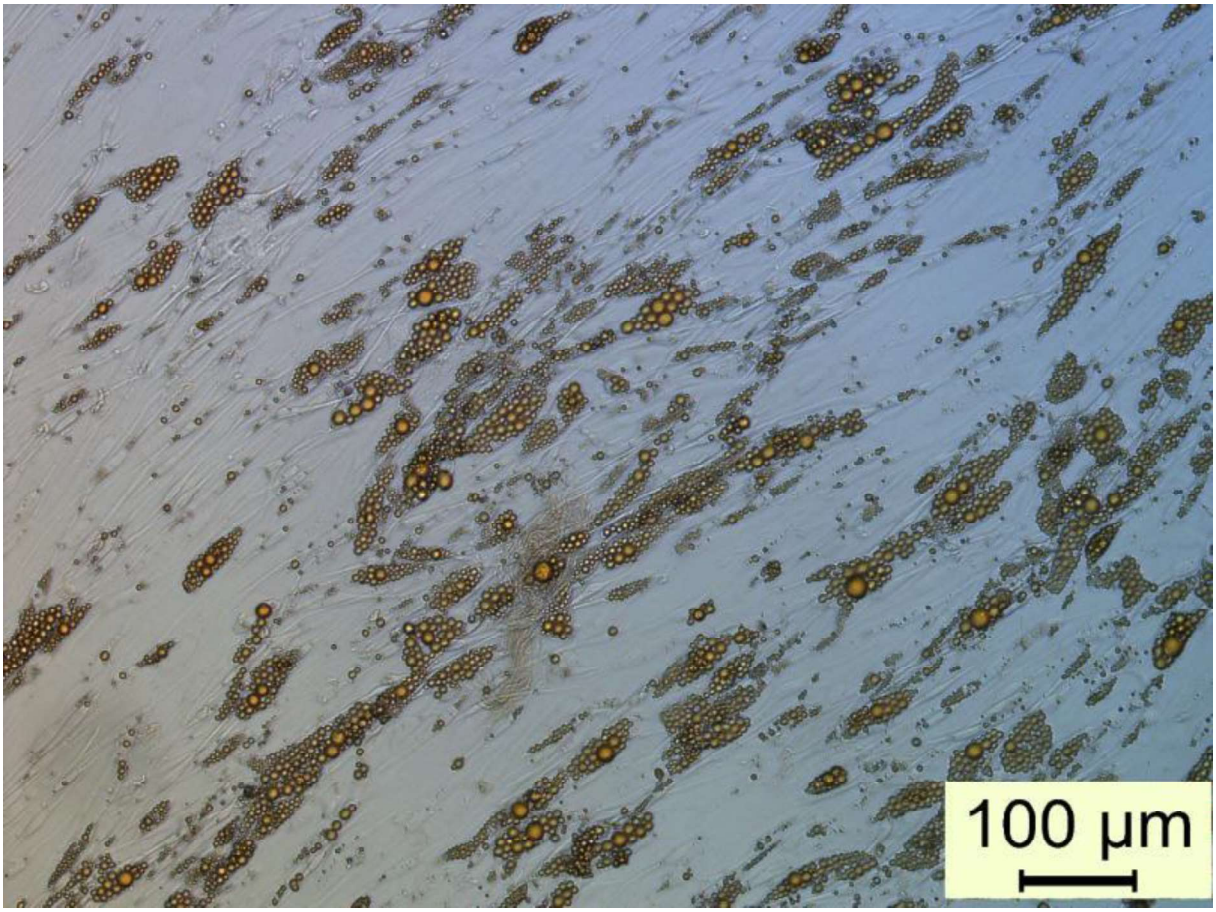

Figure 18: Sample 2, representative section, oil-red-stained.

Sample 3:

ASC in this sample were freshly isolated from lipoaspirate on the same day that it was obtained from a 57-year-old female patient with a past medical history of breast cancer. Time from isolation to 80% confluence was 7 days (mean time 8.6 days); time in P_1 to induction was 4 days (mean time 6.2 days). These growth times identify the sample as growing faster than average, although not being in the fastest growing group. Adiponectin was first detectable on day 2 of differentiation at a level of 2.4 ng/ml. Day 5 saw adiponectin at 33.7 ng/ml; it peaked on day 8 with 41.2 ng/ml adiponectin. On day 11 of differentiation, adiponectin levels had decreased to 35.6 ng/ml. The cells in this sample were uniformly fusiform and almost all exhibited lipid droplet formation. Most cells had numerous lipid droplets that were small to medium in size; no apoptosis was detectable. Figure 19 shows a representative image.

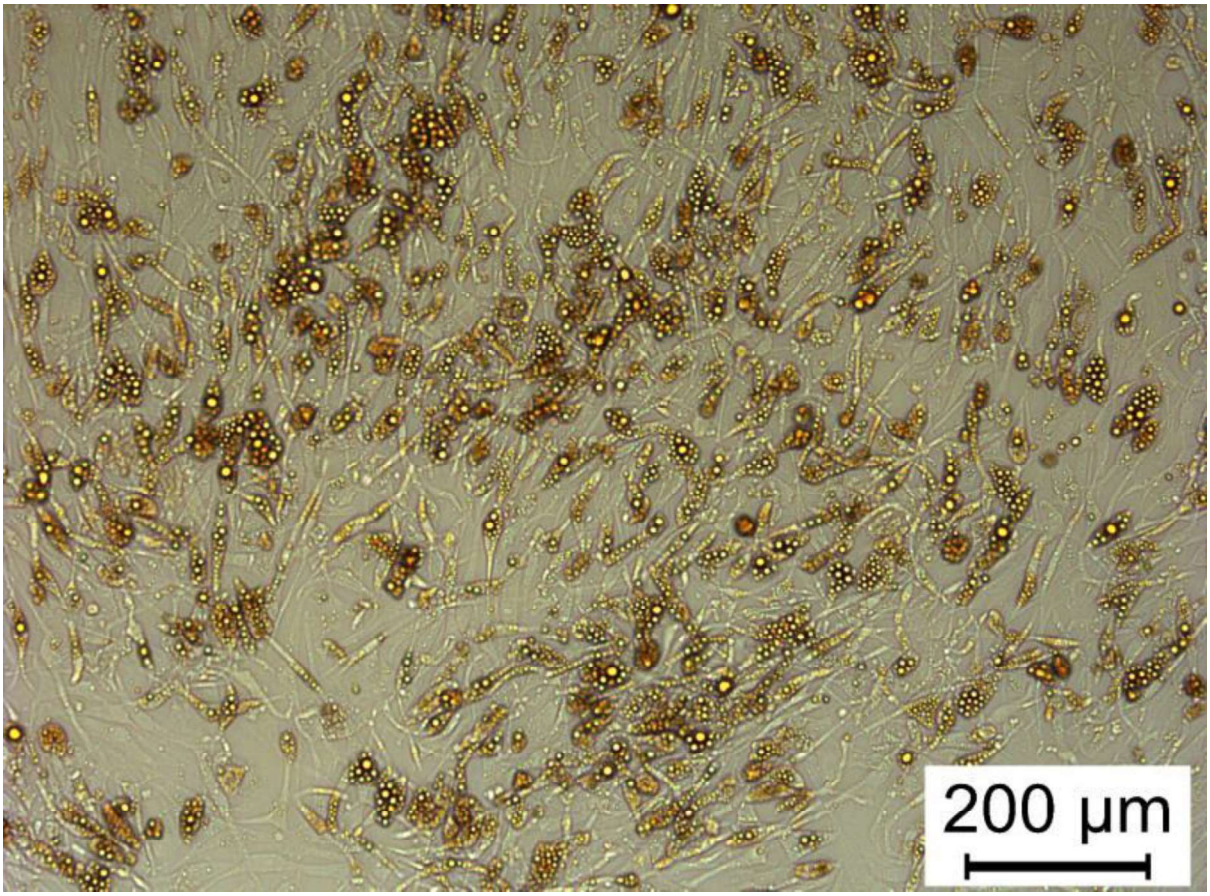

Figure 19: Sample 3, representative section, oil-red-stained.

Sample 4:

ASC in this sample were freshly isolated from lipoaspirate on the same day that it was obtained from a 54-year-old female patient undergoing breast reconstruction following subtotal breast resection after breast cancer. Time from isolation to 80% confluence was 6 days (mean time 8.6 days); time in P_1 to induction was 4 days (mean time 6.2 days). These growth times identify the sample as growwing faster than average, although some samples grew even faster. Adiponectin was first detectable on day 2 of differentiation at 4.1 ng/ml, increased to 54.7 ng/ml on day 5 and peaked at 64.6 ng/ml on day 8 before decreasing to 63.0 ng/ml on day 11. Unlike sample 3, cells in sample 4 did not differentiate and engage in lipogenesis homogeneously, despite being of a fusiform shape. Instead, a slight majority of cells created many medium to large lipid droplets, while the rest only showed minimal lipogenesis. No apoptosis was detectable. Figure 20 shows a representative region of the sample.

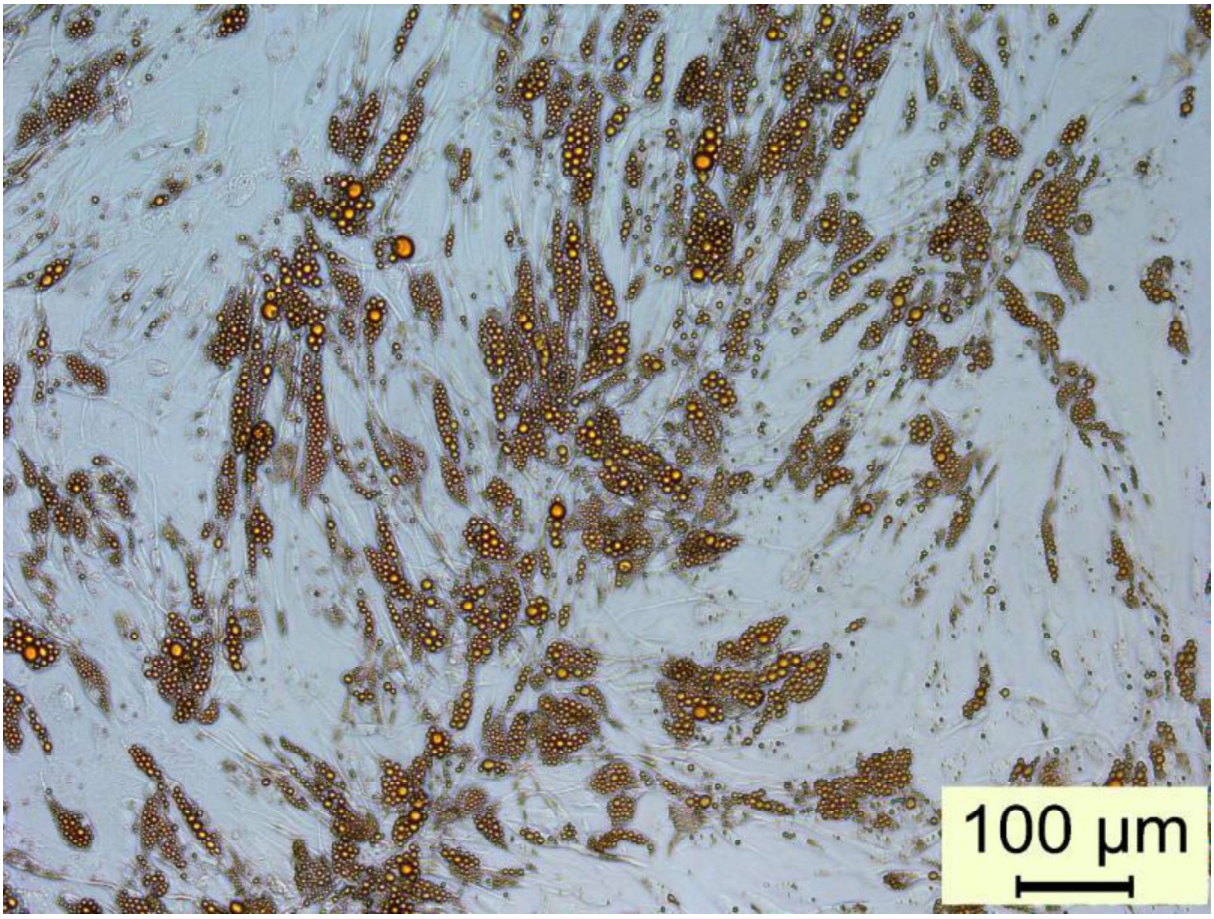

Figure 20: Sample 4, representative section, oil-red-stained.

Sample 5:

ASC in this sample were freshly isolated from lipoaspirate on the day after it was obtained from a 24-year-old female patient. Time from isolation to 80% confluence was 8 days (mean time 8.6 days); time in P_1 to induction was 6 days (mean time 6.2 days). It was, in this respect, a most average sample. Adiponectin was first detected on day 5 of differentiation, when it was measured 46.7 ng/ml. It remained at that level on day 8 and increased to 68.9 ng/ml on day 11 of differentiation. This sample exhibited strong lipogenesis with medium to large lipid droplets in approximately 75% of cells, while the remaining cells showed no lipogenesis. No indications of apoptosis were seen in any cells. Figure 21 depicts a representative section of the sample (note the higher magnification of this stitched image).

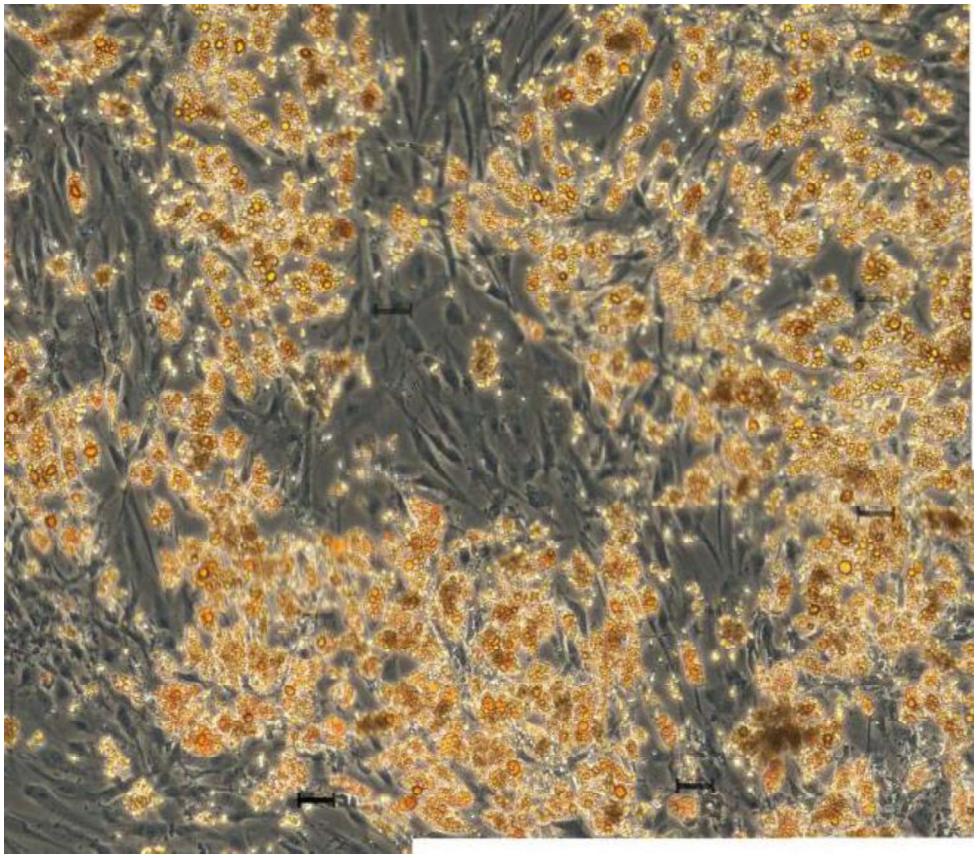

Figure 21: Sample 5, representative section, oil-red-stained, stitched image (note the various scale bars).

Sample 6:

ASC in this sample were freshly isolated from lipoaspirate on the day after it was obtained from a 36-year-old female patient undergoing breast reconstruction following removal of multiple benign cysts. Time from isolation to 80% confluence was 7 days (mean time 8.6 days); time in P_1 to induction was 6 days (mean time 6.2 days). Thus, whereas initial confluence occurred faster than average, time to confluence in P_1 was average. Adiponectin was detectable even on day 0 (i.e. in induction medium at the beginning of differentiation) at 1.7 ng/ml. Adiponectin had decreased to 0.9 ng/ml on day 2 of differentiation but surged to 71.1 ng/ml on day 5 and peaked at 100.5 ng/ml on day 8 of differentiation. On day 11, adiponectin levels had decreased slightly to 95.6 ng/ml. Cells in this sample exhibited inhomogeneous lipogenesis with some, but only a few, cells forming numerous small to medium-sized lipid droplets, whereas the majority of cells did not engage in lipogenesis. Furthermore, lipid-rich cells were found in clusters surrounded by irregularly formed non-lipogenic cells. Apoptosis was not detectable. Two representative regions of the sample are presented in figure 22.

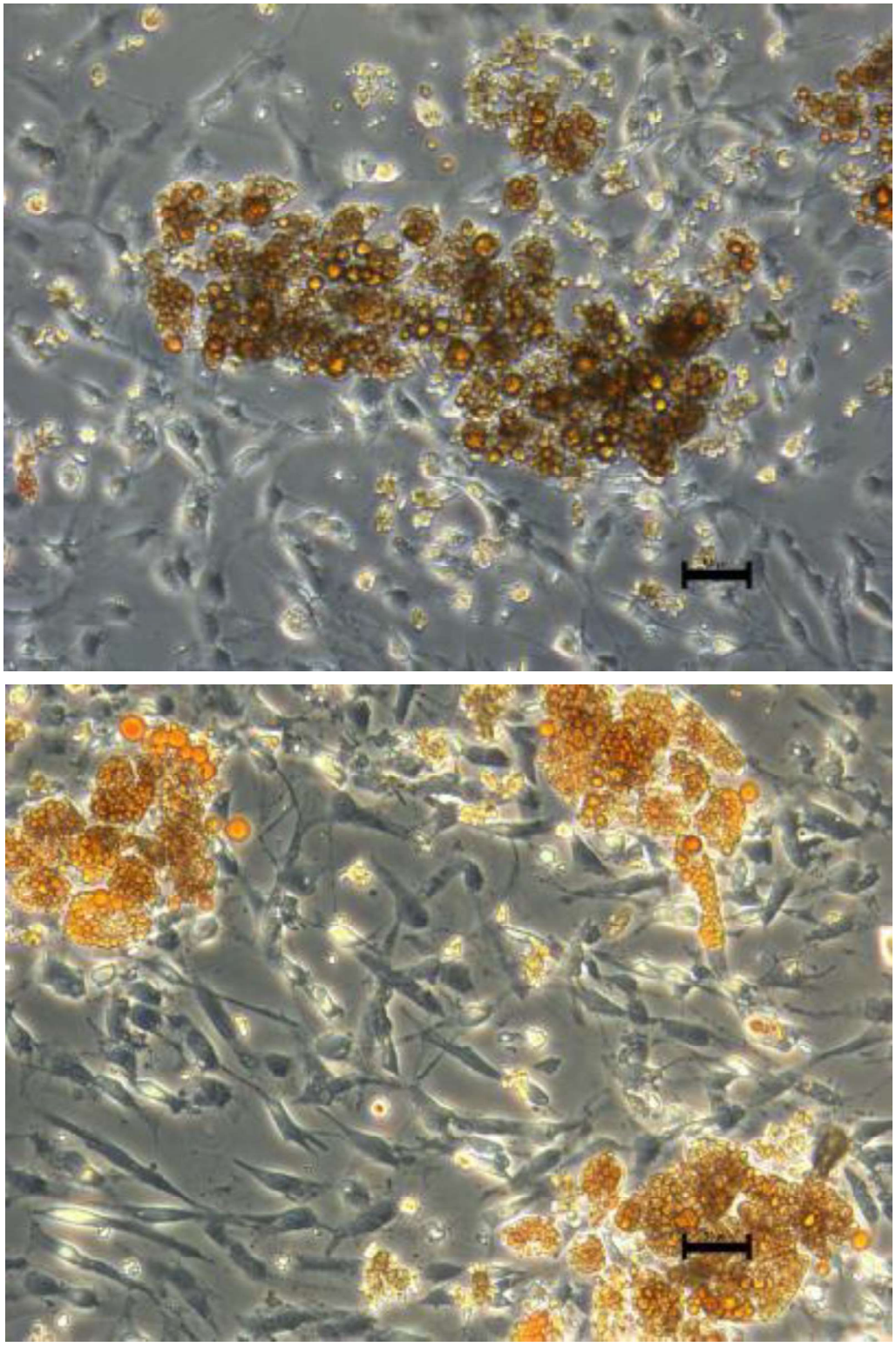

Figure 22: Sample 6, two different representative regions, oil-red-stained.

3.5.2. Variances in Anti-CD31 Immunostained Adipocyte Derived Stem Cell – Endothelial Progenitor Cell Co-cultures

To determine the extent of endothelial differentiation as indicated by immunostaining, in addition to visual inspection, the percentage of the total well surface area covered by CD31+ cells was quantified by using ImageJ and the applying a colour threshold, after which the percentage of coloured/CD31+ well surface area was calculated. Samples were assayed in duplicates (9 sets of samples) or triplicates (9 sets of samples) with respective amounts of endothelial differentiation in one set of samples and were statistically comparable (i.e. no statistically significant variance could be found) (figure 23).

Sample #	Minimum	Maximum	Mean	Standard deviation
1	5.78%	5.96%	5.87%	0.13%
2	27.7%	28%	27.85%	0.21%
3	7.01%	10.49%	8.75%	2.46%
4	13.9%	19.2%	16.55%	3.75%
5	14.16%	20.68	17.42%	4.61%
6	25.19%	25.81%	25.5%	0.44%
7	20.04%	23.98%	22.01%	2.79%
8	11.75%	20.44%	15.58%	3.75%
9	18.47%	18.59%	18.53%	0.08%
10	12%	32%	18.71%	11.51%
11	5.53%	9.99%	7.71%	2.23%
12	10.73%	15.68%	13.03%	2.49%
13	15.67%	45.4%	31.7%	15%
14	54.17%	56.88%	55.54%	1.92%
15	43.9%	48.19%	46.46%	2.26%
16	53.41%	62.58%	59%	4.90%
17	40.01%	65.96%	51.82%	13.13%
18	43.17%	56.08%	48.15%	6.94%
VEGF control	16.41%	25.77%	21.63%	2.86%
Suramin control	4.26%	10.8%	6.63%	2.23%
Medium only control	3.2%	11.4%	6.38%	2.48%

Figure 23: Minimum, maximum, mean and standard deviation of the percentage of the surface area of the well covered with CD 31+ cells. All analysed samples and all controls are included. Samples 1-7, 9 and 14 were assayed in duplicate and the remaining samples in triplicate.

Notably, 15 of the 18 samples evoked a marked increase in differentiated endothelial CD31+ cells compared with negative and medium-only controls, which also exceeded the differentiative response of the VEGF-positive control. However, samples 1, 2 and 11 exhibited low CD31+ differentiation in the negative control. In medium-only or negative-control wells, endothelial differentiation was significantly ($p < 0.05$) lower than in the aggregate of all samples, including the low-response samples 1, 2 and 11 (figure 24).

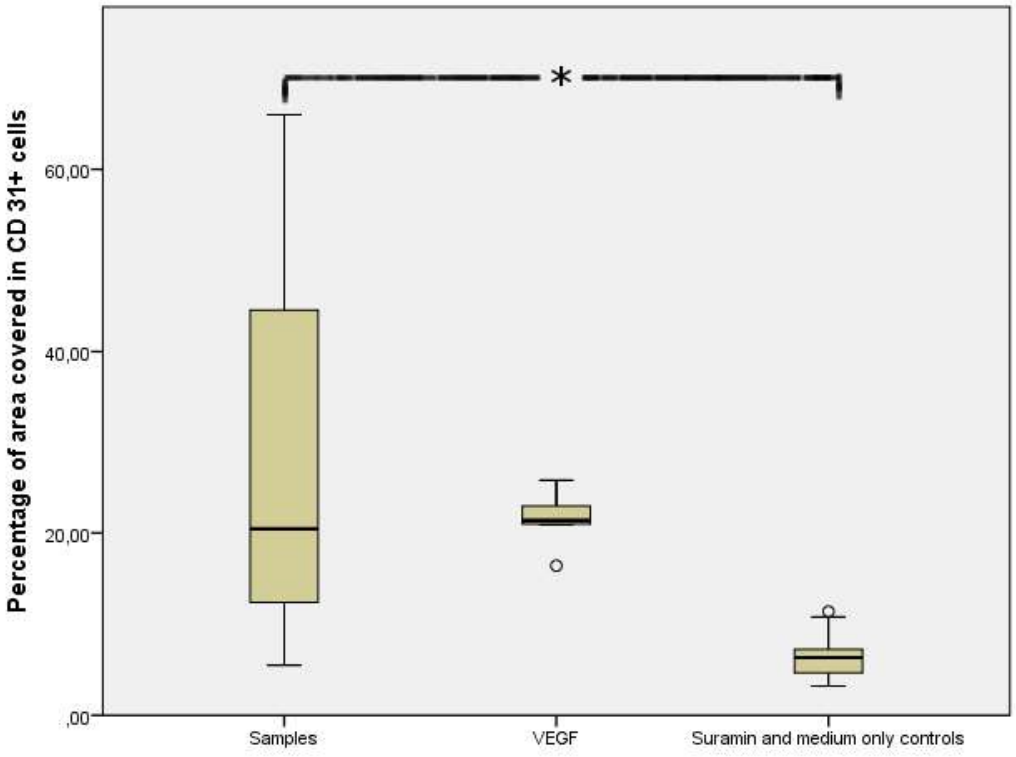

*Figure 24: Boxplot of percentage of well surface area covered by CD31+ cells. The group including all samples showing significantly ($p < 0.05$) higher CD 31+ area coverage than the group including medium only and negative (suramin added to medium) controls (marked by *).*

Co-cultures (excluding non-responding samples 1, 2 and 11) generally appeared strikingly different from the controls, with a higher extent of CD31+ cells and large branching networks. Additionally, samples with high levels of EC-differentiation often exhibited a fringed instead of a sharply circumscribed structure of CD31+ cells. The level of organisation of the cells was observed to vary greatly from highly organised, branching networks to more diffuse or random staining patterns. Compared with samples used in the experiment, the positive control wells also exhibited networks of CD31-positive cells but these were more delicate in appearance. In negative and media-only controls, no organised tubule formation was visible and the percentage of area covered by CD31+ cells was comparatively low. This further served to show that the standard medium, which was also used for the

co-culture wells, had no intrinsic pro-angiogenic properties, despite evoking the secretion of VEGF (figure 25).

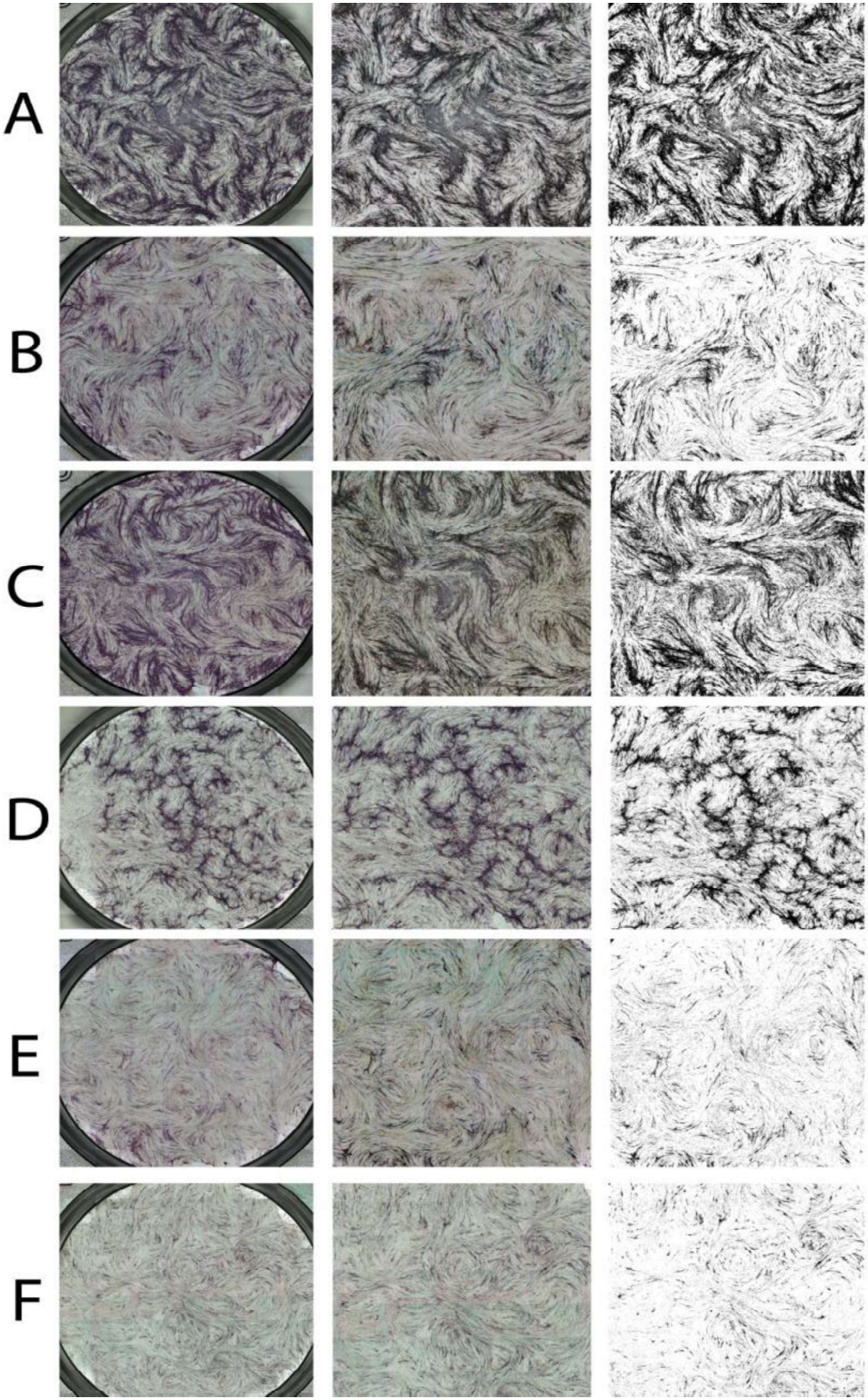
A
B
C
D
E
F

Figure 25: Aspects of various ASC – V2a co-culture samples following successful immunostaining. From left to right: Total picture, native image of the later analysed area, area recognised as being CD31+ after processing by using ImageJ. Differences in tubule formation are aapparent.

Those samples that exhibited a peak in VEGF secretion during the co-culture period were found to have highly statistically significant ($p<0.005$) higher EC-differentiation (as measured by the percentage of the well surface area covered in CD 31+ cells) compared with those samples that developed a steady increase in VEGF secretion (see also 3.3.2.) (figure 26).

	Minimum	**Maximum**	**Mean**	**Standard deviation**
Continuous increase in VEGF secretion	5.8%	28.0%	17.6%	7.2%
Peak in VEGF secretion during co-culture period	5.5%	66.0%	34.0%	20.0%

Figure 26: Minima, maxima, means and standard deviations of the percentage of well surface area covered by CD31+ cells dependent on the VEGF secretion pattern of the corresponding co-culture. The observed variances are highly statistically significant ($p<0.005$).

In summary, the presence of ASC in a co-culture can undoubtedly be claimed to enhance EC differentiation as confirmed by the increase in VEGF (compare 3.3.2.) and immunohistochemic evidence. More specifically, EC differentiation appears to be triggered by mechanisms other than one involving VEGF, as observed levels in co-cultures were consistently lower than in the positive control (containing VEGF) and, in agreement with other findings, to exhibit an inter-individually different degree of effectivenss.

4. Discussion

4.1. Conclusion of Findings

The study presented herein has confirmed that human cells capable of adipogenesis in vitro can readily be isolated and cultivated from fresh samples of lipoaspirate. Furthermore, the practicability of the cryopreservation and later cultivation of those cells has been demonstrated. Flow cytometry supports the hypothesis that the initially isolated cells are pluripotent MSC (especially because of their expression of CD73 and CD90) or adipocyte progenitor cells at early stages of commitment or differentiation. This method has also shown that the isolation and purification process do not have an overly adverse effect on cell viability and further reveals a high purification rate with almost no endothelial cells or other (haematopoietic) stem cells occurring in the primary culture.

Although cell growth in P_0 exhibited significant variance, cells showed more comparable growth rates in P_1, indicating an intrinsically consistent growth in undifferentiated ASC after the removal of non-proliferating cells (see 3.1. and 3.2.). When adiponectin secretion was used as a marker for adipocyte differentiation, as previously performed– by, for example, Martella et al. [151] and Smith et al. [152] (also suggested in a review by Fu et al. [153]), adipogenesis following standardised differentiation treatment could be demonstrated in 90% of the samples. Adiponectin levels generally increased more over the first 5 days of cultivation and reached a plateau towards the end of the differentiation period. Inter-individually, immense variances were seen in absolute adiponectin levels. The reason that the remaining 10% of the samples failed to react to this differentiation scheme could not by explained by divergence in processing times or the available patient data (see 3.3.1.). As expected, oil-red staining confirmed the formation of lipid droplets in adiponectin-secreting samples. Here, samples appeared inter-individually morphologically different (see 3.4.1.) but exhibited the expected correlation between adiponectin levels and lipid droplet formation. The ASC – EC co-culture experiment established that ASC are able to induce EC differentiation in endothelial progenitor cells in vitro without further stimuli and that EC differentiation varied both with regard to its extent and macroscopic appearance after immunostaining. Overall, the instigated EC differentiation was significant compared with controls and, in some samples, exceeded that of positive control samples by a wide margin. In agreement with these findings, the macroscopic appearance of co-cultured samples varied widely from the delicate structures of differentiated (CD31+) EC to branching and tree-like forms (see 3.4.2.). VEGF was used to monitor EC differentiation, as it is a well-researched marker [154,155]. It revealed two distinct patterns of VEGF secretion of EC during the co-culture experiment: first, a constant increase in VEGF and, second, a peak in VEGF secretion at one point during differentiation followed by a reduced and relatively constant VEGF secretion for the remainder of the co-culture. The first VEGF secretion pattern correlated with higher EC differentiation rates (measured by the

percentage of CD31+ cells at the end of the co-culture period) than the latter; a difference that was highly statistically significant (see 3.3.2.).

In conclusion, patient-derived ASC behaviour in this setting deviates from that of 3T3-L1 cells, which are the most established and best-researched ASC cell line (as of July 2015, more than 5000 results can be found in a pubmed search with the keywords “3T3-L1 adipocyte differentiation” and “adipogenesis 3T3-L1”), in that a remarkable variance has been observed in all individual measurements made in this study, despite all samples undergoing an identical treatment regime. This deviation has been found not only in terms of the very high variances in secreted markers of adipogenesis / lipogenesis, but also in the observed differences in morphology following oil-red staining and the differences in EC differentiation potential.

4.2. Limitations

The findings are limited in their validity by a number of factors. First, the sample size of 30 patients was small. Whereas it allowed for inter-individual differences to be observed, a larger sample size would have resulted in improved statistical power. Additionally, a complete medical history of the patient donating a sample could not be obtained in more than 50% of the cases. This reduced the possibility of subgroup analysis and stratification according to information acquirable through anamnesis. Flow cytometry / FACS could only be performed on some of the samples but, nevertheless, supported the hypothesis of a sufficient purification of cells in the employed isolation process and of the viability of the isolated cell population. Because of the restricted resources, not all isolated samples could be further analysed by ELISA and the co-culture assay. Selection was thus made half-randomly by trying to include cells obtained from patients of different ages and medical history but ultimately involved choosing a certain number of samples without additional information. This lack of information obviously hampers the meaningfulness of the study. Method-wise, the selection of only cells adherent to plastic surface during P_0 was the only means used to purify adipocyte progenitor cells. However, not only did the flow cytometry performed deliver results supportive of sufficient purification, but also Gimble et al. found this method to be suitable and sufficient for ASC isolation in a 2007 review [156] and a later review by Locke et al. in 2009 supported this finding [157]. Because of limited resources, the number of samples used in the V2a co-culture experiment was low. Although some compensation for this shortcoming was attempted by selecting samples in a way aimed at representing their diversity (i.e. cells natively isolated from lipoaspirates and initially cryopreserved samples, plus cells from older and younger patients), a higher number of samples analysed would have boosted the validity of the study. Thus, whereas the results allow for the postulation of a trend (“it is highly probable inter-individual differences exist in ASC adipogenicity”), the low number of samples and the incompleteness of the patient data do not allow us to assume any causalities based on the obtained data and results.

However, an attempt at interpreting the results will be made and a hypothesis about possible causes and consequences will be presented below.

4.3. Interpretation and Outlook

The starting hypothesis of a difference between the in-vitro behaviour of the established 3T3-L1 cell lines and ASC isolated from human lipoaspirates cannot be conclusively confirmed or disproved in this experimental setting; nevertheless, some evidence hints at the sought differences. In this section, an argument will be made in favour of the observed variances being evidence for inter-individual differences in the adipogenic potential of the obtained ASC. However, a problem regarding the interpretation of the results (in addition to the limitations mentioned above in 4.2.) might arise because of the lack of standardised protocols for the adipogenic differentiation of human patient-obtained ASC. Although the adipogenic potential of 3T3-L1 cells was described as early as 1975 and numerous ways and means of the adipogenic differentiation of this cell-line have been discussed, no standard procedure has so far been agreed [158]. Despite insulin, IBMX and dexamethasone being generally considered necessary for adipogenic differentiation of 3T3-L1 ASC, insulin concentrations in differentiation medium in published studies range from nil to 12052 nM, dexamethasone concentrations from nil to 1000 nM and IBMX from nil to 500 nM: median concentrations employed are 860 nM insulin, 1000 nM dexamethasone and 500 nM IBMX [159]. Published formulae for the adipogenic differentiation of human ASC differ widely while the main additives are insulin, dexamethasone and indomethacin [159]. Many authors agree on an insulin concentration between 720 nM and 10000 nM [160–165], dexamethasone concentration of 1000 nM [160–165] and an indomethacin concentration ranging between 60 – 200 nM [160–165]. These compositions are comparable with the induction medium used in this study. Our concept of an induction step followed by a differentiation step that employs a different medium has also successfully been undertaken with various compositions of differentiation media in a number of studies [138,166–168]. However, in those studies that made use of two distinct media for induction and differentiation, no actual common ground in medium composition could be found. As a base medium MEM, DMEM or DMEM / F-12 (in a 1:1 ratio) was used. Including our medium composition, 4 out of 5 groups added insulin in concentrations ranging over two orders of magnitude (500 nM to 66 µM) to their respective media. FCS was used at a concentration of 5% by us and by one other group. Whereas, apart from insulin, only an antibiotic-antimycotic concentrate and glutamine were added to our differentiation medium, other groups have used additional additives, such as transferrin [138,166,168,167], glitazones [167,168], corticosteroids [166,168,138], IBMX [166], biotin and pantothenate [167]. Despite the variances in composition, all media successfully evoked adipogenic differentiation, indicating that adipogenesis as the “natural” programming of ASC can easily be activated. As detailed in the materials and methods and the results sections, our cryopreservation, thawing and isolation protocols followed standardised

protocols and delivered consistent results. Moreover, the induction and differentiation processes employed in this study were similar to the published methods of other groups (see above) and succeeded in regularly evoking an adipogenic response in vitro. These findings provide the first support of the hypothesis that the observed differences in growth rates and adiponectin secretion during differentiation are caused by inter-individual ASC differences on a cellular level [169].

External factors that could have affected ASC after explantation (i.e. *ex vivo*) should also be considered, as they could have affected the samples for various periods of time, thus possibly imitating intrinsic inter-individual differences. In this context, ASC samples probably had to sustain various periods of hypoxia during the collection and then the transport of the tissue to the laboratory for isolation. However, ASC have been shown to be relatively resistant to hypoxia and to be able to be cultivated after several days under hypoxic conditions [170,171]. These findings make a significant impairment of adipogenic potential attributable to prolonged hypoxia appear unlikely. Conversely, some studies have even suggested an increase in the proangiogenic potential in ASC that have sustained hypoxia [172,113]. This increase in proangiogenic potential was measured by the increased secretion of HIF, VEGF and angiogenin, a pro-angiogenic factor. In this context, various hypoxic intervals could have influenced the results in the ASC – EC co-culture experiment (also see below) [114]. Moreover, cells might have been subjected to various amounts of time in the tumescence solution used for liposuction, as syringes containing lipoaspirate and tumescence solution were usually centrifuged by scrub nurses, who may have not always been immediately able to perform this step when other OR duties were more urgent. The tumescence solution has been shown to affect ASC viability negatively [144]; thus, this circumstance might represent another possibility for ASC to have sustained damage at the cellular level leading to possible differences that are independent of the donor patient.

With regards to intrinsic factors that represent the actual determinants for the inter-individual differences postulated in this thesis, a correlation between the individual medical and family history of a patient and adiponectin secretion as a surrogate for adipogenic differentiation in culture must be assumed. The pathophysiological substrate or consequence of metabolic diseases such as type 2 diabetes or obesity has been shown to be WAT fibrosis, a condition named “adipose tissue fibrosis”. Furthermore, descendants of survivors of famines have an elevated risk of developing metabolic disorders that manifest in dysregulated adipocyte / WAT functioning (see 1.1.2.). In turn, these metabolic states also correlate with abnormal adiponectin levels. More evidence for inheritable epigenetic changes in adipocytes in vivo has also emerged in animal experiments, hinting at an “epigenetic burden” (Attig et. al) passed on to the offspring of obese test mice. Furthermore, Attig et al. found that mice born of obesity-prone parents developed more severe obesity during a high-fat diet and had a higher body fat mass than the control group, even under a later normocaloric diet regime [173]. The observed genetic changes in WAT were predominantly related to energy allocation

(glucose versus fatty acid uptake) and expenditure and to adipose tissue hypertrophy, which could lead to hypoxia and adipose tissue fibrosis [7]. As states of inflammation marked by an elevated TNF-α level are inversely correlated to serum adiponectin levels, a connection may also exist between ASC origin (possibly from chronically inflamed adipose tissue) and variable adiponectin levels in culture [174,67].

Adiponectin is the best researched adipokine and hypoadiponectinaemia is involved in all four core symptoms of metabolic syndrome. Metabolic disorders can manifest in elevated and decreased adiponectin levels; the observed differences in the ELISA performed in this study may therefore be caused by persistent epigenetic or post-translational changes in ASC affecting adiponectin secretion. In this hypothesis, "normal" or physiological adiponectin levels would lie between the pathological extremes at either end of the spectrum of recorded adiponectin levels. Epigenetic changes in ASC have been speculated to interfere with the adipogenic potential of these cells before the manifestation of metabolic disorders, thus not only contributing to the observed inter-individual differences, but also predating those types of disease (e.g. type 2 diabetes) usually listed in questionnaires related to a patient's medical history. Support for this stems from the finding that low adiponectin concentrations are an independent risk factor for developing hypertension within a five year observation period [70]. However, the mentioned study did not include any investigation of adipose tissue and, so, the presence of adipose tissue fibrosis at baseline remains unclear, although this would have given information about the sequence of changes eventually leading to metabolic syndrome.

The observed variances in pro-angiogenic ASC potential could also be rooted in a patient's medical history. As sufficient vasculature has been established as being essential for physiological WAT functioning, the ASC – EC co-culture experiment allows an insight into the significant inter-individual differences of the angiogenic potential of ASC. Nevertheless, although numerous models of angiogenesis have been established in vivo (such as the chick chorioallantoic membrane assay [175] or the rabbit cornea model [176]), the setting in an animal model invariably brings external, uncontrollable and possibly confounding factors into an experiment. Potential distortions of measurements and the effort involved in performing an in-vivo trial have led us to the conclusion that such an approach was both undesirable and impractical. In contrast, an in-vitro approach utilising the V2a assay appeared more feasible to us, in addition to being more cost effective and easier to conduct. It also allowed a standardised procedure to be carried out and, thus, a more reliable quantification of possible differences in EC differentiation.

The results of the co-culture experiment confirmed that an intrinsic angiogenic response could be provoked solely by co-culturing ASC with endothelial progenitor cells. Hence, the proangiogenic properties of ASC can be considered as having been confirmed. Although neither hypoxia nor nutritional stress were present at any time-point during the culturing of the ASC before their addition

to the pre-cultured V2a-cells or during the actual co-cultivating process, variable degrees of endothelial differentiation could be observed, exhibiting once again the inter-individual differences in ASC. However, as mentioned above, the cells might have sustained variable periods of hypoxia before being transferred into P_0. As also mentioned before, hypoxia has the potential of (positively) influencing ASC angiogenicity. In this case, the observed variances would have (at least partly) been attributable to conditions experienced by cells only from outside the donor and not of a truly intrinsic nature.

With respect to the differences observed regarding the general aspect of co-cultured samples compared with each other and with controls, the presence of ASC can be proposed to have interfered with a coordinated endothelial progenitor cell expansion. This idea implies two different underlying principles. Depending on the expansion speed of ASC, endothelial progenitor cells might have been curbed in their growth by the comparatively faster expanding ASC. Vice versa, relatively slower ASC expansion rates would have allowed an undisturbed growth of endothelial progenitor cells thereby causing a smoother macroscopic aspect. However, the high rates of EC differentiation might have been caused by an ASC growth-dependent presence of stimulating factors but not of VEGF, as the levels of this cytokine did not correlate with EC differentiation or tubule formation. However, the fringed aspect of CD31+ cell networks, indicating a high overall cell count, was often correlated with a high rate of endothelial differentiation. Cytokines other than VEGF, such as HIF, should be taken into account when searching for the stimulus of ASC-driven angiogenesis.

By using ASC of passage one or two, the presence of cell types other than ASCs seems highly unlikely. Therefore, subpopulations of endothelial progenitor cells that potentially might lead to a misinterpretation of our results would not be expected in our cultures. However, ASC might also have transformed into EC during the co-cultivation period of 13 days. Obviously, this experiment does not clarify whether the markedly increased VEGF levels are a result of ASC secretion, V2a-cell secretion or both. Nevertheless, we have confirmed that human ASC stimulate angiogenesis in vitro, even without specific external pro-angiogenic stimuli. As stated above, studies indicate that widespread diseases such as metabolic syndrome, type 2 diabetes or morbid obesity, which are known to manifest themselves as pathologies of WAT, affect ASC at a fundamental level. Thus, inter-individual differences in ASC can be assumed to manifest themselves not only in variances in the potential for adipogenic differentiation, but possibly also in their potential for promoting angiogenesis. In metabolic syndrome and insulin resistance, WAT has been shown to enter a state of chronic low-grade inflammation, marked by a change of WAT-resident macrophages from the "anti-inflammatory" M2 type to the "pro-inflammatory" M1 type and by the immigration of circulating M1 macrophages and elevated activation levels of NK-cells, all of which lead to the remodelling of WAT ECM into a more rigid type and to a higher cell turnover [124]. This, in turn, would lead to hypoxia through the increased distance between the capillaries and adipocytes, with neoangiogenesis being concomitantly impaired by the

aforementioned more rigid ECM structure, eventually leading to a self-maintaining vicious circle of chronic inflammation, hypoxia, adipose tissue fibrosis and curbed neoangiogenesis [25]. Sustained inflammation might eventually evoke epigenetic changes in ASC populations leading to altered behaviour of these cells, even under non-hypoxic, nutritionally optimal and stable conditions, as observed in our experiment. Prolonged inflammatory states have previously been shown to induce epigenetic changes in cells [177,178]. Furthermore, since ASC are subjected to stress and hypoxia during the liposuction process, which has been shown to impair their viability, even the surviving cells might be permanently damaged, resulting in altered behaviour through epigenetic changes [179]. Local anaesthetics used in the tumescence solution in liposuction have also been shown to affect ASC viability negatively [144]. However, as all samples were obtained by using the same tumescence composition, possible effects (if any) would be caused by variable exposure times of ASC to the tumescence solution, as mentioned above. The demonstration of spontaneous VEGF secretion by ASC, as first performed as early as 2004, and the subsequent evidence of VEGF release enhancement through the creation of hypoxic conditions do not suffice to explain the differences in EC differentiation observed, as cultivation took place under non-hypoxic/non-inflamed conditions [180]. In contrast, hypoxically conditioned ASC exhibited higher angiogenic potential. Whatever the reason for the variable endothelial differentiation, VEGF secretion by either ASC or V2a only appears to be indirectly (if at all) correlated with it. Additionally, VEGF is present when, as demonstrated with assays performed on controls, endothelial differentiation is random and minimal, implying that the VEGF release by undifferentiated endothelial cells fails to cause endothelial differentiation. With suramin being a highly potent inhibitor of angiogenesis [181], the absence of EC differentiation is obviously expected, but the presence of elevated VEGF levels in the media-only control group in combination with the equally low level of EC differentiation compared with the negative control group is surprising [182]. As VEGF is also a survival factor for EC and their progenitor cells, the measured levels might represent a baseline value that is necessary for survival but that is not sufficient for differentiation [183]. No definite conclusions can be drawn from the ASC – EC co-culture experiment as too many variables remain unaccounted for; however, we have established a proof of concept of an in-vitro co-culture, an application not included in the kit manufacturer's protocol, and the demonstration of significant inter-individual variances in a crucial ASC property, in addition to the aforementioned differences in adipogenic potential. This further supports the hypothesis of actual variances in the cell pool.

Thus, whereas further and more detailed research will be necessary to clarify the causes of our findings, ASC can be concluded to exhibit an inter-individually varying degree of activity in standardised environments. These differences may contribute to the frequently reported problem of the unpredictable resorption rates of the transplant after the autologous transplantation of adipose tissue. Deeper insights into the mechanisms behind this behaviour may eventually allow more predictable

outcomes when soft tissue defects are treated by using adipose tissue with its otherwise very favourable properties (it is readily available and easily obtainable, it has an autologous nature and is malleable and it shows re-growth) as a filler [146]. If, in the future, a reliable method of predicting adipocyte growth in vivo is introduced, then the prospect of seeding precisely calculated numbers of purified (and possibly preconditioned) ASC into tissues for augmentation by adipogenic differentiation will become feasible. The imaginable uses of this technique, beyond the augmentation of vocal folds in ear-nose-throat surgery, are countless.

5. Appendix

5.1. References

1. Dympna Gallagher, Steven B Heymsfield, Moonseong Heo, Susan A Jebb, Peter R Murgatroyd, Yoichi Sakamoto (2000) Healthy percentage body fat ranges: an approach for developing guidelines based on body mass index. Am J Clin Nutr 72 (3): 694–701. Available: http://ajcn.nutrition.org/content/72/3/694.full.
2. Hausman DB, DiGirolamo M, Bartness TJ, Hausman GJ, Martin RJ (2001) The biology of white adipocyte proliferation. Obes Rev 2 (4): 239–254.
3. Friedl KE, Moore RJ, Martinez-Lopez LE, Vogel JA, Askew EW, Marchitelli LJ, Hoyt RW, Gordon CC (1994) Lower limit of body fat in healthy active men. Journal of applied physiology (Bethesda, Md. : 1985) 77 (2): 933–940.
4. Tran TT, Yamamoto Y, Gesta S, Kahn CR (2008) Beneficial effects of subcutaneous fat transplantation on metabolism. Cell Metabolism 7 (5): 410–420.
5. Silvana Baglioni1., Giulia Cantini1., Giada Poli, Michela Francalanci, Roberta Squecco, Alessandra Di Franco. Elisa Borgogni, Salvatore Frontera, Gabriella Nesi, Francesco Liotta, Marcello Lucchese, Giuliano Perigli, Fabio Francini, Gianni Forti, Mario Serio, Michaela Luconi (2012) Functional Differences in Visceral and Subcutaneous Fat Pads Originate from Differences in the Adipose Stem Cell. PLoS ONE 7 (5): e36569. Available: http://journals.plos.org/plosone/article/asset?id=10.1371/journal.pone.0036569.PDF.
6. Tchkonia T, Lenburg M, Thomou T, Giorgadze N, Frampton G, Pirtskhalava T, Cartwright A, Cartwright M, Flanagan J, Karagiannides I, Gerry N, Forse RA, Tchoukalova Y, Jensen MD, Pothoulakis C, Kirkland JL. (2007) Identification of depot-specific human fat cell progenitors through distinct expression profiles and developmental gene patterns. American Journal of Physiology - Endocrinology and Metabolism 292 (1): E298-E307.
7. Hoffstedt J, Arner E, Wahrenberg H, Andersson DP, Qvisth V, Löfgren P, Rydén M, Thörne A, Wirén M, Palmér M, Thorell A, Toft E, Arner P (2010) Regional impact of adipose tissue morphology on the metabolic profile in morbid obesity. Diabetologia 53 (12): 2496–2503.
8. Gartner LP, Hiatt JL (2012) Color Atlas and Text of Histology: Wolters Kluwer Health.
9. Neels JG, Thinnes T, Loskutoff DJ (2004) Angiogenesis in an in vivo model of adipose tissue development. FASEB journal : official publication of the Federation of American Societies for Experimental Biology 18 (9): 983–985.
10. Nishimura S1, Manabe I, Nagasaki M, Hosoya Y, Yamashita H, Fujita H, Ohsugi M, Tobe K, Kadowaki T, Nagai R, Sugiura S (2007) Adipogenesis in obesity requires close interplay between differentiating adipocytes, stromal cells, and blood vessels. Diabetes 56 (6): 1517–1526.
11. Lijnen HR (2008) Angiogenesis and obesity. Cardiovascular Research 78 (2): 286–293.
12. Alexander JK, Dennis EW, Smith WG, Amad KH, Duncan WC, Austin RC (1962-1963) Blood volume, cardiac output, and distribution of systemic blood flow in extreme obesity. Cardiovascular Research Center bulletin 1: 39–44.
13. Divoux A, Clément K (2011) Architecture and the extracellular matrix: the still unappreciated components of the adipose tissue. Obes Rev 12 (5): e494-503.
14. Lim JM, Sherling D, Teo CF, Hausman DB, Lin D, Wells L (2008) Defining the regulated secreted proteome of rodent adipocytes upon the induction of insulin resistance. Journal of proteome research 7 (3): 1251–1263.
15. Pierleoni C, Verdenelli F, Castellucci M, Cinti S (1998) Fibronectins and basal lamina molecules expression in human subcutaneous white adipose tissue. European journal of histochemistry : EJH 42 (3): 183–188.
16. Chen X, Cushman SW, Pannell LK, Hess S (2005) Quantitative proteomic analysis of the secretory proteins from rat adipose cells using a 2D liquid chromatography-MS/MS approach. Journal of proteome research 4 (2): 570–577.
17. Spencer M, Unal R, Zhu B, Rasouli N, McGehee RE Jr, Peterson CA, Kern PA (2011) Adipose tissue extracellular matrix and vascular abnormalities in obesity and insulin resistance. J. Clin. Endocrinol. Metab. 96 (12): E1990-8. Accessed 21 April 2015.

18. Spiegelman BM, Ginty CA (1983) Fibronectin modulation of cell shape and lipogenic gene expression in 3T3-adipocytes. Cell 35 (3 Pt 2): 657–666.
19. Taleb S, Cancello R, Clement K, Lacasa D (2006) Cathepsin s promotes human preadipocyte differentiation: possible involvement of fibronectin degradation. Endocrinology 147 (10): 4950–4959.
20. Bauters D, Scroyen I, van Hul M, Lijnen HR (2015) Gelatinase A (MMP-2) promotes murine adipogenesis. Biochimica et biophysica acta 1850 (7): 1449–1456.
21. Bouloumie A, Sengenes C, Portolan G, Galitzky J, Lafontan M (2001) Adipocyte produces matrix metalloproteinases 2 and 9: involvement in adipose differentiation. Diabetes 50 (9): 2080–2086.
22. Yan J, Yang S, Zhang J, Zhu T (2009) BMP6 reverses TGF-beta1-induced changes in HK-2 cells: implications for the treatment of renal fibrosis. Acta pharmacologica Sinica 30 (7): 994–1000.
23. Bauters D, van Hul M, Lijnen HR (2014) Gelatinase B (MMP-9) gene silencing does not affect murine preadipocyte differentiation. Adipocyte 3 (1): 50–53.
24. Catalán V, Gómez-Ambrosi J, Rodríguez A, Ramírez B, Silva C, Rotellar F, Gil MJ, Cienfuegos JA, Salvador J, Frühbeck G (2009) Increased adipose tissue expression of lipocalin-2 in obesity is related to inflammation and matrix metalloproteinase-2 and metalloproteinase-9 activities in humans. Journal of molecular medicine (Berlin, Germany) 87 (8): 803–813.
25. Khan T, Muise ES, Iyengar P, Wang ZV, Chandalia M, Abate N, Zhang BB, Bonaldo P, Chua S, Scherer PE (2009) Metabolic dysregulation and adipose tissue fibrosis: role of collagen VI. Mol. Cell. Biol. 29 (6): 1575–1591.
26. Iyengar P, Espina V, Williams TW, Lin Y, Berry D, Jelicks LA, Lee H, Temple K, Graves R, Pollard J, Chopra N, Russell RG, Sasisekharan R, Trock BJ, Lippman M, Calvert VS, Petricoin EF 3rd, Liotta L, Dadachova E, Pestell RG, Lisanti MP, Bonaldo P, Scherer PE (2005) Adipocyte-derived collagen VI affects early mammary tumor progression in vivo, demonstrating a critical interaction in the tumor/stroma microenvironment. The Journal of Clinical Investigation 115 (5): 1163–1176.
27. Lee RH, Kim B, Choi I, Kim H, Choi HS, Suh K, Bae YC, Jung JS (2004) Characterization and Expression Analysis of Mesenchymal Stem Cells from Human Bone Marrow and Adipose Tissue. Cell Physiol Biochem 14 (4-6): 311–324. Available: http://www.karger.com/Article/FullText/80341.
28. Crisan M, Yap S, Casteilla L, Chen CW, Corselli M, Park TS, Andriolo G, Sun B, Zheng B, Zhang L, Norotte C, Teng PN, Traas J, Schugar R, Deasy BM, Badylak S, Buhring HJ, Giacobino JP, Lazzari L, Huard J, Péault B (2008) A Perivascular Origin for Mesenchymal Stem Cells in Multiple Human Organs. Cell Stem Cell 3 (3): 301–313.
29. Wagner W, Wein F, Seckinger A, Frankhauser M, Wirkner U, Krause U, Blake J, Schwager C, Eckstein V, Ansorge W, Ho AD (2005) Comparative characteristics of mesenchymal stem cells from human bone marrow, adipose tissue, and umbilical cord blood. Experimental Hematology 33 (11): 1402–1416.
30. Tomiyama K, Murase N, Stolz DB, Toyokawa H, O'Donnell DR, Smith DM, Dudas JR, Rubin JP, Marra KG (2008) Characterization of Transplanted Green Fluorescent Protein+ Bone Marrow Cells into Adipose Tissue. STEM CELLS 26 (2): 330–338. Available: http://onlinelibrary.wiley.com/doi/10.1634/stemcells.2007-0567/full.
31. Cawthorn WP, Scheller EL, MacDougald OA (2012) Adipose tissue stem cells meet preadipocyte commitment: going back to the future. J. Lipid Res. 53 (2): 227–246.
32. Rodeheffer MS, Birsoy K, Friedman JM (2008) Identification of White Adipocyte Progenitor Cells In Vivo. Cell 135 (2): 240–249.
33. Zuk PA, Zhu M, Ashjian P, De Ugarte DA, Huang JI, Mizuno H, Alfonso ZC, Fraser JK, Benhaim P, Hedrick MH (2002) Human adipose tissue is a source of multipotent stem cells. Mol. Biol. Cell 13 (12): 4279–4295.
34. Spencer M, Yao-Borengasser A, Unal R, Rasouli N, Gurley CM, Zhu B, Peterson CA, Kern PA (2010) Adipose tissue macrophages in insulin-resistant subjects are associated with collagen VI and fibrosis and demonstrate alternative activation. American Journal of Physiology - Endocrinology and Metabolism 299 (6): E1016-E1027.
35. Spalding KL, Arner E, Westermark PO, Bernard S, Buchholz BA, Bergmann O, Blomqvist L, Hoffstedt J, Näslund E, Britton T, Concha H, Hassan M, Rydén M, Frisén J, Arner P (2008) Dynamics of fat cell turnover in humans. Nature 453 (7196): 783–787.
36. BJ K, J H (1979) Isotopic labeling of DNA in rat adipose tissue: evidence for proliferating cells associated with mature adipocytes. J Lipid Res 20 (6): 691–704.

37. Naaz A, Holsberger DR, Iwamoto GA, Nelson A, Kiyokawa H, Cooke PS (2004) Loss of cyclin-dependent kinase inhibitors produces adipocyte hyperplasia and obesity. FASEB J 18 (15): 1925–1927. Available: http://www.fasebj.org/content/18/15/1925.full.
38. Henninger, A. M. Josefin, Eliasson B, Jenndahl LE, Hammarstedt A (2014) Adipocyte Hypertrophy, Inflammation and Fibrosis Characterize Subcutaneous Adipose Tissue of Healthy, Non-Obese Subjects Predisposed to Type 2 Diabetes. PLoS ONE 9 (8): e105262. Available: http://journals.plos.org/plosone/article/asset?id=10.1371/journal.pone.0105262.PDF.
39. Gustafson B, Hedjazifar S, Gogg S, Hammarstedt A, Smith U (2015) Insulin resistance and impaired adipogenesis. Trends in endocrinology and metabolism: TEM 26 (4): 193–200.
40. Kim SM, Lun M, Wang M, Senyo SE, Guillermier C, Patwari P, Steinhauser ML (2014) Loss of White Adipose Hyperplastic Potential Is Associated with Enhanced Susceptibility to Insulin Resistance. Cell Metabolism 20 (6): 1049–1058.
41. Marques BG, Hausman DB, Martin RJ (1998) Association of fat cell size and paracrine growth factors in development of hyperplastic obesity. The American journal of physiology 275 (6 Pt 2): R1898-908.
42. Hallenborg P, Petersen RK, Feddersen S, Sundekilde U, Hansen JB, Blagoev B, Madsen L, Kristiansen K (2014) PPARγ ligand production is tightly linked to clonal expansion during initiation of adipocyte differentiation. J. Lipid Res. 55 (12): 2491–2500. Available: http://www.jlr.org/content/55/12/2491.full.
43. Druet C, Stettler N, Sharp S, Simmons RK, Cooper C, Smith GD, Ekelund U, Lévy-Marchal C, Jarvelin MR, Kuh D, Ong KK (2012) Prediction of childhood obesity by infancy weight gain: an individual-level meta-analysis. Paediatric and perinatal epidemiology 26 (1): 19–26.
44. Araújo EP, De Souza CT, Gasparetti AL, Ueno M, Boschero AC, Saad MJ, Velloso LA (2005) Short-term in vivo inhibition of insulin receptor substrate-1 expression leads to insulin resistance, hyperinsulinemia, and increased adiposity. Endocrinology 146 (3): 1428–1437.
45. Berends LM, Fernandez-Twinn DS, Martin-Gronert MS, Cripps RL, Ozanne SE (2013) Catch-up growth following intra-uterine growth-restriction programmes an insulin-resistant phenotype in adipose tissue. International Journal of Obesity 37 (8): 1051.
46. Winer JP, Janmey PA, McCormick ME, Funaki M (2009) Bone marrow-derived human mesenchymal stem cells become quiescent on soft substrates but remain responsive to chemical or mechanical stimuli. Tissue engineering. Part A 15 (1): 147–154.
47. Chun TH, Hotary KB, Sabeh F, Saltiel AR, Allen ED, Weiss SJ (2006) A pericellular collagenase directs the 3-dimensional development of white adipose tissue. Cell 125 (3): 577–591.
48. Takada I, Kouzmenko AP, Kato S (2009) Wnt and PPARgamma signaling in osteoblastogenesis and adipogenesis. Nature reviews. Rheumatology 5 (8): 442–447.
49. Hauner H, Brunner S, Amann-Gassner U (2013) The role of dietary fatty acids for early human adipose tissue growth. The American journal of clinical nutrition 98 (2): 549S-55S.
50. Fernandez-Twinn DS, Wayman A, Ekizoglou S, Martin MS, Hales CN, Ozanne SE (2005) Maternal protein restriction leads to hyperinsulinemia and reduced insulin-signaling protein expression in 21-mo-old female rat offspring. American journal of physiology. Regulatory, integrative and comparative physiology 288 (2): R368-73.
51. Ozanne SE, Dorling MW, Wang CL, Nave BT (2001) Impaired PI 3-kinase activation in adipocytes from early growth-restricted male rats. American journal of physiology. Endocrinology and metabolism 280 (3): E534-9.
52. Hammarstedt A, Graham TE, Kahn BB (2012) Adipose tissue dysregulation and reduced insulin sensitivity in non-obese individuals with enlarged abdominal adipose cells. Diabetology & metabolic syndrome 4 (1): 42.
53. Muise ES, Souza S, Chi A, Tan Y, Zhao X, Liu F, Dallas-Yang Q, Wu M, Sarr T, Zhu L, Guo H, Li Z, Li W, Hu W, Jiang G, Paweletz CP, Hendrickson RC, Thompson JR, Mu J, Berger JP, Mehmet H (2013) Downstream Signaling Pathways in Mouse Adipose Tissues Following Acute In Vivo Administration of Fibroblast Growth Factor 21. PLoS ONE 8 (9): e73011. Available: http://journals.plos.org/plosone/article/asset?id=10.1371/journal.pone.0073011.PDF.
54. Lord JM, Flight IHK, Norman RJ (2003) Insulin-sensitising drugs (metformin, troglitazone, rosiglitazone, pioglitazone, D-chiro-inositol) for polycystic ovary syndrome. The Cochrane database of systematic reviews (3): CD003053.

55. Weyer C, Funahashi T, Tanaka S, Hotta K, Matsuzawa Y, Pratley RE, Tataranni PA (2001) Hypoadiponectinemia in obesity and type 2 diabetes: close association with insulin resistance and hyperinsulinemia. J. Clin. Endocrinol. Metab. 86 (5): 1930–1935.
56. Andrews RC, Walker BR (1999) Glucocorticoids and insulin resistance: old hormones, new targets. Clinical Science 96 (5): 513–523.
57. Hotamisligil GS, Shargill NS, Spiegelman BM (1993) Adipose expression of tumor necrosis factor-alpha: direct role in obesity-linked insulin resistance. Science (New York, N.Y.) 259 (5091): 87–91.
58. Hotamisligil GS, Peraldi P, Budavari A, Ellis R, White MF, Spiegelman BM (1996) IRS-1-Mediated Inhibition of Insulin Receptor Tyrosine Kinase Activity in TNF-α- and Obesity-Induced Insulin Resistance. Science 271 (5249): 665–670.
59. Gao Z, Zhang X, Zuberi A, Hwang D, Quon MJ, Lefevre M, Ye J (2004) Inhibition of insulin sensitivity by free fatty acids requires activation of multiple serine kinases in 3T3-L1 adipocytes. Molecular endocrinology (Baltimore, Md.) 18 (8): 2024–2034.
60. Halberg N, Khan T, Trujillo ME, Wernstedt-Asterholm I, Attie AD, Sherwani S, Wang ZV, Landskroner-Eiger S, Dineen S, Magalang UJ, Brekken RA, Scherer PE. (2009) Hypoxia-Inducible Factor 1α Induces Fibrosis and Insulin Resistance in White Adipose Tissue. Mol. Cell. Biol. 29 (16): 4467–4483. Available: http://mcb.asm.org/content/29/16/4467.full.
61. Ingalls AM, Dickie MM, Snell GD (1950) Obese, a new mutation in the house mouse. The Journal of heredity 41 (12): 317–318.
62. Zhang Y, Proenca R, Maffei M, Barone M, Leopold L, Friedman JM (1994) Positional cloning of the mouse obese gene and its human homologue. Nature 372 (6505): 425–432.
63. Thamer C, Machann J, Tschritter O, Haap M, Wietek B, Dahl D, Bachmann O, Fritsche A, Jacob S, Stumvoll M, Schick F, Häring HU (2002) Relationship between Serum Adiponectin Concentration and Intramyocellular Lipid Stores in Humans. Horm Metab Res 34 (11/12): 646–649.
64. Halaas JL, Gajiwala KS, Maffei M, Cohen SL, Chait BT, Rabinowitz D, Lallone RL, Burley SK, Friedman JM (1995) Weight-reducing effects of the plasma protein encoded by the obese gene. Science (New York, N.Y.) 269 (5223): 543–546.
65. Pelleymounter MA, Cullen MJ, Baker MB, Hecht R, Winters D, Boone T, Collins F (1995) Effects of the obese gene product on body weight regulation in ob/ob mice. Science (New York, N.Y.) 269 (5223): 540–543.
66. Nedvídková J, Smitka K, Kopský V, Hainer V (2005) Adiponectin, an adipocyte-derived protein. Physiol Res 54 (2): 133–140.
67. Ouchi N, Kihara S, Funahashi T, Nakamura T, Nishida M, Kumada M, Okamoto Y, Ohashi K, Nagaretani H, Kishida K, Nishizawa H, Maeda N, Kobayashi H, Hiraoka H, Matsuzawa Y (2003) Reciprocal Association of C-Reactive Protein With Adiponectin in Blood Stream and Adipose Tissue. Circulation 107 (5): 671–674. Available: http://circ.ahajournals.org/content/107/5/671.full.
68. Yamauchi T, Kamon J, Waki H, Imai Y, Shimozawa N, Hioki K, Uchida S, Ito Y, Takakuwa K, Matsui J, Takata M, Eto K, Terauchi Y, Komeda K, Tsunoda M, Murakami K, Ohnishi Y, Naitoh T, Yamamura K, Ueyama Y, Froguel P, Kimura S, Nagai R, Kadowaki T (2003) Globular adiponectin protected ob/ob mice from diabetes and ApoE-deficient mice from atherosclerosis. J. Biol. Chem. 278 (4): 2461–2468.
69. Yamauchi T, Kamon J, Ito Y, Tsuchida A, Yokomizo T, Kita S, Sugiyama T, Miyagishi M, Hara K, Tsunoda M, Murakami K, Ohteki T, Uchida S, Takekawa S, Waki H, Tsuno NH, Shibata Y, Terauchi Y, Froguel P, Tobe K, Koyasu S, Taira K, Kitamura T, Shimizu T, Nagai R, Kadowaki T (2003) Cloning of adiponectin receptors that mediate antidiabetic metabolic effects. Nature 423 (6941): 762–769.
70. Chow WS, Cheung BM, Tso AW, Xu A, Wat NM, Fong CH, Ong LH, Tam S, Tan KC, Janus ED, Lam TH, Lam KS (2007) Hypoadiponectinemia as a predictor for the development of hypertension: a 5-year prospective study. Hypertension 49 (6): 1455–1461.
71. Motoshima H, Wu X, Mahadev K, Goldstein BJ (2004) Adiponectin suppresses proliferation and superoxide generation and enhances eNOS activity in endothelial cells treated with oxidized LDL. Biochemical and biophysical research communications 315 (2): 264–271.
72. Chen H, Montagnani M, Funahashi T, Shimomura I, Quon MJ (2003) Adiponectin Stimulates Production of Nitric Oxide in Vascular Endothelial Cells. J. Biol. Chem. 278 (45): 45021–45026. Available: http://www.jbc.org/content/278/45/45021.full.

73. Wang Y, Lam KS, Xu JY, Lu G, Xu LY, Cooper GJ, Xu A (2005) Adiponectin Inhibits Cell Proliferation by Interacting with Several Growth Factors in an Oligomerization-dependent Manner. J. Biol. Chem. 280 (18): 18341–18347. Available: http://www.jbc.org/content/280/18/18341.full.
74. Masaie H, Oritani K, Yokota T, Takahashi I, Shirogane T, Ujiie H, Ichii M, Saitoh N, Maeda T, Tanigawa R, Oka K, Hoshida Y, Tomiyama Y, Kanakura Y (2007) Adiponectin binds to chemokines via the globular head and modulates interactions between chemokines and heparan sulfates. Experimental Hematology 35 (6): 947–956.
75. Park P, McMullen MR, Huang H, Thakur V, Nagy LE (2007) Short-term Treatment of RAW264.7 Macrophages with Adiponectin Increases Tumor Necrosis Factor-α (TNF-α) Expression via ERK1/2 Activation and Egr-1 Expression role of TNF-α in adiponectin-stimulated interleukin-10 production J. Biol. Chem. 282 (30): 21695–21703. Available: http://www.jbc.org/content/282/30/21695.full.
76. Kumada M, Kihara S, Ouchi N, Kobayashi H, Okamoto Y, Ohashi K, Maeda K, Nagaretani H, Kishida K, Maeda N, Nagasawa A, Funahashi T, Matsuzawa Y (2004) Adiponectin specifically increased tissue inhibitor of metalloproteinase-1 through interleukin-10 expression in human macrophages. Circulation 109 (17): 2046–2049.
77. Tsatsanis C, Zacharioudaki V, Androulidaki A, Dermitzaki E, Charalampopoulos I, Minas V, Gravanis A, Margioris AN (2005) Adiponectin induces TNF-alpha and IL-6 in macrophages and promotes tolerance to itself and other pro-inflammatory stimuli. Biochemical and biophysical research communications 335 (4): 1254–1263.
78. Winder WW, Hardie DG (1999) AMP-activated protein kinase, a metabolic master switch: possible roles in type 2 diabetes. Am. J. Physiol. 277 (1 Pt 1): E1-10.
79. Wirth A (2008) Adipositas. Ätiologie, Folgekrankheiten, Diagnostik, Therapie ; mit 60 Tabellen. Heidelberg: Springer. XV, 422 S p.
80. Farr OM, Fiorenza C, Papageorgiou P, Brinkoetter M, Ziemke F, Koo BB, Rojas R, Mantzoros CS (2014) Leptin therapy alters appetite and neural responses to food stimuli in brain areas of leptin-sensitive subjects without altering brain structure. J. Clin. Endocrinol. Metab. 99 (12): E2529-38.
81. Schwartz MW, Seeley RJ, Campfield LA, Burn P, Baskin DG (1996) Identification of targets of leptin action in rat hypothalamus. Journal of Clinical Investigation 98 (5): 1101–1106.
82. Bouloumie A, Marumo T, Lafontan M, Busse R (1999) Leptin induces oxidative stress in human endothelial cells. FASEB J 13 (10): 1231–1238.
83. Ghantous CM, Azrak Z, Hanache S, Abou-Kheir W, Zeidan A (2015) Differential Role of Leptin and Adiponectin in Cardiovascular System. Differential Role of Leptin and Adiponectin in Cardiovascular System. Int J Endocrinol 2015: 534320. Available: http://europepmc.org/articles/PMC4433709?pdf=render.
84. Yamagishi SI, Edelstein D, Du XL, Kaneda Y, Guzmán M, Brownlee M (2001) Leptin induces mitochondrial superoxide production and monocyte chemoattractant protein-1 expression in aortic endothelial cells by increasing fatty acid oxidation via protein kinase A. J Biol Chem 276 (27): 25096–25100.
85. Maingrette F, Renier G (2003) Leptin increases lipoprotein lipase secretion by macrophages: involvement of oxidative stress and protein kinase C. Diabetes 52 (8): 2121–2128.
86. Luan B, Goodarzi MO, Phillips NG, Guo X, Chen YD, Yao J, Allison M, Rotter JI, Shaw R, Montminy M (2014) Leptin-Mediated Increases in Catecholamine Signaling Reduce Adipose Tissue Inflammation via Activation of Macrophage HDAC4. Cell Metabolism 19 (6): 1058–1065. Available: http://www.cell.com/article/S1550413114001296/fulltext.
87. MacKenzie KF, Clark K, Naqvi S, McGuire VA, Nöehren G, Kristariyanto Y, van den Bosch M, Mudaliar M, McCarthy PC, Pattison MJ, Pedrioli PG, Barton GJ, Toth R, Prescott A, Arthur JS (2013) PGE(2) induces macrophage IL-10 production and a regulatory-like phenotype via a protein kinase A-SIK-CRTC3 pathway. Journal of immunology (Baltimore, Md. : 1950) 190 (2): 565–577.
88. Jéquier E (2002) Leptin Signaling, Adiposity, and Energy Balance. Annals of the New York Academy of Sciences 967 (1): 379–388. Available: http://onlinelibrary.wiley.com/doi/10.1111/j.1749-6632.2002.tb04293.x/full.
89. Minokoshi Y, Haque MS, Shimazu T (1999) Microinjection of leptin into the ventromedial hypothalamus increases glucose uptake in peripheral tissues in rats. Diabetes 48 (2): 287–291.

90. German J, Kim F, Schwartz GJ, Havel PJ, Rhodes CJ, Schwartz MW, Morton GJ (2009) Hypothalamic leptin signaling regulates hepatic insulin sensitivity via a neurocircuit involving the vagus nerve. Endocrinology 150 (10): 4502–4511.
91. Fujikawa T, Coppari R (2015) Living without insulin: the role of leptin signaling in the hypothalamus. Front Neurosci 9: 108.
92. Wabitsch M, Funcke JB, Lennerz B, Kuhnle-Krahl U, Lahr G, Debatin KM, Vatter P, Gierschik P, Moepps B, Fischer-Posovszky P (2014) Biologically Inactive Leptin and Early-Onset Extreme Obesity. N Engl J Med 372 (1): 48–54.
93. Yan QW, Yang Q, Mody N, Graham TE, Hsu CH, Xu Z, Houstis NE, Kahn BB, Rosen ED (2007) The adipokine lipocalin 2 is regulated by obesity and promotes insulin resistance. Diabetes 56 (10): 2533–2540.
94. Guo H, Jin D, Chen X (2014) Lipocalin 2 is a regulator of macrophage polarization and NF-kappaB/STAT3 pathway activation. Molecular endocrinology (Baltimore, Md.) 28 (10): 1616–1628.
95. Yang K, Guan H, Arany E, Hill DJ, Cao X (2008) Neuropeptide Y is produced in visceral adipose tissue and promotes proliferation of adipocyte precursor cells via the Y1 receptor. FASEB J 22 (7): 2452–2464. Available: http://www.fasebj.org/content/22/7/2452.full.
96. Kuo LE, Kitlinska JB, Tilan JU, Li L, Baker SB, Johnson MD, Lee EW, Burnett MS, Fricke ST, Kvetnansky R, Herzog H, Zukowska Z (2007) Neuropeptide Y acts directly in the periphery on fat tissue and mediates stress-induced obesity and metabolic syndrome. Nature medicine 13 (7): 803.
97. Sano H, Kane S, Sano E, Mîinea CP, Asara JM, Lane WS, Garner CW, Lienhard GE (2003) Insulin-stimulated phosphorylation of a Rab GTPase-activating protein regulates GLUT4 translocation. The Journal of biological chemistry 278 (17): 14599–14602.
98. Stenmark H, Olkkonen VM (2001) The Rab GTPase family. Genome Biology 2 (5): reviews3007. Available: http://www.genomebiology.com/content/pdf/gb-2001-2-5-reviews3007.pdf.
99. Sarrazin S, Lamanna WC, Esko JD (2011) Heparan Sulfate Proteoglycans. Cold Spring Harbor Perspectives in Biology 3 (7).
100. Davies BS, Beigneux AP, Barnes RH 2nd, Tu Y, Gin P, Weinstein MM, Nobumori C, Nyrén R, Goldberg I, Olivecrona G, Bensadoun A, Young SG, Fong LG (2010) GPIHBP1 is responsible for the entry of lipoprotein lipase into capillaries. Cell Metabolism 12 (1): 42–52.
101. Bishop JR, Passos-Bueno MR, Fong L, Stanford KI, Gonzales JC, Yeh E, Young SG, Bensadoun A, Witztum JL, Esko JD, Moulton KS (2010) Deletion of the basement membrane heparan sulfate proteoglycan type XVIII collagen causes hypertriglyceridemia in mice and humans. PloS one 5 (11): e13919.
102. Mead J, Irvine S, Ramji D (2002) Lipoprotein lipase: structure, function, regulation, and role in disease. Journal of Molecular Medicine. J Mol Med 80 (12): 753–769.
103. Yost TJ, Jensen DR, Haugen BR, Eckel RH (1998) Effect of dietary macronutrient composition on tissue-specific lipoprotein lipase activity and insulin action in normal-weight subjects. The American journal of clinical nutrition 68 (2): 296–302.
104. Pohl J, Ring A, Korkmaz Ü, Ehehalt R, Stremmel W (2005) FAT/CD36-mediated Long-Chain Fatty Acid Uptake in Adipocytes Requires Plasma Membrane Rafts. Mol. Biol. Cell 16 (1): 24–31. Available: http://www.molbiolcell.org/content/16/1/24.full.
105. Stahl A, Evans JG, Pattel S, Hirsch D, Lodish HF (2002) Insulin Causes Fatty Acid Transport Protein Translocation and Enhanced Fatty Acid Uptake in Adipocytes. Developmental Cell 2 (4): 477–488.
106. Bartness TJ, Bamshad M (1998) Innervation of mammalian white adipose tissue: implications for the regulation of total body fat. The American journal of physiology 275 (5 Pt 2): R1399-411.
107. Alberti, K. G. M. M., Zimmet P, Shaw J (2006) Metabolic syndrome—a new world-wide definition. A Consensus Statement from the International Diabetes Federation. Diabetic Medicine 23 (5): 469–480. Available: http://onlinelibrary.wiley.com/doi/10.1111/j.1464-5491.2006.01858.x/full.
108. Sniderman AD, Faraj M (2007) Apolipoprotein B, apolipoprotein A-I, insulin resistance and the metabolic syndrome. Current opinion in lipidology 18 (6): 633–637.
109. Pasarica M, Sereda OR, Redman LM, Albarado DC, Hymel DT, Roan LE, Rood JC, Burk DH, Smith SR (2009) Reduced Adipose Tissue Oxygenation in Human Obesity Evidence for Rarefaction, Macrophage Chemotaxis, and Inflammation Without an Angiogenic Response. Diabetes 58 (3): 718–725. Available: http://diabetes.diabetesjournals.org/content/58/3/718.full.

110. Summers LK, Samra JS, Humphreys SM, Morris RJ, Frayn KN (1996) Subcutaneous abdominal adipose tissue blood flow: variation within and between subjects and relationship to obesity. Clinical science (London, England : 1979) 91 (6): 679–683.
111. Hotamisligil GS (2003) Inflammatory pathways and insulin action. International journal of obesity and related metabolic disorders : journal of the International Association for the Study of Obesity 27 Suppl 3: S53-5.
112. Scherer PE, Bickel PE, Kotler M, Lodish HF (1998) Cloning of cell-specific secreted and surface proteins by subtractive antibody screening. Nature biotechnology 16 (6): 581–586.
113. De Barros S, Dehez S, Arnaud E, Barreau C, Cazavet A, Perez G, Galinier A, Casteilla L, Planat-Bénard V (2013) Aging-related decrease of human ASC angiogenic potential is reversed by hypoxia preconditioning through ROS production. Molecular therapy : the journal of the American Society of Gene Therapy 21 (2): 399–408.
114. Hsiao ST, Lokmic Z, Peshavariya H, Abberton KM, Dusting GJ, Lim SY, Dilley RJ (2013) Hypoxic conditioning enhances the angiogenic paracrine activity of human adipose-derived stem cells. Stem cells and development 22 (10): 1614–1623.
115. Nian M, Lee P, Khaper N, Liu P (2004) Inflammatory Cytokines and Postmyocardial Infarction Remodeling. Circulation Research 94 (12): 1543–1553. Available: http://circres.ahajournals.org/content/94/12/1543.full.
116. Bertola A, Ciucci T, Rousseau D, Bourlier V, Duffaut C, Bonnafous S, Blin-Wakkach C, Anty R, Iannelli A, Gugenheim J, Tran A, Bouloumié A, Gual P, Wakkach A (2012) Identification of adipose tissue dendritic cells correlated with obesity-associated insulin-resistance and inducing Th17 responses in mice and patients. Diabetes 61 (9): 2238–2247.
117. Bourlier V, Zakaroff-Girard A, Miranville A, De Barros S, Maumus M, Sengenes C, Galitzky J, Lafontan M, Karpe F, Frayn KN, Bouloumié A (2008) Remodeling phenotype of human subcutaneous adipose tissue macrophages. Circulation 117 (6): 806–815.
118. Nishimura S, Manabe I, Nagasaki M, Eto K, Yamashita H, Ohsugi M, Otsu M, Hara K, Ueki K, Sugiura S, Yoshimura K, Kadowaki T, Nagai R (2009) CD8+ effector T cells contribute to macrophage recruitment and adipose tissue inflammation in obesity. Nature medicine 15 (8): 914–920.
119. Stefanovic-Racic M, Yang X, Turner MS, Mantell BS, Stolz DB, Sumpter TL, Sipula IJ, Dedousis N, Scott DK, Morel PA, Thomson AW, O'Doherty RM (2012) Dendritic cells promote macrophage infiltration and comprise a substantial proportion of obesity-associated increases in CD11c+ cells in adipose tissue and liver. Diabetes 61 (9): 2330–2339.
120. Shaul ME, Bennett G, Strissel KJ, Greenberg AS, Obin MS (2010) Dynamic, M2-like remodeling phenotypes of CD11c+ adipose tissue macrophages during high-fat diet--induced obesity in mice. Diabetes 59 (5): 1171–1181.
121. Feuerer M, Herrero L, Cipolletta D, Naaz A, Wong J, Nayer A, Lee J, Goldfine AB, Benoist C, Shoelson S, Mathis D (2009) Lean, but not obese, fat is enriched for a unique population of regulatory T cells that affect metabolic parameters. Nature medicine 15 (8): 930–939.
122. Winer S, Chan Y, Paltser G, Truong D, Tsui H, Bahrami J, Dorfman R, Wang Y, Zielenski J, Mastronardi F, Maezawa Y, Drucker DJ, Engleman E, Winer D, Dosch HM (2009) Normalization of obesity-associated insulin resistance through immunotherapy. Nature medicine 15 (8): 921–929.
123. Yang H, Youm YH, Vandanmagsar B, Ravussin A, Gimble JM, Greenway F, Stephens JM, Mynatt RL, Dixit VD (2010) Obesity increases the production of proinflammatory mediators from adipose tissue T cells and compromises TCR repertoire diversity: implications for systemic inflammation and insulin resistance. Journal of immunology (Baltimore, Md. : 1950) 185 (3): 1836–1845.
124. O'Rourke RW, Gaston GD, Meyer KA, White AE, Marks DL (2013) Adipose tissue NK cells manifest an activated phenotype in human obesity. Metabolism: clinical and experimental 62 (11): 1557–1561.
125. Lee B, Lee J (2014) Cellular and molecular players in adipose tissue inflammation in the development of obesity-induced insulin resistance. Biochimica et biophysica acta 1842 (3): 446–462.
126. Koza RA, Nikonova L, Hogan J, Rim JS, Mendoza T, Faulk C, Skaf J, Kozak LP (2006) Changes in gene expression foreshadow diet-induced obesity in genetically identical mice. PLoS genetics 2 (5): e81.

127. Heijmans BT, Tobi EW, Stein AD, Putter H, Blauw GJ, Susser ES, Slagboom PE, Lumey LH (2008) Persistent epigenetic differences associated with prenatal exposure to famine in humans. Proceedings of the National Academy of Sciences of the United States of America 105 (44): 17046–17049.
128. Thurner S, Klimek P, Szell M, Duftschmid G, Endel G, Kautzky-Willer A, Kasper DC (2013) Quantification of excess risk for diabetes for those born in times of hunger, in an entire population of a nation, across a century. Proceedings of the National Academy of Sciences of the United States of America 110 (12): 4703–4707.
129. Jousse C, Parry L, Lambert-Langlais S, Maurin AC, Averous J, Bruhat A, Carraro V, Tost J, Letteron P, Chen P, Jockers R, Launay JM, Mallet J, Fafournoux P (2011) Perinatal undernutrition affects the methylation and expression of the leptin gene in adults: implication for the understanding of metabolic syndrome. FASEB journal : official publication of the Federation of American Societies for Experimental Biology 25 (9): 3271–3278.
130. Ravelli AC, van der Meulen JH, Michels RP, Osmond C, Barker DJ, Hales CN, Bleker OP (1998) Glucose tolerance in adults after prenatal exposure to famine. Lancet (London, England) 351 (9097): 173–177.
131. Jufvas A, Sjödin S, Lundqvist K, Amin R, Vener AV, Strålfors P (2013) Global differences in specific histone H3 methylation are associated with overweight and type 2 diabetes. Clinical epigenetics 5 (1): 15.
132. Matsui Y, Tomaru U, Miyoshi A, Ito T, Fukaya S, Miyoshi H, Atsumi T, Ishizu A (2014) Overexpression of TNF-alpha converting enzyme promotes adipose tissue inflammation and fibrosis induced by high fat diet. Experimental and molecular pathology 97 (3): 354–358.
133. Strissel KJ, Stancheva Z, Miyoshi H, Perfield JW 2nd, DeFuria J, Jick Z, Greenberg AS, Obin MS (2007) Adipocyte Death, Adipose Tissue Remodeling, and Obesity Complications. Diabetes 56 (12): 2910–2918. Available: http://diabetes.diabetesjournals.org/content/56/12/2910.full.
134. Zuk P (2013) The ASC: Critical Participants in Paracrine-Mediated Tissue Health and Function. In: Andrades JA, editor. Regenerative medicine ad tissue engineering. Rijeka: InTech.
135. Dominici M, Le Blanc K, Mueller I, Slaper-Cortenbach I, Marini F, Krause D, Deans R, Keating A, Prockop Dj, Horwitz E (2006) Minimal criteria for defining multipotent mesenchymal stromal cells. The International Society for Cellular Therapy position statement. Cytotherapy 8 (4): 315–317.
136. Maleki M, Ghanbarvand F, Reza Behvarz M, Ejtemaei M, Ghadirkhomi E (2014) Comparison of mesenchymal stem cell markers in multiple human adult stem cells. Int J Stem Cells 7 (2): 118–126.
137. Merfeld-Clauss S, Lupov IP1, Lu H1, Feng D1, Compton-Craig P1, March KL1, Traktuev DO (2014) Adipose Stromal Cells Differentiate Along a Smooth Muscle Lineage Pathway Upon Endothelial Cell Contact via Induction of Activin A. Circulation Research 115 (9): 800–809. Available: http://circres.ahajournals.org/content/115/9/800.full.
138. Wosnitza M, Hemmrich K, Groger A, Gräber S, Pallua N (2007) Plasticity of human adipose stem cells to perform adipogenic and endothelial differentiation. Differentiation 75 (1): 12–23.
139. De Francesco F, Tirino V, Desiderio V, Ferraro G, D'Andrea F, Giuliano M, Libondi G, Pirozzi G, De Rosa A, Papaccio G (2009) Human CD34/CD90 ASCs are capable of growing as sphere clusters, producing high levels of VEGF and forming capillaries. PLoS ONE 4 (8): e6537.
140. Koh YJ, Koh BI, Kim H, Joo HJ, Jin HK, Jeon J, Choi C, Lee DH, Chung JH, Cho CH, Park WS, Ryu JK, Suh JK, Koh GY (2011) Stromal vascular fraction from adipose tissue forms profound vascular network through the dynamic reassembly of blood endothelial cells. Arterioscler. Thromb. Vasc. Biol. 31 (5): 1141–1150.
141. Hu H, He ML, Tao R, Sun HY, Hu R, Zang WJ, Yuan BX, Lau CP, Tse HF, Li GR (2009) Characterization of ion channels in human preadipocytes. Journal of Cellular Physiology 218 (2): 427–435. Available: http://onlinelibrary.wiley.com/doi/10.1002/jcp.21617/full.
142. Lefterova MI, Haakonsson AK, Lazar MA, Mandrup S (2014) PPARgamma and the global map of adipogenesis and beyond. Trends in endocrinology and metabolism: TEM 25 (6): 293–302.
143. Huang HY, Chen SZ, Zhang WT, Wang SS, Liu Y, Li X, Sun X, Li YM, Wen B, Lei QY, Tang QQ (2013) Induction of EMT-like response by BMP4 via up-regulation of lysyl oxidase is required for adipocyte lineage commitment. Stem Cell Res 10 (3): 278–287.
144. Keck M, Zeyda M, Gollinger K, Burjak S, Kamolz LP, Frey M, Stulnig TM (2010) Local anesthetics have a major impact on viability of preadipocytes and their differentiation into adipocytes. Plastic and reconstructive surgery 126 (5): 1500–1505.

145. Illouz YG (1983) Body contouring by lipolysis: a 5-year experience with over 3000 cases. Plast. Reconstr. Surg. 72 (5): 591–597.
146. Blacam C de, Momoh AO, Colakoglu S, Tobias AM, Lee BT (2011) Evaluation of clinical outcomes and aesthetic results after autologous fat grafting for contour deformities of the reconstructed breast. Plastic and reconstructive surgery 128 (5): 411e-418e.
147. Storck K, Ell J, Regn S, Rittler-Ungetüm B, Mayer H, Schantz T, Müller D, Buchberger M (2015) Optimization of in vitro cultivation strategies for human adipocyte derived stem cells. Adipocyte: 1–7.
148. Bunnell BA, Flaat M, Gagliardi C, Patel B, Ripoll C (2008) Adipose-derived stem cells: isolation, expansion and differentiation. Methods 45 (2): 115–120. Accessed 21 April 2015.
149. Sattler G, Augustin M, editors (2003) Lehrbuch der Liposuktion. 17 Tabellen. Stuttgart: Thieme. 274 p.
150. Lee JA, Parrett BM, Conejero JA, Laser J, Chen J, Kogon AJ, Nanda D, Grant RT, Breitbart AS (2003) Biological alchemy: engineering bone and fat from fat-derived stem cells. Ann Plast Surg 50 (6): 610–617.
151. Martella E, Bellotti C, Dozza B, Perrone S, Donati D, Lucarelli E (2014) Secreted adiponectin as a marker to evaluate in vitro the adipogenic differentiation of human mesenchymal stromal cells. Cytotherapy 16 (11): 1476–1485.
152. Smith NC, Fairbridge NA, Pallegar NK, Christian SL (2015) Dynamic upregulation of CD24 in pre-adipocytes promotes adipogenesis. Adipocyte 4 (2): 89–100.
153. Fu Y, Luo N, Klein RL, Garvey WT (2005) Adiponectin promotes adipocyte differentiation, insulin sensitivity, and lipid accumulation. Journal of lipid research 46 (7): 1369–1379.
154. Leung DW, Cachianes G, Kuang WJ, Goeddel DV, Ferrara N (1989) Vascular endothelial growth factor is a secreted angiogenic mitogen. Science (New York, N.Y.) 246 (4935): 1306–1309.
155. Breier G, Albrecht U, Sterrer S, Risau W (1992) Expression of vascular endothelial growth factor during embryonic angiogenesis and endothelial cell differentiation. Development 114 (2): 521–532. Available: http://dev.biologists.org/content/114/2/521.full.pdf.
156. Gimble JM, Katz AJ, Bunnell BA (2007) Adipose-derived stem cells for regenerative medicine. Circulation research 100 (9): 1249–1260.
157. Locke M, Windsor J, Dunbar PR (2009) Human adipose-derived stem cells: isolation, characterization and applications in surgery. ANZ Journal of Surgery 79 (4): 235–244. Available: http://onlinelibrary.wiley.com/doi/10.1111/j.1445-2197.2009.04852.x/full.
158. Green H, Kehinde O (1975) An established preadipose cell line and its differentiation in culture II. Factors affecting the adipose conversion. Cell 5 (1): 19–27.
159. Scott MA, Nguyen VT, Levi B, James AW (2011) Current methods of adipogenic differentiation of mesenchymal stem cells. Stem cells and development 20 (10): 1793–1804.
160. Zimmerlin L, Donnenberg VS, Pfeifer ME, Meyer EM, Péault B, Rubin JP, Donnenberg AD (2010) Stromal vascular progenitors in adult human adipose tissue. Cytometry. Part A : the journal of the International Society for Analytical Cytology 77 (1): 22–30.
161. Park JR, Jung JW, Seo MS, Kang SK, Lee YS, Kang KS (2010) DNER modulates adipogenesis of human adipose tissue-derived mesenchymal stem cells via regulation of cell proliferation. Cell proliferation 43 (1): 19–28.
162. Ghosh S, Dean A, Walter M, Bao Y, Hu Y, Ruan J, Li R (2010) Cell density-dependent transcriptional activation of endocrine-related genes in human adipose tissue-derived stem cells. Experimental cell research 316 (13): 2087–2098.
163. Moioli EK, Chen M, Yang R, Shah B, Wu J, Mao JJ (2010) Hybrid adipogenic implants from adipose stem cells for soft tissue reconstruction in vivo. Tissue engineering. Part A 16 (11): 3299–3307.
164. Yu G, Wu X, Dietrich MA, Polk P, Scott LK, Ptitsyn AA, Gimble JM (2010) Yield and characterization of subcutaneous human adipose-derived stem cells by flow cytometric and adipogenic mRNA analyzes. Cytotherapy 12 (4): 538–546.
165. Lee JE, Kim I, Kim M (2010) Adipogenic differentiation of human adipose tissue-derived stem cells obtained from cryopreserved adipose aspirates. Dermatologic surgery : official publication for American Society for Dermatologic Surgery [et al.] 36 (7): 1078–1083.
166. van Harmelen V, Röhrig K, Hauner H (2004) Comparison of proliferation and differentiation capacity of human adipocyte precursor cells from the omental and subcutaneous adipose tissue depot of obese subjects. Metabolism 53 (5): 632–637.

167. Li H, Zimmerlin L, Marra KG, Donnenberg VS, Donnenberg AD, Rubin JP (2011) Adipogenic potential of adipose stem cell subpopulations. Plastic and reconstructive surgery 128 (3): 663–672.
168. Wu P, Sato K, Yukawa S, Hikasa Y, Kagota K (2001) Differentiation of stromal-vascular cells isolated from canine adipose tissues in primary culture. The Journal of veterinary medical science / the Japanese Society of Veterinary Science 63 (1): 17–23.
169. Goh BC, Thirumala S, Kilroy G, Devireddy RV, Gimble JM (2007) Cryopreservation characteristics of adipose-derived stem cells: maintenance of differentiation potential and viability. Journal of tissue engineering and regenerative medicine 1 (4): 322–324.
170. Weijers EM, Van Den Broek LJ, Waaijman T, Van Hinsbergh VW, Gibbs S, Koolwijk P (2011) The influence of hypoxia and fibrinogen variants on the expansion and differentiation of adipose tissue-derived mesenchymal stem cells. Tissue engineering. Part A 17 (21-22): 2675–2685.
171. Frazier TP, Gimble JM, Kheterpal I, Rowan BG (2013) Impact of low oxygen on the secretome of human adipose-derived stromal/stem cell primary cultures. Special section : The Mesenchymal Stem Cell secretome in Regenerative Medicine. Biochimie 95 (12): 2286–2296.
172. Stubbs SL, Hsiao ST, Peshavariya HM, Lim SY, Dusting GJ, Dilley RJ (2012) Hypoxic preconditioning enhances survival of human adipose-derived stem cells and conditions endothelial cells in vitro. Stem cells and development 21 (11): 1887–1896.
173. Attig L, Vigé A, Gabory A, Karimi M, Beauger A, Gross MS, Athias A, Gallou-Kabani C, Gambert P, Ekstrom TJ, Jais JP, Junien C (2013) Dietary alleviation of maternal obesity and diabetes: increased resistance to diet-induced obesity transcriptional and epigenetic signatures. PloS one 8 (6): e66816.
174. Maeda N, Shimomura I, Kishida K, Nishizawa H, Matsuda M, Nagaretani H, Furuyama N, Kondo H, Takahashi M, Arita Y, Komuro R, Ouchi N, Kihara S, Tochino Y, Okutomi K, Horie M, Takeda S, Aoyama T, Funahashi T, Matsuzawa Y (2002) Diet-induced insulin resistance in mice lacking adiponectin/ACRP30. Nature medicine 8 (7): 731–737.
175. Vu MT, Smith CF, Burger PC, Klintworth GK (1985) An evaluation of methods to quantitate the chick chorioallantoic membrane assay in angiogenesis. Laboratory investigation; a journal of technical methods and pathology 53 (4): 499–508.
176. Gimbrone MA, JR, Leapman SB, Cotran RS, Folkman J (1972) Tumor dormancy in vivo by prevention of neovascularization. The Journal of experimental medicine 136 (2): 261–276.
177. Iliopoulos D, Hirsch HA, Struhl K (2009) An epigenetic switch involving NF-kappaB, Lin28, Let-7 MicroRNA, and IL6 links inflammation to cell transformation. Cell 139 (4): 693–706.
178. Stenvinkel P, Karimi M, Johansson S, Axelsson J, Suliman M, Lindholm B, Heimbürger O, Barany P, Alvestrand A, Nordfors L, Qureshi AR, Ekström TJ, Schalling M (2007) Impact of inflammation on epigenetic DNA methylation - a novel risk factor for cardiovascular disease. Journal of internal medicine 261 (5): 488–499.
179. Kang S, Kim S, Sung J (2014) Cellular and molecular stimulation of adipose-derived stem cells under hypoxia. Cell Biology International 38 (5): 553–562. Available: http://onlinelibrary.wiley.com/doi/10.1002/cbin.10246/full.
180. Rehman J, Traktuev D, Li J, Merfeld-Clauss S, Temm-Grove CJ, Bovenkerk JE, Pell CL, Johnstone BH, Considine RV, March KL (2004) Secretion of angiogenic and antiapoptotic factors by human adipose stromal cells. Circulation 109 (10): 1292–1298.
181. Waltenberger J, Mayr U, Frank H, Hombach V (1996) Suramin is a potent inhibitor of vascular endothelial growth factor. A contribution to the molecular basis of its antiangiogenic action. J. Mol. Cell. Cardiol. 28 (7): 1523–1529.
182. Bahramsoltani M, Plendl J (2007) Different ways to antiangiogenesis by angiostatin and suramin, and quantitation of angiostatin-induced antiangiogenesis. APMIS : acta pathologica, microbiologica, et immunologica Scandinavica 115 (1): 30–46.
183. Saharinen P, Eklund L, Pulkki K, Bono P, Alitalo K (2011) VEGF and angiopoietin signaling in tumor angiogenesis and metastasis. Trends in molecular medicine 17 (7): 347–362.